Laboratorio de Microscopías Avanzadas

Annual Report 2011

LMA
LABORATORIO DE MICROSCOPIAS AVANZADAS

Laboratorio de Microscopías Avanzadas

Annual Report 2011

LMA
LABORATORIO DE MICROSCOPIAS AVANZADAS

Index

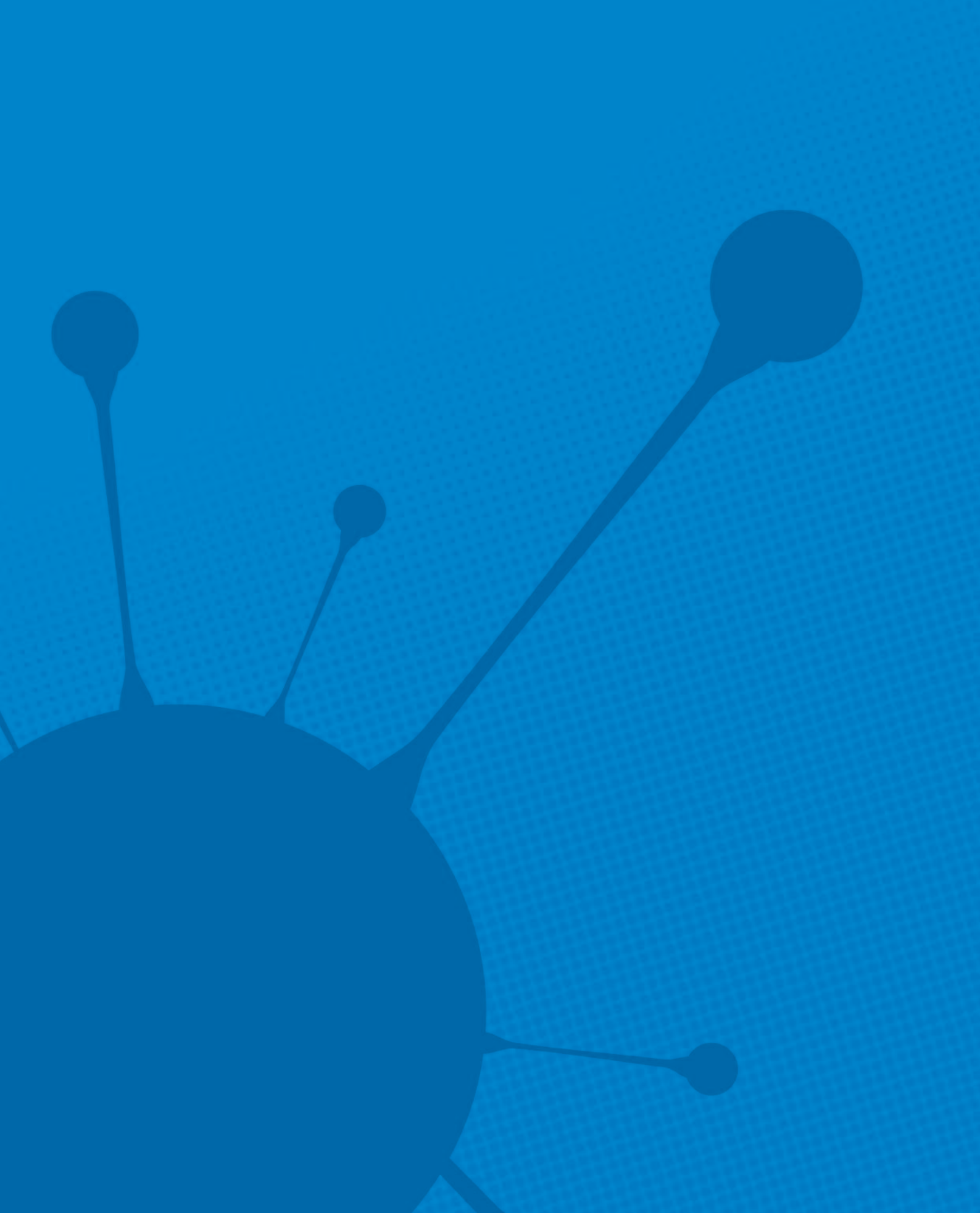

Introduction

Manuel Ricardo Ibarra García
Director

The Laboratory of Advanced Microscopies (Laboratorio de Microscopías Avanzadas, LMA) emerges in our scientific environment as a result of the fruitful activity in the field of new materials and the need to cover the requirements of new infrastructures for the observation and processing of the matter at nanoscale and even at atomic level.

> *"The Nanosciences are one of the most promising fields of research of today and their development demands not only facilities for the fabrication of nanostructures but also absolutely requires advanced tools for the characterization of these nanostructures. No progress would have been possible on superlattices, quantum dots, nanomagnets, etc without a precise characterization to guide the fabrication and, then, permit the interpretation and modeling of the experimental results…"*
>
> **Albert Fert,** Nobel Prize in Physics in 2007,
> in his Letter of support for the creation of the LMA

A long trajectory of the Institute of Materials Science of Aragón (ICMA) and a clear positioning of the Institute of Nanoscience of Aragón (INA) as a reference center at national level was the seed of the new project in which in an innovative manner new advanced microscopies were combined: Dual Beam (DB), Transmission Electron Microscopy (TEM) and Scanning Probe Microscopy (SPM). This has been one of the most recognized peculiarities of the LMA and it is being considered one of the powerful sources for a real contribution to the scientific knowledge development in Nanoscience.

Two major challenges have been overcome, providing a new scientific atmosphere: the existence of top level scientific instrumentation and the attraction of young new researchers, who at this moment constitute a major achievement of this project.

The Aragón Government and the University of Zaragoza have been the supporters during the first steps of this new facility through an agreement with the Spanish Ministry of Science and Innovation within the framework of the national ICTS Program (Infraestructuras Científico-Técnicas Singulares). The first step was the acquisition and setup of the equipments at the new building for the Research Institutes of the University of Zaragoza at the Campus Rio Ebro. The second step has been the consolidation and maintenance of the facility under long-term partial financial support of the Aragón government.

The LMA aims to develop stable institutional collaborations such as the Transpyrenean Associated Laboratory for Electron Microscopy (TALEM) with the Centre CEMES (CNRS, Toulouse). Recently, the LMA joined the European Consortium for advanced development of TEM (ESTEEMII) in which the main European TEM groups are involved.

The LMA is open to the overall scientific community both at national or international level and during the short term of operation, large number of scientist and companies have profited from their singular characteristics. As a summary, relevant achievements have been obtained in the fields of: nanofabrication, morphologic and electronic characterization with atomic resolution and atomic manipulation.

Foreword

José María De Teresa Nogueras
Coordinator

The LMA agreements were signed at the end of 2009 with two main objectives. One is to provide service, facilitating the access of any researcher or company to the existing advanced infrastructures in the LMA, and another one is to generate top scientific and technological results by the local researchers. The LMA was conceived as an open and research-driven facility, which is reflected in the way it is managed. The three areas of research, DB, TEM and SPM work autonomously on the daily basis, following their respective needs and supervised by three researchers belonging respectively to the staff of CSIC, the CNRS and the Freie University of Berlin. My role as coordinator, starting in May 2011, is to assist the three areas to develop efficiently their work respecting the main objectives previously mentioned and with a fluid connection with the LMA director. It has been a pleasure for me to coordinate the writing of the first LMA scientific report, including the main scientific and technological achievements obtained along 2011. Given the short history of the LMA, I have been strongly impressed by those achievements, which include for example one publication in Science (vol. 334, page 1377) thanks to the external service provided by the LMA, several publications in Nature Materials, Nanoletters and ACS Nano by researchers belonging to INA and ICMA and many services provided to companies and researchers. This could not have been possible without the strong commitment and solid knowledge of all the people involved in the project: director, area supervisors, scientists, technical staff and administration. I thank all of them for their contribution to the LMA venture and in particular to the 2011 LMA annual report.

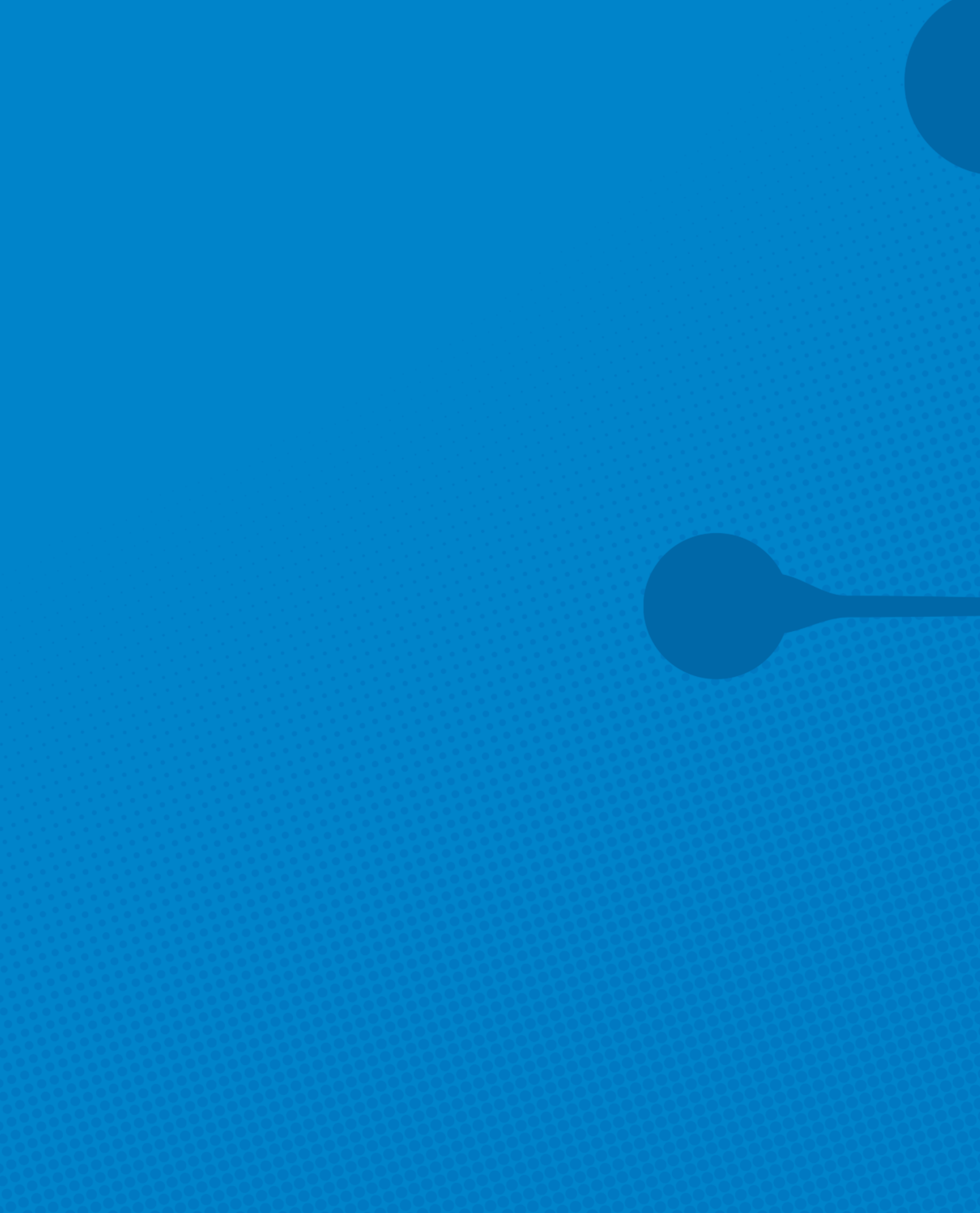

About LMA

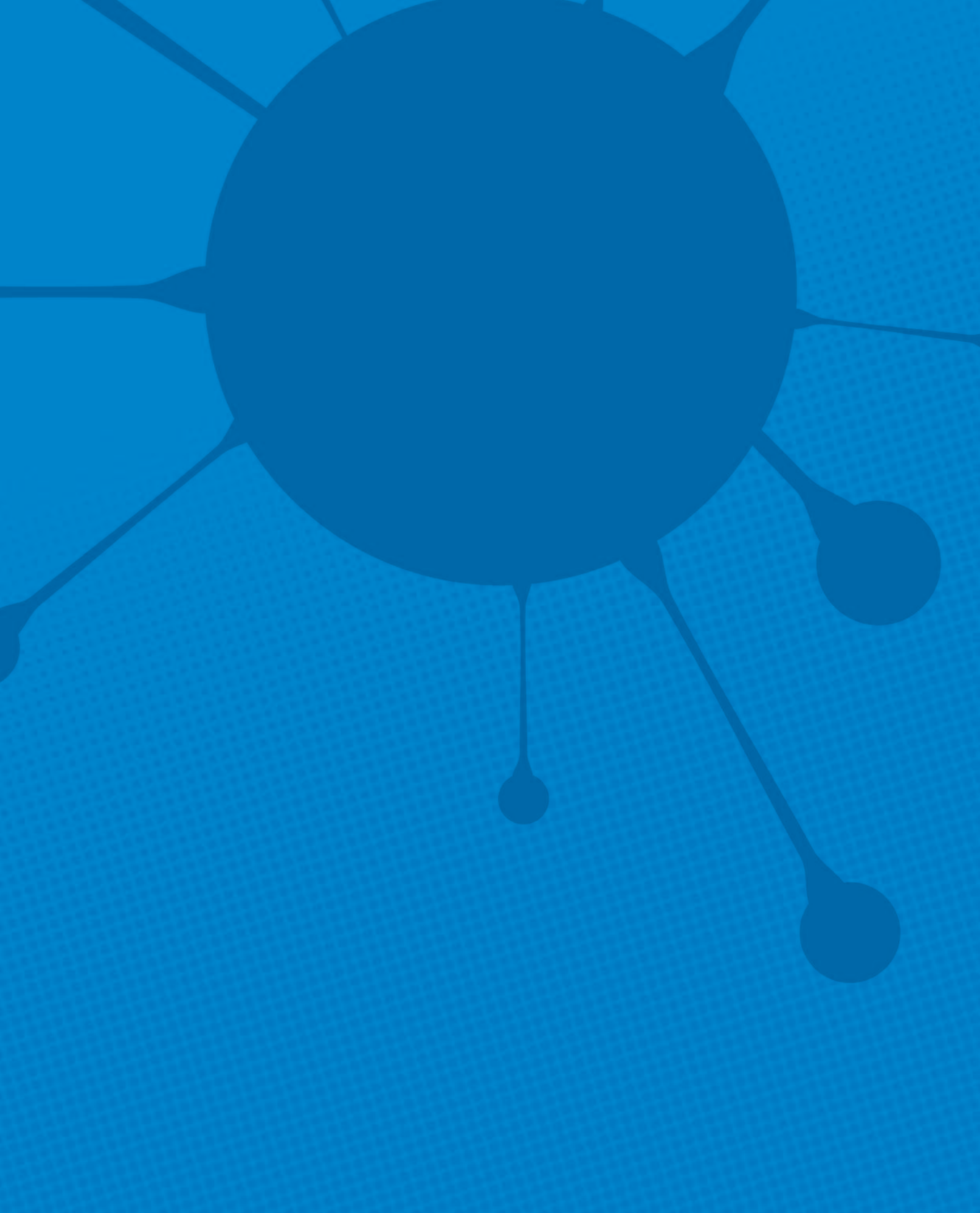

About LMA

Unique facilities for the biggest expectations

The Advanced Microscopies Laboratory (LMA) represents a unique initiative both at national and international level. Its aim is to provide the Scientific Community with the most advanced existing infrastructures in Local Probe and Electron Microscopy for the observation, characterization, nanopatterning and handling of materials at atomic scale, as well as with a wide range of scientific tools devoted to characterization, processing and handling procedures at the nanometric scale.

Its location within the Institute of Nanoscience of Aragon (INA) guarantees an environment of complementary associated infrastructures and excellence-driven scientific and technical human resources which, together with the unique equipment of LMA, will boost research capacity in Nanoscience in Spain, as well as the development of new related technologies.

All LMA scientific instruments and the expertise of the scientists and technical staff involved are available for public and private research centers and for the industry in general, who find in this facility a unique research capacity and technological development only available in very few research centers worldwide.

Laboratorio de Microscopías Avanzadas
Edificio I+D
Campus Río Ebro
C/ Mariano Esquillor, s/n.
50018 Zaragoza (Spain)
Tel. +34 976 762 980
Fax +34 976 762 777
Email: lma@unizar.es
http://ina.unizar.es/lma

Organization Chart

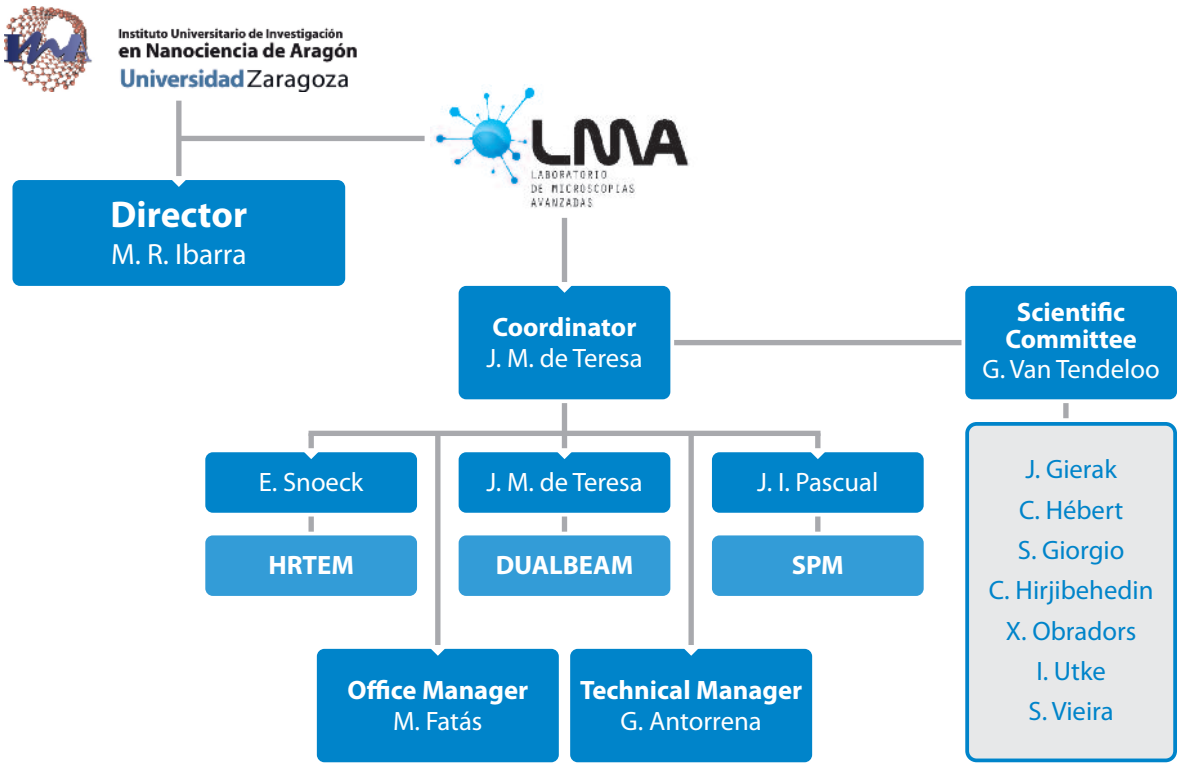

The LMA depends administratively on the University of Zaragoza through the Instituto de Nanociencia de Aragón. The director of INA is also the director of the LMA. An international Scientific Committee evaluates periodically the activities of the LMA and provides assessment for improvement. The LMA scientific activities are managed by three area supervisors, coordinated by the LMA coordinator. Each area supervisor is responsible for the equipments and technical staff assigned to its area and in general for all the organizational issues of the area.

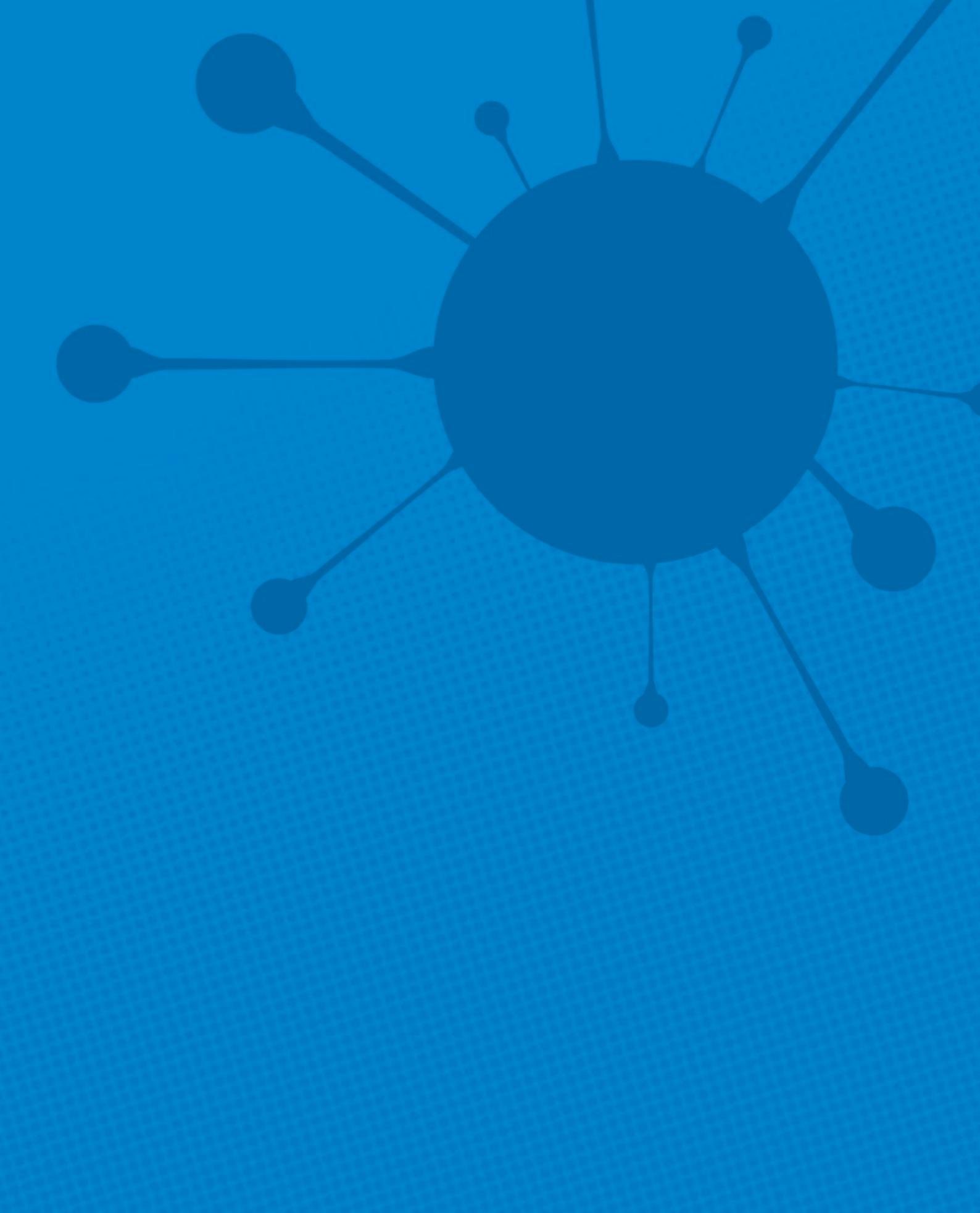

Scientific Committee members

Prof. Gustaf Van Tendeloo
University of Antwerp (Belgium)

Prof. G. Van Tendeloo got his PhD at the Antwerp University under the direction of Prof. S. Amelinckx. He has been nominated in 1988 professor in physics at the University of Antwerp where he developed TEM technics for Materials Sciences studies. He led the electron microscopy laboratory (EMAT) in Antwerp since 2003. His main activities concern advanced electron microscopy, fine structure of interfaces, nanotubes and nanowires, nanoparticles and mesoporous materials. Prof. G Van Tendeloo is the author of ~700 publications in international journals, has given invited talks in more than 100 international conferences, is the editor of "Handbook of Microscopy" and of "Handbook on Nanoscopy". He is member of the editorial board of 6 ISI journals and his "H" factor is 58. He was leading the European IP3 project ESTEEM (2005-2011).

Dr. Jacques Gierak
LPN – CNRS (France)

Jacques Gierak is the responsible for the Focused Ion Beam (FIB) activity at the Laboratory for Photonics and Nanostructures (LPN) since 1995. He is involved in FIB research activity since 1984, as he joined the LPN laboratory now located in Marcoussis (France). He is graduated from the "Conservatoire National des Arts et Métiers" Paris in the Physics-Electronics dept., owner of a DEA in instrumentation, and of a PhD thesis. The recent FIB machines he has developed have all reached the international state-of-the-art. He holds 10 patents, 3 in explotaition and 70 publications. CNRS Cristal Medalist Prize obtained in 2003 and Yves Rocard Prize from the French Physics Society in 2007. Thus, he is considered to be one of the world experts in FIB.

Prof. Suzanne Giorgio
INaM – CNRS (France)

Prof. S. Giorgio got her PhD at the University Aix-Marseille. She has been nominated "Chargé de Recherche" at CNRS in 1983 and Professor at the Marseille University in 2004. She is the head of Department "Materials Science" at the Ecole Supérieure d'Ingénieur de Luminy (ESIL – Marseille) and is in charge of the "Scientific Diffusion" at the University (Université de la Méditerranée). Prof. S. Giorgio is an electron microscopist specialized in catalysis and "in-situ". She is working on the relations between the reactivity of metal clusters and their structural properties and has developed a new technique of environmental microscopy at high pressure of gas (< 30 mbar) and high temperature (<350°C), in a closed reactor inside a sample holder, connected to a mass spectrometer to analyse the reaction products during the modification of the crystalline structure at the atomic scale. She is the author of more than 70 papers and has "H" factor of 20

Prof. Cécile Hébert
EPFL (Switzerland)

Cécile Hébert obtained her master degree (physics) and her Ph.D degree (design of a new energy filter for TEM) at the Ecole Centrale in Paris. She then has been working on the calculation of the fine structure of ionisation edges in EELS. As a research assistant at the Vienna University of Technology, she was one of the main participant to the CHIRALTEM project dealing with the measurement of magnetic circular dichroism in the electron microscope. She currently leads the Center for Electron Microscopy at the EPFL. She is the author of more than 150 papers with an "H" factor of 32.

Dr. Cyrus Hirjibehedin
London Center for Nanotechnology (UK)

Dr. Hirjibehedin is an expert in atomic magnetism. He got his Ph.D. in 2004, in Columbia University, and spent a extended period at IBM Almaden Research Center. There he performed reknown works in the field of manipulation of magnetic properties of individual atoms. In 2008 he became member of the London Institute of nanotechnology, at the University College London, where he leads a research group on low temperature atomic magnetism. His contributions to our understanding of magnetic interactions at the nanometer scale have been crucial.

Dr. Xavier Obradors
ICMAB – CSIC

Prof. Xavier Obradors got his degree in Physics in the University of Barcelona in 1978, a DEA in Solid State Physics in Toulouse and a PhD in Physics in the University of Barcelona in 1982. He is Research Professor at CSIC since 1992 and the current Director of the Institute of Materials Science in Barcelona (ICMAB). He holds more than 400 publications and an "h" factor of 37. He has received several awards, in particular, the National Prize "Blas Cabrera" of Physical Sciences, Materials and Earth studies, Spain 2003. His research activity is broad, including materials preparation with controlled microstructures and the search for the comprehension of the physical mechanisms underlaying the magnetic and superconducting properties of the materials. The generation of industrially significant knowledge, both in materials processing and in electrotechnical device development, has been strongly stimulated by him. Several initiatives of technological transfer within an European scenario have been carried out by him.

Dr. Ivo Utke
EMPA (Switzerland)

Dr. Ivo Utke holds a PhD thesis from the Humboldt University of Berlin since 1995. Between this date and 2004 he held several positions at the EFPL (Switzerland) and since 2005 he is a Senior Scientist at EMPA-Thun. He is a world expert in R&D in Nanoscience and Nanotechnology with charged particle beams. In particular, he has focused on the fundamental and applied studies of Focused Electron Beam Induced Deposition and Etching (metals, dielectrics, semiconductors). He has developed charged particle beam techniques and other technologies (lithography, lift-off) as rapid, maskless, minimally-invasive prototyping tools. He has strong experience in the fabrication of prototypes in the field of nano-optics, nano-electronics, scanning probes, and bio-applications.

Prof. Sebastián Vieira
Universidad Autónoma de Madrid

Prof. Sebastián Vieira is full professor at the Universidad Autónoma de Madrid and one of the founding members of the department of Condensed Matter, in the 70s. He leads the group of Low Temperature Physics, traditionally oriented to the study of the thermal properties of solids, mainly of disordered ones, with calorimetric, dilatometric and thermal transport techniques. Today, he extended his research areas to the physics of nanoscopic systems, at low temperatures, and the fabrication and characterization of superconducting nanostructures.

Scientific Committee 2011 Report

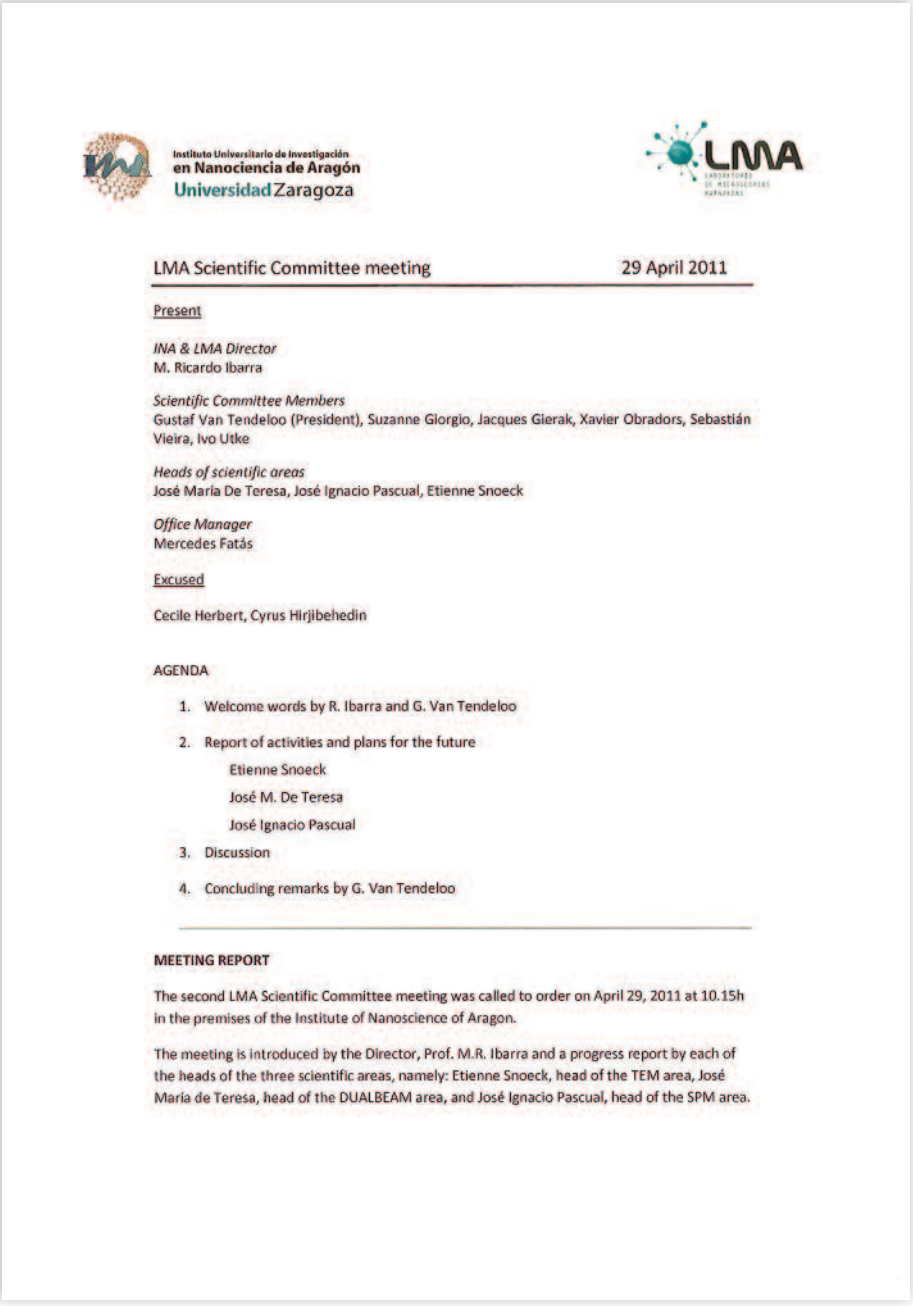

Instituto Universitario de Investigación en Nanociencia de Aragón
Universidad Zaragoza

LMA

LMA Scientific Committee meeting 29 April 2011

Present

INA & LMA Director
M. Ricardo Ibarra

Scientific Committee Members
Gustaf Van Tendeloo (President), Suzanne Giorgio, Jacques Gierak, Xavier Obradors, Sebastián Vieira, Ivo Utke

Heads of scientific areas
José María De Teresa, José Ignacio Pascual, Etienne Snoeck

Office Manager
Mercedes Fatás

Excused

Cecile Herbert, Cyrus Hirjibehedin

AGENDA

1. Welcome words by R. Ibarra and G. Van Tendeloo
2. Report of activities and plans for the future
   Etienne Snoeck
   José M. De Teresa
   José Ignacio Pascual
3. Discussion
4. Concluding remarks by G. Van Tendeloo

MEETING REPORT

The second LMA Scientific Committee meeting was called to order on April 29, 2011 at 10.15h in the premises of the Institute of Nanoscience of Aragon.

The meeting is introduced by the Director, Prof. M.R. Ibarra and a progress report by each of the heads of the three scientific areas, namely: Etienne Snoeck, head of the TEM area, José María de Teresa, head of the DUALBEAM area, and José Ignacio Pascual, head of the SPM area.

Instituto Universitario de Investigación en Nanociencia de Aragón
Universidad Zaragoza

LMA

Regarding the general structure of LMA, there is a suggestion made by the Director to incorporate a coordinating figure to the organizational chart. Taking into account the structure and the complexity that the LMA already has, with 45 people, the Scientific Committee finds it convenient to create such coordination position to simplify and to facilitate the communication between the LMA Director and the three heads of the different scientific areas and they also agree to designate José María de Teresa, who is CSIC Research Professor as well as UZ Associated Professor, as this designation shows that LMA is an open lab, a very positive feature, specially for the agreement which is being negotiated for CSIC to be involved in the Lab.

The progress reports lead to the following conclusions by the Scientific Committee:

- The dual beam area is particularly impressive because it covers a wide range of applications, beyond the common use of this type of equipment.
- Regarding the SPM area, it is suggested to focus the research lines rather than covering a wide spectrum of scientific directions.
- The TEM area is very promising, but it should think about what scientific orientation it is going to take and it is suggested to focus the research on high-impact results, leaving aside more-routine type of research. It is important to determine its own specialization.
- Regarding LMA as a whole, it will be very important to attract scientists from all over Spain to make use these complex instruments. Special focus should be on showing the possibilities to a broader scientific community. It is suggested to have a person dedicated to approach scientists, such as crystallographers, metallurgists, soft matter researchers....
- In order to improve cooperation, interaction and exchange of opinions, it is also suggested to organize thematic workshops for users and potential users.
- Institutional visibility should be increased and further interaction with industry should also be sought. LMA has to show what it is capable to do. A good instrument could be the organization of events devoted to industry, or to have someone devoted exclusively to industry.
- Finally, LMA must be congratulated for the excellent work done so far since the last meeting one year ago.

Gustaaf Van Tendeloo
President of the Scientific committee

Human Resources

Management

M. Ricardo Ibarra	*Director*	ibarra@unizar.es
José Mª De Teresa	*Scientific Coordinator*	deteresa@unizar.es
Guillermo Antorrena	*Technical Manager*	ganto@unizar.es
Mercedes Fatás	*Office Manager*	mfatas@unizar.es

TEM

Arenal, Raúl	*Researcher, ARAID Foundation*	arenal@unizar.es
Custardoy, Laura	*Sample Prep Technician*	lauracs@unizar.es
Fdez. Pacheco, Rodrigo	*TEM Technician*	pacheco@unizar.es
Ibarra, Alfonso	*TEM Technician*	aibarra@unizar.es
Magén César	*Researcher, ARAID Foundation*	cmagend@unizar.es
Mayoral, Álvaro	*Postdoctoral Researcher*	amayoral@unizar.es
Rodríguez, Luis Alfredo	*PhD Student*	luisaf85@unizar.es
Snoeck Etienne	*Head of TEM Area*	etienne.snoeck@cemes.fr

SPM

Arnaudas, José Ignacio	*Full Professor*	arnaudas@unizar.es
Cea, Pilar	*Associate Professor*	pilarcea@unizar.es
Ciria, Miguel	*Tenured Scientist, CSIC*	ciria@unizar.es
Coffey, David	*PhD Student*	dcoffeyb@unizar.es
de Miguel, Rocío	*PhD Student*	rociodmv@unizar.es
Díez José, Luis	*SPM Technician*	jlx@unizar.es
Gracia, Ana Isabel	*Researcher, ARAID Foundation*	aglostao@unizar.es

Marcuello, Carlos	*PhD Student*	cmarcuel@unizar.es
Martín, Carlos	*SPM Technician*	carmarsa@unizar.es
Martín, Santiago	*Researcher, Juan de La Cierva Program*	smartins@unizar.es
Moro, María	*PhD Student*	mmoro@unizar.es
Pascual, José Ignacio	*Head of SPM Area*	pascualj@unizar.es
Piantek, Marten	*Researcher, JAE-DOC Program, CSIC*	piantek@unizar.es
Serrano, Luis	*PhD Student*	serrale@unizar.es
Serrate, David	*Researcher, Ramón y Cajal Program*	serrate@unizar.es

DUAL BEAM

Casado, Laura	*Dual Beam Technician*	laurac@unizar.es
Córdoba, Rosa	*Dual Beam Technician*	rocorcas@unizar.es
Cuestas, Carlos	*SEM Technician*	cayllon@unizar.es
De Teresa, José Mª	*Head of DUAL BEAM Area*	deteresa@unizar.es
Goya, Gerardo	*Associate Research Professor*	goya@unizar.es
Irusta, Silvia	*Associate Research Professor*	sirusta@unizar.es
Marquina, Clara	*Research Professor, CSIC*	clara@unizar.es
Mtez. De la Fuente, Jesús	*Researcher, ARAID Foundation*	jmfuente@unizar.es
Pardo, José Ángel	*Associate Professor*	jpardo@unizar.es
Rivas, Isabel	*Clean Room Technician*	irivas@unizar.es
Sesé, Javier	*Associate Research Professor*	jsese@unizar.es
Simón, Gala	*Clean Room Technician*	gala@unizar.es
Tejero, Luis	*Technician*	tejero77@unizar.es
Torres, Teobaldo	*Dual Beam Technician*	teo@unizar.es
Valero, Rubén	*Clean Room Technician*	rvalero@unizar.es

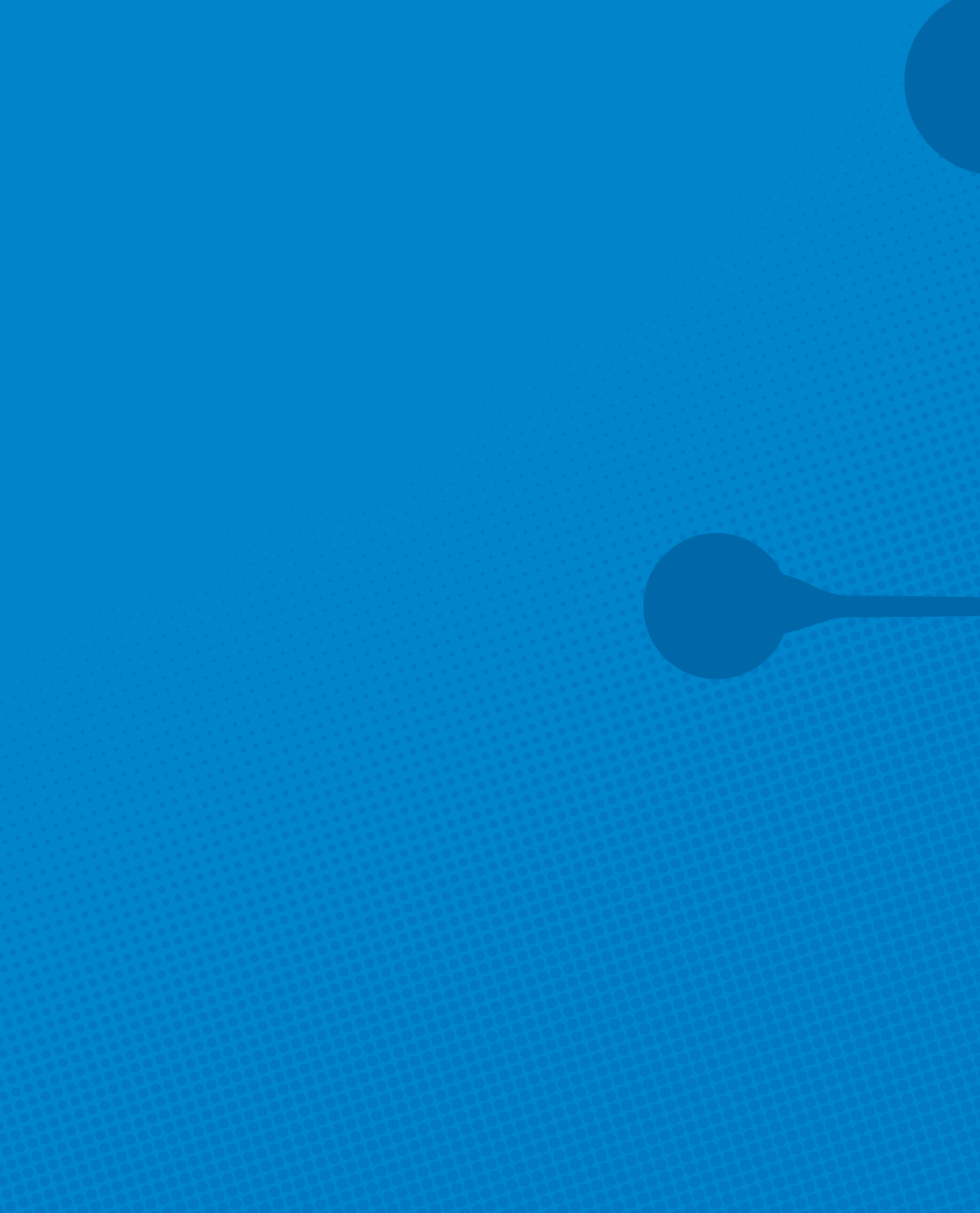

The Laboratories

The Laboratories

Transmission Electron Microscopy Laboratories (UHRTEM and HRTEM)

Researchers committed to the LMA project:

> Prof. Etienne Snoeck
> Dr. Raúl Arenal
> Dr. César Magén
> Dr. Álvaro Mayoral

LMA Technical Staff:

> Dr. Rodrigo Fernández-Pacheco
> Dr. Alfonso Ibarra
> MSc. Laura Custardoy

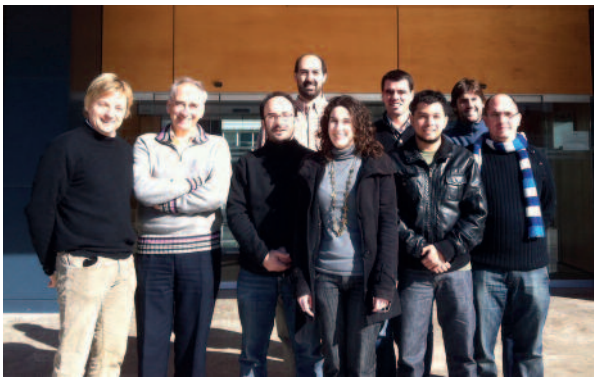

There are four TEM instruments available at the Transmission Electron Microscopy Laboratories, two being so-called "conventional" TEM within the HRTEM Laboratory, and two being Cs corrected microscopes of the very last generation at the UHRTEM Laboratory.

A) The high resolution transmission electron microscopy Laboratory (HRTEM) with two "conventional" TEMs

T20 – FEI microscope.

This 200 kV TEM equipped with a LaB_6 electron source, is fitted with a "SuperTwin®" objective lens allowing a point resolution of 2.4 Å. It is equipped with a 2K x 2K Veleta High speed CCD camera (Olympus) with a large field of view. This microscope, which is manly used for size and morphological studies of nano-objects, has been fitted with a cryo set-up allowing for the study of electron irradiation sensitive biological and inorganic materials at liquid Nitrogen temperature

F30 – FEI microscope.

This 300 kV Field Emission Gun (FEG) TEM is fitted with a SuperTwin® lens allowing a point resolution of 1.9 Å. This TEM can work in TEM and STEM mode. For Z-contrast imaging in STEM mode, it is fitted with a High-Angle Annular Dark Field (HAADF) detector. This TEM is equipped for spectroscopy experiments performed either in EDS (X-Ray Microanalysis) or in Electron Energy Loss spectroscopy (EELS). For the latter, it is fitted with the "Tridiem" Gatan Energy Filter (GIF). This EELS set-up allows Energy Filtered TEM (EFTEM) images to be recorded as well as line spectra or spectrum imaging experiments to be performed. A 2K x 2K Ultrascan CCD camera (Gatan) is located before the GIF for TEM imaging. In addition to these capabilities the F30 TEM

is also fitted with a Lorentz lens which permits the study of magnetic materials in an environment free of magnetic field (for magnetic domain imaging). Furthermore, the F30 allows tomography experiments to be performed both in TEM and STEM mode using a dedicated single tilt holder (+/- 70°) from Fischione.

B) The UHRTEM Laboratory with two "dedicated" Cs-corrected TEMs

A TITAN STEM microscope dedicated to EELS and STEM HAADF studies.

This Scanning Transmission Electron Microscope works either in TEM or in STEM mode at voltages between 60 kV and 300 kV. It then can be used at low voltage to analyse electron irradiation sensitive materials. It is fitted with the last generation of a high brightness Schotky emitter developed by FEI (the so called "X-FEG" gun) a monochromator and a Gatan 2k x 2k CCD camera.

STEM: As this microscope is devoted for STEM and EELS experiments, it is equipped with a CETCOR Cs-probe corrector from CEOS Company allowing for the formation of an electron probe of 0.08 nm mean size. The TEM is equipped with all the STEM facilities (BF, DF, ADF and HAADF detectors) and 0.08 nm spatial resolution has indeed been achieved in STEM-HAADF mode.

EELS and EDS: For EELS experiments, the microscope is fitted with a Gatan Energy Filter Tridiem 866 ERS and a monochromator. An energy resolution of 0.14 eV has been recently achieved with this setup. In addition, an EDS (EDAX) detector allows performing EDX experiments in scanning mode with a spatial resolution of about ~0.2 nm.

Lorentz and holography: Beside these analytical capabilities, the Titan STEM corrected microscope is fitted with a Lorentz lens and an electrostatic biprism allowing Lorentz and medium resolution electron holography experiments to be carried out in a field-free environment (as needed for magnetic materials studies). Tomography: In addition, a tomography set-up with a +/- 70° single tilt stage permits to perform 3D analyses either in TEM or STEM modes.

A TITAN^3 microscope dedicated to Ultra High Resolution TEM imaging

This TEM also works at voltages between 60 and 300 kV. It is located in a "box" (cube) to avoid mechanical and thermal perturbation (see figure). It contains a normal FEG (Shottky emitter) and a Gatan 2k x 2k CCD camera for (HR)TEM images acquisition.

HREM: As this microscope is devoted for High Resolution Transmission Electron Microscopy (HRTEM) studies, it is equipped with a SuperTwin® objective lens and a CETCOR Cs-objective corrector from CEOS Company allowing a point to point resolution of 0.08 nm.

STEM: In addition this Titan^3 is equipped with the basic STEM facilities (BF, DF detectors) for STEM imaging at medium resolution

EELS: a Gatan Energy Filter Tridiem 863 allows Titan^3 to perform EELS experiments in a standard and routine way (energy resolution of ~0.7 eV).

Lorentz and holography: As for the dedicated Titan STEM, beside these spectroscopy capabilities, the Titan^3 corrected microscope is fitted with a Lorentz lens and an electrostatic biprism allowing Lorentz and medium resolution electron holography experiments to be carried on.

C) Sample Preparation Laboratory

TEM is based in the use of transmitted electrons to form images of the materials. However, the electron is a strongly interacting charged particle and TEM samples are required to be extremely thin (tens of nm) to be electron transparent. Some materials are inherently electron transparent (nanoparticles, nanotubes…), but most of them (bulk materials, thin films, devices…) have much larger dimensions and it is frequently required to carry out a TEM sample preparation procedure to make them thin. The LMA has set the most advanced Sample Preparation Laboratory equipped with the necessary instruments to perform this task. Among the many procedures to produce electron transparent specimens, the most important and frequently used is based on mechanical thinning of the materials in a highly controlled way. This produces a flat specimen of a few microns thickness with defect-less surfaces that afterwards follows a low-angle, low-energy ion milling of the surfaces to achieve extremely thin areas ready for TEM observation. Nowadays, this task can be also performed in many cases by means of Focused Ion Beam (FIB) techniques in the DualBeam equipments available at the LMA providing large flat electron transparent areas selected with high accuracy, which is ideal, for instance, in the TEM sample preparation of nanodevices.

Sample Preparation Laboratory of the LMA.

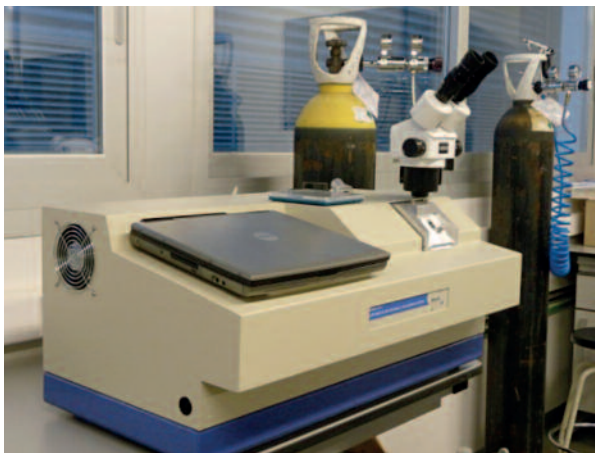

Ion mill equipment to obtain electron transparent areas in the samples for the TEM observation.

Research Lines

Study of nanosystems for physical or biological applications. The aim of the studies of these nano-objects is to establish correlations between the structures at the nanometer scale of these nano-objets with their functional properties. The line is closely connected to the two "Nanobiomedicine" and "Nanomaterials" research lines at INA. The systems being studied are magnetic and non-magnetic nanoparticles (metallic or oxide), semiconducting nanostructures, zeolite and mesoporous compounds. The TEM techniques involved in this research line are: Energy Electron Loss Spectroscopy (EELS) performed at the high spatial and energy resolution, High Resolution imaging in TEM (Q-HRTEM) and STEM (HAADF), and Tomography. These studies are performed on the two Titan G2 60-300 microscopes.

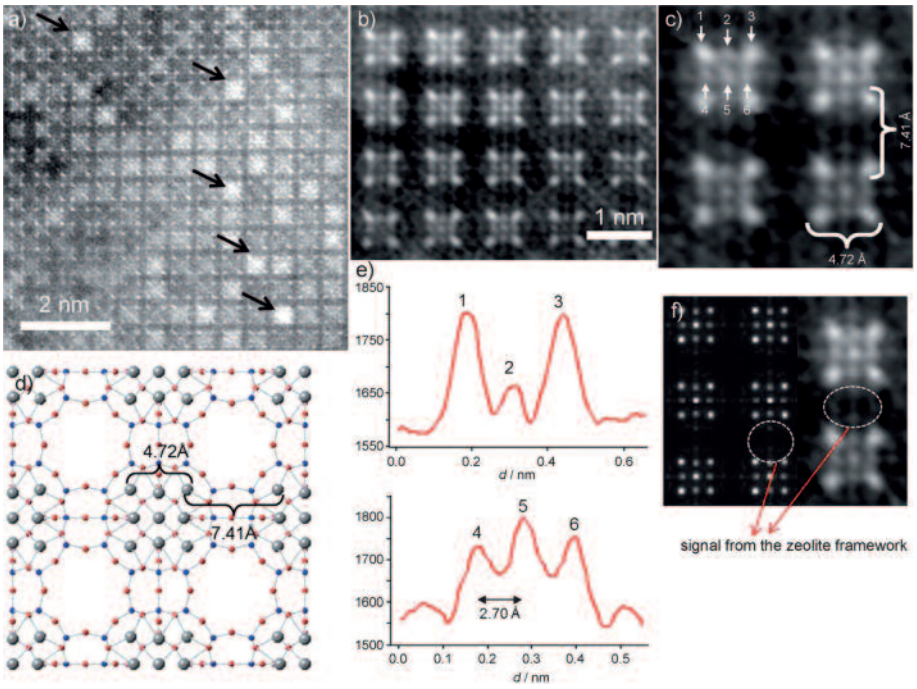

Aberration-corrected STEM-HAADF image of the silver zeolite A (AgA) along the [001] direction, where the white spots are single atomic columns and the black arrows point to Ag clusters in the alpha cages. b, c) Fourier-filtered images of the atomic distribution where the four columns of Ag at the corners of the sodalite cage are separated by 4.72 Å and each sodalite cage is separated by 7.41 Å; the Ag6 cluster is also observed in these cages. d) Proposed model with the Ag atoms in grey. e) Intensity profiles performed on the atoms marked as 1, 2, and 3 in (c) and 4, 5, and 6 with the interatomic distance between these atoms being 2.70 Å. f) Multislice STEM simulation along the [001] direction using 300 kV, Cs=0 mm, a defocus value of 0, a probe convergence semiangle of 24 mrad, and a collection angle of 70–200 mrad. The experimental image is shown alongside, and in both cases the zeolite framework signal is marked by white circles.

Study of interfaces in heterostructures. This activity is closely related to works carried out in the "Physics of Nanosystems" research line within INA. Our work addresses the structural properties (defects, epitaxy, strain) studied by Quantitative HRTEM and the chemistry and electronic structure of the interfaces investigated by the analysis of the EELS core loss fine structure of interfaces in thin films or multilayers either of 3d metals or in oxide (perovskite or spinel type). The TEM techniques involved in these studies are: Quantitative High Resolution TEM, STEM HAADF and Energy Electron Loss Spectroscopy (EELS) performed at the high spatial and energy resolution developed on the two **Titan G2** microscopes.

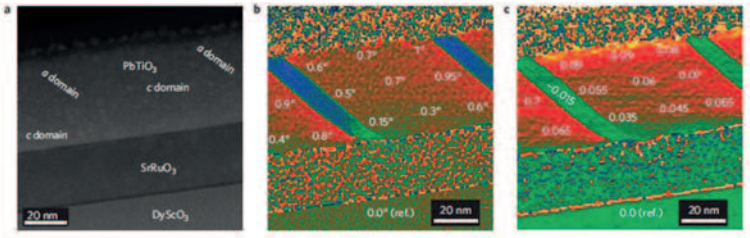

***Direct imaging of strain gradients from aberration corrected STEM images**. HAADF-STEM and GPA of the $PbTiO_3$ thin film grown on a $SrRuO_3$ buffer layer deposited on a $DyScO_3$ substrate and studied in cross-section. a, HAADF image, showing the structure. b, The map of lattice rotations shows that the upper layers are more relaxed, and therefore more inclined, than those close to the interface. c, The out-of-plane strain ezz (relative to the $DyScO_3$ substrate, c = 3:95 Å) shows a higher tetragonality in the right-hand side of the c-domain than in the left-hand side (obtuse). The difference arises from the local stress concentrations required to 'flatten' the interface of the ferroelastic film onto the substrate.*

Development of Electron Holography and Lorentz Microscopy. Electron holography allows recovering the phase of the electron beam that has interacted with a thin TEM sample. Measuring this phase shift gives information about the local electrostatic potential and magnetic induction within the sample and about the surrounding stray fields. Thus, it is possible to measure locally and quantitatively these internal fields with a resolution of few nanometers and map the electrostatic and magnetic potentials in and in the vicinity of the thin sample. Lorentz microscopy also permits the measurement of local magnetic induction on larger area but with a lower spatial resolution. In addition, information about the local strain within the sample can be obtained measuring the phase shift of diffracted beams in strained crystal. This can be done using the so-called Dark Field Electron Holography ("Holodark") method. It is then possible to locally correlate the structure and composition of a given materials or nanosystem to the fields (magnetic, electrostatic and strain) associated to a specific structure. For instance, this is of great interest in the study of the magnetic properties of magnetic nanoparticles or thin films used for magnetic or spintronic applications, or the effect of strain in electronic devices. The Lorentz microscopy and electron holography experiments are mainly developed on the Titan^3 microscope.

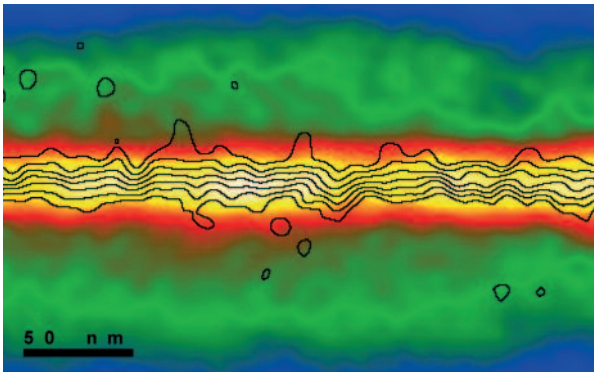

Electron Holography on a 8.6 nm thick and 30 nm wide Co-nanowire deposited by FEBID: Electrostatic and magnetic contributions to the electron beam phase shift: The magnetic flux is superimposed over the electrostatic phase shift image.

Within the TEM activities on magnetic and spintronic nanosystems, a particularly important topic deals with the "in-situ" experiments. Most of the electron holography and Lorentz experiments on magnetic materials are performed in the remnant state, while it is of great interest to study the magnetic device in more realistic conditions, i.e. under the application of an external magnetic field or even when an electric current flows through it. In that sense, a research project is underway to study the dynamics of magnetic domains under the application of on an external magnetic field or due to the spin torque effect of a polarized current either by electron holography or Lorentz microscopy. The aim is to study the influence of local defects, interfaces, constrictions, etc… on the nucleation processes and propagation of magnetic domain walls at the nanometer scale on nano-objects. These "in-situ" experiments are mainly developed on the Titan^3 microscope and partly on the F30 using the Lorentz capabilities of these two microscopes

Plasmonics. Works are focused on the low-energy excitations, involving holes and electrons in valence and conduction bands, as well as collective modes of conduction electrons (plasmons). Thus, it will concern nanophotonic aspects. Such kind of studies are now possible due to the improvement of the energy or spectral resolution obtained using the monochromators in the TEMs. The capabilities of the probe corrected and monochromated Titan G2 in terms of energy resolution combined to the spatial resolution permit the study of the optical response of nanomaterials (in the spectral range between 0.5 to 5 eV). It is aimed to study the optical properties of metallic nanomaterials focusing on the dependence of the plasmonic excitations with the size and shape of the nano-objects. In a second step, the plasmon interactions between neighboring objects will be addressed. Such studies will be carried out in spectroscopic experiments both in EELS and also in Energy Filtered imaging mode (EFTEM).

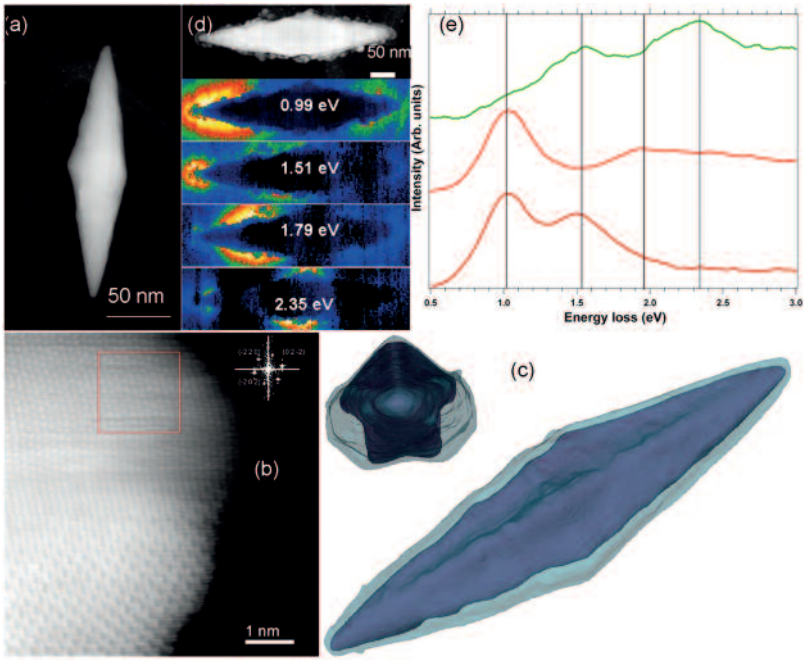

(a) HAADF image of Au-Ag NP. (b) HR-HAADF image of the tip of the NP, corresponding to Ag shell. (c) 3D modeling of one of the NP obtained from a HAADF-STEM tomogram showing the morphology of the NP and bi-pyramidal structure type core-shell (Au-Ag). (d) Spectrum-image (SPIM) acquired one of these Au-Ag NP and the spatial distribution of their excited surface plasmon resonances (SPR). (e) Spectra extracted from this SPIM at different regions corresponding to different SPR.

Study of carbon-based and heteroatomic (based on boron and/or carbon and/or nitrogen) nanostructures such as nanotubes (NT), nanodiamond, and graphene. Electron microscopy is an essential and powerful technique for studying these nanomaterials at the (sub)nanometer scale. The use of HRTEM, electron diffraction and EELS techniques provide very rich information not only about their atomic structure and configuration, but also about their physical and chemical properties. Understanding the growth mechanism of these nanostructures is of particular interest in order to improve their production not only quantitatively but mainly in a controlled way, having access to a particular kind of nano-object. Furthermore, the atomic configuration of these nano-structures, as well as their electronic and chemical properties, is also investigated. These studies are carried out in the two **Titan G2** which both allow working at low voltages (60, 80 kV) with the highest resolution achievable. That is a major advantage of the LMA for the study of such materials sensitive to electron irradiation.

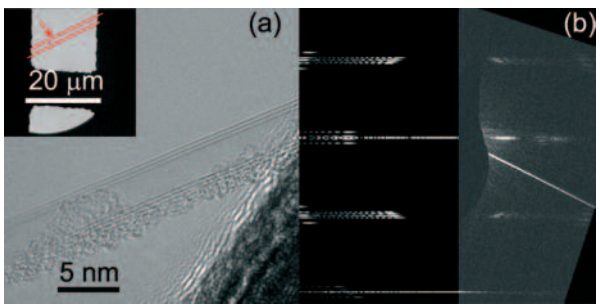

(a) HRTEM image of a triple-walled (TW) carbon nanotube (inset: low-magnification micrograph of this NT). (b) Experimental and simulated electron diffraction patterns (EDP) of this TW-NT, respectively. These EDP are unambiguously assigned to a (21, 21) @ (28, 26) @ (36, 29) NT.

Laboratories for Local Probe Microscopy

Researchers committed to the LMA project:

> Prof. José Ignacio Pascual
> Prof. José Ignacio Arnaudas
> Prof. Carlos Gómez-Moreno
> Dr. Pilar Cea
> Dr. Miguel Ciria
> Dr. Ana Isabel Gracia
> Dr. Santiago Martin
> Dr. Marten Piantek
> Dr. David Serrate

LMA Technical Staff:

> Dr. José Luis Díez
> D. Carlos Martín

The available facilities in the SPM section of the LMA are composed by seven SPM equipments combined in three different laboratories:

A) Low-temperature, ultra high vacuum (UHV-LT) probe microscopy Laboratory

The laboratory of UHV-LT is specifically designed for surface science microscopy and spectroscopy methods. The aim is to cover a wide variety of problems in surface science, from molecular chemistry to atomic magnetism. Three systems are equipped with different preparation techniques under UHV conditions, as well as equipped with large variety of epitaxial growth facilities. Force- and Tunnel-based methodologies can be combined, allowing to investigate substrates with different electronic properties. The accessible temperature range for experiments is from 0.5 K to 1300 K.

Ultra low Temperature STM with axial magnetic field and variable temperature SPM.

This equipment is specifically oriented to investigate atomic scale magnetism and to high resolution spectroscopy of molecules and atoms, as well as to study the dynamics of atoms and molecules as a function of temperature. It includes two UHV STMs, one of them running at a base temperature of 1K (possibly extended down to 0.5K by using He3 as refrigerating liquid) and a variable temperature STM (from 100 K to 1300 K), with a fast and flexible measurement approach. Two chambers connected to the STMs but with independent vacuum allow the preparation of samples in situ and the epitaxial growth of organic and inorganic ultra-thin films on surfaces. The details of the equipments are the following:

> **Low T STM #1:** Joule Thomson cryostat (1K-10K) UHV-STM; 3 T axial B field. Metal and organic epitaxy *in situ*.

> **Variable T STM/AFM:** Aarhus variable temperature (100K-1300K) STM, Non-contact-AFM.

> **Preparation:** LEED/Auger characterization facilities; 9 Molecular Beam Epitaxy pockets (5 of them with fast reload option), 1 effusion cell.

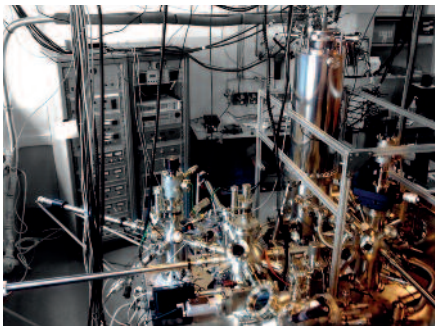

Low Temperature STM in UHV.

This equipment is oriented to investigate metal-on-metal epitaxy of rare earths. It is specially oriented to the growth of magnetic thin films and nanostructures. The equipment runs at a base pressure of 4 K and has been optimized to deposition of rare-earth metals on tungsten substrates.

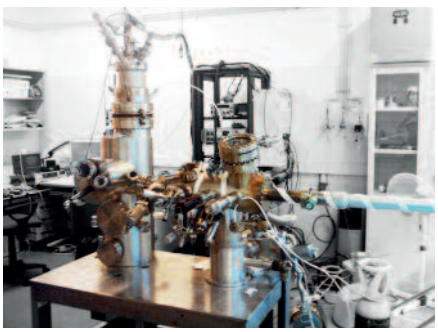

> **Low T STM #2:** Low temperature (5K) UHV STM.

> **Preparation:** Metal epitaxy, and LEED/Auger characterization facilities.

Low temperature STM/AFM in UHV.

This set up includes the last development in UHV non-contact AFM. Working at a base temperature of 5K, the use of a qPlus sensor allows to simultaneously acquire local tunneling and force spectroscopy. Measurement of both forces and conductance is especially interesting in the field of molecular physics on surfaces. Force microscopy is also especially suitable to work on isolating surfaces. This experimental set up has been equipped with various methods to deposit organic materials on inorganic surfaces. The research lines are oriented to molecular interactions, self-assembly and magnetic, electronic and structural properties of hybrid metal-organic films.

> **Low T STM/AFM:** Low temperature (5K) UHV STM equipped with a qPlus sensor allows to correlate resonance frequency shifts of a quartz tuning fork with the gradient of forces between tip and sample.

> **Preparation:** Metal epitaxy, and K-cell of sublimation of organic materials.

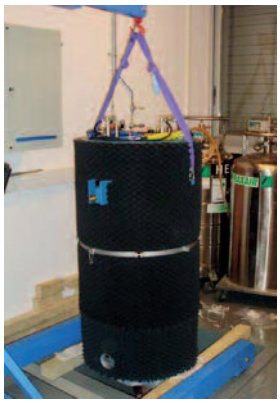

B) Laboratory of high magnetic fields

The laboratory of high magnetic fields offers the possibility of combining probe measurements (AFM, MFM, STM) with ultra-low temperatures and a high vector magnetic field. It is composed of one single equipment: a variable temperature (2K-300K) STM/AFM/MFM in a large-bore insert, inserted into a superconducting electromagnet reaching 8T/2T vector magnetic field. The equipment has a quick load facility, allowing mounting a new sample and measuring in just a couple of hours. Additionally, a Variable Temperature module allows one to continuously change the temperature from 2 K, its lowest temperature, to 300 K. The laboratory is especially suitable for combination of local probe inspection with electrical magneto-transport measurements as, for example, scanning gate microscopy. Therefore, it runs research lines oriented towards low temperature magnetism, transport through nanodevices and spintronics.

Several characteristics of this equipment are the following:

–AFM/MFM head with interferometric sensor.
–STM/Tuning Fork head
–Variable temperature insert (1.5K-300K) cryostat.
–8 T (vertical) and 2 T (in-plane) superconducting magnet, combined to a rotating platform allows to apply vector fields in three dimensions.
–Compatible chip carrier with dual-beam and pulsed field facilities.

C) Laboratory of probe microscopies in environmental conditions

The biology, chemistry and physics community, all of them potential users of the SPM facilities, demands a set of microscopy tools with large versatility and able of working under different environmental (more real) conditions. The laboratory of probe microscopy in environmental conditions collect force and tunnel microscopies that allows a quick investigation of samples in liquid, electrolytes, or in atmosphere with controlled humidity and/or composition.

Atomic Force Microscopy

AFM is a key technique in Nanosciences, supporting multidisciplinary activities. Hence it is a central facility in the LMA. A special room with outstanding vibration isolation stages is dedicated to hold the equipments. In addition, a highly specialized technical scientist is in charge of the support to external users, training of frequent and experienced users and maintenance of the equipments. The equipments stand for their completeness. Measurements can be performed under different conditions like liquids, electrolytes, or atmosphere with controlled level of humidity. They can perform high sensitive Force spectroscopy and working under magnetic field in the Magnetic Force Microscopy mode.

Equipments:

(1) *Cervantes Fullmode SPM* from Nanotec Electrónica S.L. AFM/MFM/STM equipped with variable magnetic field and liquid cell.

(2) *Multimode 8* from Veeco-Bruker. SPM equipped with KPM, conductive AFM, liquid and electrochemistry cells, PicoForce module for force spectroscopy measures, and variable temperature.

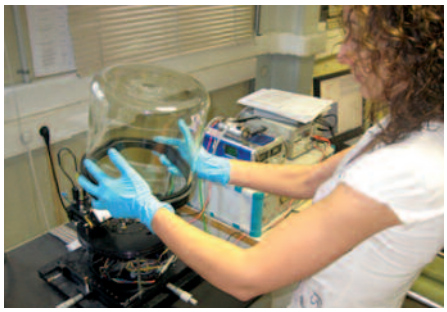

Cervantes Fullmode SPM from Nanotec Electrónica

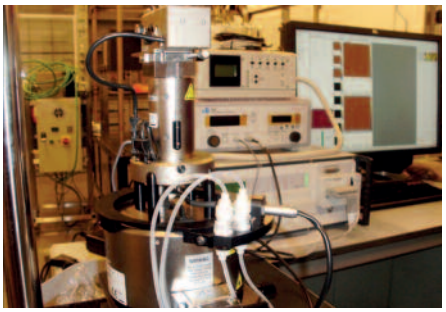

Multimode 8 from Veeco-Bruker

Research lines

The research lines performed within the SPM area are framed in the fields of Physics, Chemistry and Biology, with strong focus in Nanoscience.

Supported by the strong background in magnetism both at INA/UZ and ICMA in Zaragoza, an important goal is to explore its limits at the atomic scale. In this sense, the low temperature UHV facilities provides the possibility of growing magnetic nanostructures (nanowires, atomic chains, quantum corrals) and resolve magnetic information at the atomic scale.

In addition, the new tools will also allow the establishment of new initiatives, indeed new in Zaragoza. In relation with biology, the focus is centered on using force spectroscopy to resolve intermolecular forces that govern recognition between biomolecules. This approach can be also extended down to the atomic scale with a newly developed method, the qPlus sensor STM, which allows to measure and quantify weak interaction forces between single molecular groups. Furthermore, a constitutive interest is being developed in exploring the fundamental properties of electronic transport through individual molecules and through molecular self-assemblies. The goal is to identify molecular-active channels, and the related charge quantization effects, that may be extended to molecular-based electronic devices. In this sense, the use of an electrolyte as an external gating is more than an attractive endeavor.

More specifically, the research lines are structured as follows:

Magnetism on surfaces – Spin Polarized STM

Atomic magnetism and manipulation. The unique capability of STM techniques are being exploited to alter the matter in the atomic or molecular scale with simultaneous electronic and magnetic characterization with atomic resolution. Recent developments on this field point to the possibility of downscaling stable magnetic moments to the scale of a single atom or artificial nanostructures constructed in an atom-by-atom fashion. The profound implications in magnetic data storage lead this research line to pursues a pioneering understanding of low

dimensional magnetism using single atomic spins as building blocks of our sample system.

Experiments are being conducted to explore interactions among neighboring atoms. The magnetic playground which enables a direct control of the atomic spin is the combined action of magnetocrystalline anisotropy, quantum fluctuations, and various exchange interactions with the substrate. Investigations address atomic nanostructures, constructed through controlled atomic manipulation, and magnetic adatoms deposited on ultra-thin insulating thin films, acting as spacers between adatom and substrate.

A particular challenge is using atoms with large values of the intrinsic magnetic anisotropy (large spin orbit coupling) in the fabrication of magnetic structures formed by simply a few atoms. The adsorption and manipulation of rare-earth adatoms on the W(110) surface are being explored. The electronic state of the free ion is expected to be retained at the single atom scale, offering the possibility to study the magnetism of a lanthanide with 13 electrons in the f shell.

Rare earth nanostructures. The goal of this line is the study of the competing interactions (dipolar, elastic, electronic,…) that are responsible for the self-organization of metal-on-metal systems, with special emphasis on rare earth adatoms. The so-created self-organization may give rise to individual atom arrays, as well as to extended nanostructures with different dimensionality, depending on the specific preparation procedure. These systems can be therefore envisaged to have an interesting outcome of quantum size effects in the electronic and magnetic properties of such nanostructures, with the goal of raising the superparamagnetic limit by tuning the shape of the magnetic nano-object at the atomic length scale.

The preparation procedure of materials is characterized well below the monolayer, which becomes important in order to obtain long-range self organized materials instead of an assembly of defective polycrystalline arrays of nanoparticles. Current investigations focus on rare earths deposited at room temperature on W(110), well below one monolayer. W(110) is particularly interesting because it provides a structural anisotropy, steering the growth of one dimensional metal systems.

Molecular Science on surfaces:

SUPRAMOL. The goal of this research line is to investigate the assembly of organic and metal-organic networks on surfaces mediated by coordination as well as covalent and non-covalent interactions. A deep understanding of the growth-controlling mechanisms can be used to develop new fashions in bottom-up technology that allows the fabrication of new functionalized materials. In collaboration with organic chemistry groups at the University of Zaragoza, several strategies of supramolecular chemistry, known to be effective in solution, will be explored on inorganic surfaces.

MOLMAG. The goal is the control of the molecular magnetism of single metal-organic molecules on inorganic surface. The influence of the substrate on different molecular

model systems by means of STM and qPlus-AFM at low temperatures is therefore investigated. Beyond the basic understanding of the interaction mechanisms, a targeted implementation of those compounds into a purposive host matrix will open the way towards new functionalized materials.

Nanodevices, transport and spintronics:

SPINTRONICS. The goal of this research line is to identify active transport channels in nanometer-size devices grown on electrical gates, their spin polarization and their electrical properties as a function of the magnetic state. There is a close collaboration with the FIB/SEM area to produce nanowires, dots, rings, flakes,… using the existing nanodeposition facilities, to contact them with three terminals and inspect the transport characteristics with the local probe devices. It is expected to identify spin channels and accumulation at interfaces, to observe thermo magnetic transport properties and, in general, to map in space magnetic and electrical response to external actions in three terminal devices.

Nanobiology and new nanobiomaterials:

Molecular recognition. The goal is the measurement of the intermolecular forces that govern the recognition processes between biomolecules using force spectroscopy. By careful analysis of the breaking force at various pulling speeds, it is possible to map the energy landscape of the chemical bond under mechanical force. This leads to interesting results in the study of antibody-antigen, protein-protein, protein-DNA and even protein-living cell interactions at the single-molecule level. Works are also underway in the analysis of different biological processes under relevant physiological conditions using AFM imaging to know the models of binding and estimate parameters on the formation of the complexes.

Ferritin-based nanomaterials. Preparation of nanoparticles in the cavity of the protein ferritin. These nanomaterials are used as a model for studying the physical properties at very low temperatures of particles with a size intermediate between the atom and the macroscopic magnets. These NPs can be applied to the area of biomedicine.

Dip-pen nanolithography (DPN). This is a scanning probe lithography technique where an AFM tip is used to directly transfer reagents to a surface via a solvent meniscus. DPN is used to organize a great variety of molecules and particles on different surfaces with nanoscopic resolution. Ferritin containing nanoparticles are being positioned in the most sensitive areas of new microsensors to explore the signal of a few NPs, and nanostructuring these materials for the study of their properties on surface.

Transport in and through molecular films:

Molecular electronics. The incorporation of molecules into electronic nanoscale devices requires the development of sophisticated techniques and robust protocols for wiring them into addressable arrays, as well as methods for measuring and controlling their

electrical properties. Research is focused on understanding the influence of molecular structure and assembling process of materials on the electrical characteristics at the molecular scale.

Transport properties of molecular junctions are being characterized by using bottom-up methods driving molecular self-assembly and Langmuir-Blodgett techniques, combined with SPM methods.

The conductance properties of a molecular junction depend not only on the molecule(s) themselves, but also on parameters like the nature of the electrodes' material, the detailed contact geometry (i.e., hybridization at the molecule-electrode interfaces), the temperature and the local environment of the system (vacuum or air, solvent, etc.). There is particular interest in studying the different types of organic-metal contacts as well as in controlling the conductivity of the molecular assemblies by tuning the oxidation state of redox end groups or the spin state of magnetic moieties.

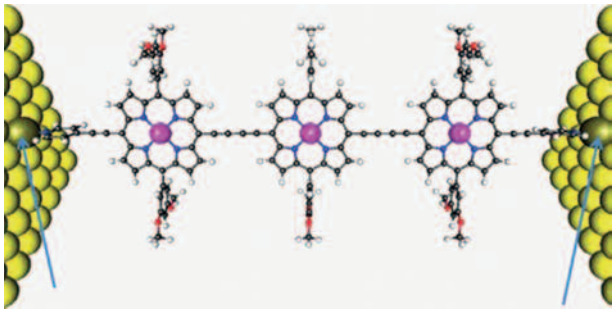

Schematic representation of the butadiyne-linked trimer between gold leads, when the porphyrin rings lie in one plane. Axial ligands (pyridine) binding to the Zn centres are also not shown (these inhibit aggregation of the molecules and are observed to promote the formation of Au | oligoporphyrin | Au junctions in the STM experiments). The terminal N atoms are bonded to gold adatoms on each electrode surface (A–A configuration). Atom colouring: C, dark grey; H, light grey; N, blue; O, red; Zn, pink; Au, yellow.

DUAL BEAM Laboratories

Researchers committed to the LMA project:

> Prof. José María De Teresa
> Prof. Clara Marquina
> Dr. Gerardo Goya
> Dr. Jesús Martínez de la Fuente
> Dr. Javier Sesé
> Dr. Silvia Irusta
> Dr. José Ángel Pardo

LMA Technical Staff:

> Dr. Guillermo Antorrena
> MSc. Rosa Córdoba
> MSc. Laura Casado
> MSc. Teobaldo Torres
> MSc. Carlos Cuestas
> MSc. Rubén Valero
> MSc. Gala Simón
> MSc. Isabel Rivas

Dual Beam Laboratory in Clean Room

Helios 600 dual beam equipment installed inside the Clean Room of the INA building.

In the Clean Room facilities of the institute, several lithography facilities permit to pattern structures at the micro- and nano-meter scale and to create devices. In particular, the two dual beam equipments assigned to nanolithography and lamellae preparation are placed on two concrete platforms inside the 125 m^2 10000-class Clean Room. The first dual beam equipment is the Helios 600 model and has been working since December 2009 at the same place. It consists of a 30 kV field-emission scanning electron column and a 30 kV Ga focused ion beam placed at 52º one from each other. The ion column is able to work properly at low voltage (5 kV and lower), allowing the preparation of lamellae with low ion damage. Thus, in this equipment 54 lamellae have been prepared in 2011 by the technical staff, with high enough quality for atomic-resolution TEM imaging. In this equipment, there are five gas injectors as well, allowing the growth of nanodeposits with high resolution. In this equipment it has been possible to grow W-based superconducting nanodeposits with lateral size of 40 nm and Co-based ferromagnetic nanodeposits with lateral size 30 nm, these ultranarrow dimensions being at the forefront of the research in these topics.

Helios 650 equipment installed inside the Clean Room of the INA building.

The second dual beam inside the Clean Room was installed in December 2010 and the model is Helios 650. Such a model is an improved version of the Helios 600 one. Thus, the SEM column has resolution of 0.9 nm and it bears a monochromator and beam deceleration. The FIB column is differentially vacuum-pumped at the lowest part, allowing a well-defined beam profile impacting on the sample surface. Preliminary results with such a column indicate that ultranarrow nanodeposits can be grown. This FIB column is nicely suited for lamellae preparation too, in combination with the Omniprobe nanomanipulator. The equipment has got 5 gas injectors and electrical microprobes. This equipment is expected to work properly for the requested main tasks: lamellae preparation and nanolithography based on ion patterning, electron beam lithography and nanodeposition.

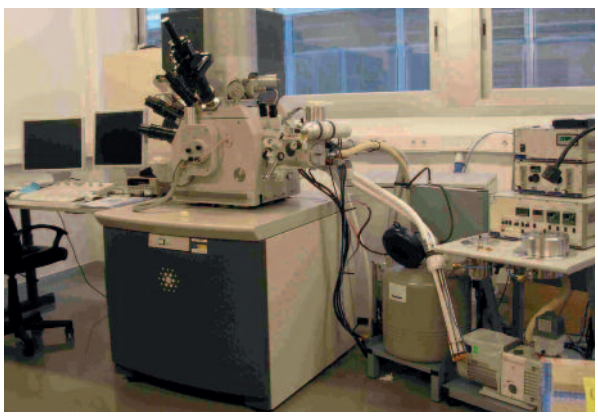

Nova 200 dual beam equipment and the cryo-transfer setup, installed at INA building

Life Sciences Laboratory

The third dual beam equipment is used for life sciences and has been installed in the same room as the environmental SEM and the field-emission SEM. The third dual beam is based on the Nova 200 model (existing in our laboratory since November 2006) but upgraded with a cryo-transfer chamber. This equipment has worked properly since 2007 and in combination with the cryo-transfer set-up is being used to produce series of ion-cuts of cells embedded in resin or frozen with the help of liquid nitrogen. These images will be used to produce 3-dimensional reconstructions. Appropriate software for 3-dimensional compositional reconstructions based on energy-dispersive x-ray micro-analysis is also included in this equipment. If needed, the equipment also holds an Omniprobe nanomanipulator for lamellae preparation as well as 5 gas injectors.

An environmental SEM, model Quanta 250, is installed in the same room as the Nova 200 dual beam. The SEM column allows beam deceleration, which permits to keep resolution of 1.4 nm even at 1 kV electron landing voltage. The Quanta equipment can work under three different pressure ranges, the maximum pressure being 4000 Pa, thus close to ambient pressure. This allows observation of life-sciences samples without previous metallic coating. The equipment allows the use of a Wet-STEM, which permits to inspect samples with controlled humidity, this being crucial in life-science samples in order to maintain the same conditions as hold when functional. The equipment can also use a heater to perform observation on samples heated up to 1000 Celsius degrees.

Environmental SEM, Quanta FEG 250 equipment, installed at the INA building

Field-emission SEM, INSPECT equipment, installed at the INA building

The last SEM equipment, the Inspect model, is a general-purpose field-emission SEM for high-resolution imaging and composition analysis by energy-dispersive x-ray microanalysis.

Laboratory of Microstructural Characterization and Spectroscopy

The XRD and the XPS-AES equipments are installed in the room devoted to microstructural and spectroscopy sample analysis. Those equipments have been working since 2006 and providing a great variety of useful results for most of the research groups at INA and other centres and companies mentioned later. In the following, the main characteristics of these equipments are mentioned:

XRD (Bruker D8 Advance, four-circle diffractometer).

- Copper anode.
- Eulerian cradle.
- Parallel-beam optics.
- Incident- and diffracted-beam monochromators.
- Scintillation counter and 2D detector (GADDS).
- Analysis software and database.

XPS-AES (Kratos):

- Analysis chamber with base pressure < 10^{-9} Torr
- Multi-detector energy analyser and 2D image in parallel
- Monochromator
- Ar ion milling
- Electron gun for AES
- Charge neutralizer
- Sample holder for 4-axis high-precision displacements

XRD (left image) and the XPS-AES (right image) equipments, installed at INA

Research lines

Several researchers from the local research institutes (INA and ICMA most frequently) develop a wide variety of research lines using the dual beams, environmental and high-vacuum SEM, XRD and XPS-AES equipments. Hereafter, a brief summary of those research lines are included:

The dual beam equipments inside the Clean Room are involved in the development of the following research lines:

- Lamellae preparation for subsequent TEM investigation of their physical and chemical properties. This activity is significant as there are many situations in which one needs to analyze with high precision the physical and/or chemical properties of a small part of one material/sample. This activity is frequently requested by many researchers belonging to different research groups, especially those working directly on TEM research and Thin Film Growth.
- Nanoelectronics and Spintronics based on 2-dimensional systems such as graphene and ultrathin bismuth films, with high carrier mobility and long spin diffusion length. The aim is to fabricate nanodevices with new or improved functionalities in terms of signal output, power consumption, integration, etc.
- Magnetic nanostructures based on cobalt grown by focused electron beam induced deposition for applications in magnetic domain wall manipulation for information storage and magnetic logic and Hall sensors for magnetic sensing.
- Superconducting nanostructures based on W nanodeposits grown by focused ion beam induced deposition for spectroscopic studies, finite size effects and vortex-based fluxtronics. These W nanodeposits have been found to be an ideal system to study the physics of vortex lattices in combination with Scanning Tunnelling Microscopy.
- Nanocontacts for giant magnetoresistance, Andreev reflection studies and nanoelectronics. These nanocontacts have been grown so far using thin films or nanodeposits with ferromagnetic or superconducting properties.
- Magnetic properties of antidot networks fabricated by electron beam lithography and focused ion beam.
- Fabrication of nanocalorimeters for magnetic refrigeration with molecular magnets.
- New superconducting SQUID sensors for ac susceptometry and study of qubits in the mK range.

- Tailored magnetic anisotropy in epitaxial magnetic heterostructures after nanolithography.
- Magnetotransport in nanowires lithographied out of epitaxial magnetic thin films.

In the equipments concerning life science dual beam and environmental SEM, the following research lines are currently being developed:

- Thermosensitive hidrogels based on dendritic macromolecules derived from Pluronic®. These systems are interesting for tissue regeneration.
- Supramolecular hidrogels based on glicolipids modified with photosensitive groups. These systems are interesting as carrier agents sensitive to light stimulii.
- Studies of hyperthermia using magnetic nanoparticles. Currently, dendritic cells are being cultured with magnetic nanoparticles for Trojan horse approach to cancer treatment.
- Efficient biosensing using different strategies for the biofunctionalization of metallic nanoparticles and the chemical modification of enzimes and proteins as recognition reagents.
- Nanotherapy using multifunctional biofunctionalized nanoparticles. By using inorganic nanoparticles and organic ligands biologically active, research focuses on cancer therapy.
- Morphology and metastructure resulting from the interaction between cells and nanoparticles, with applications in neuron regeneration, magnetotransfection, magnetic hyperthermia and controlled drug delivery.
- Nanoparticle internalization inside vegetal cells for basic studies of transport in plants as well as studies of advanced treatments on plants.

The XRD equipment is mainly used by researchers growing epitaxial thin films in the following applications:

- High-resolution diffraction, X-ray reflectivity, texture
- Magnetic thin films and heterostrucutres for applications in spintronics
- Multiferroic thin films
- Thermoelectric thin films and films showing spin-Seebeck effects
- Magnetic multilayers with tailored magnetic anisotropy

The XPS equipment is mainly used in the following research lines :

- Mixed matrix membranes used for gas separation.
- Guest molecules in zeolitic materials used for the adsorption of light hydrocarbon and olefin/paraffin separation.
- Labeling of nanoparticles to study the nanosafety in work environments.
- Polymeric nanocomposites with enhanced thermal properties.
- Nanoparticles synthesized by conventional and microwave heating used as catalysts in microreactors.
- Zeolitic based cantilevers for the detection of contaminants in the ppb order.

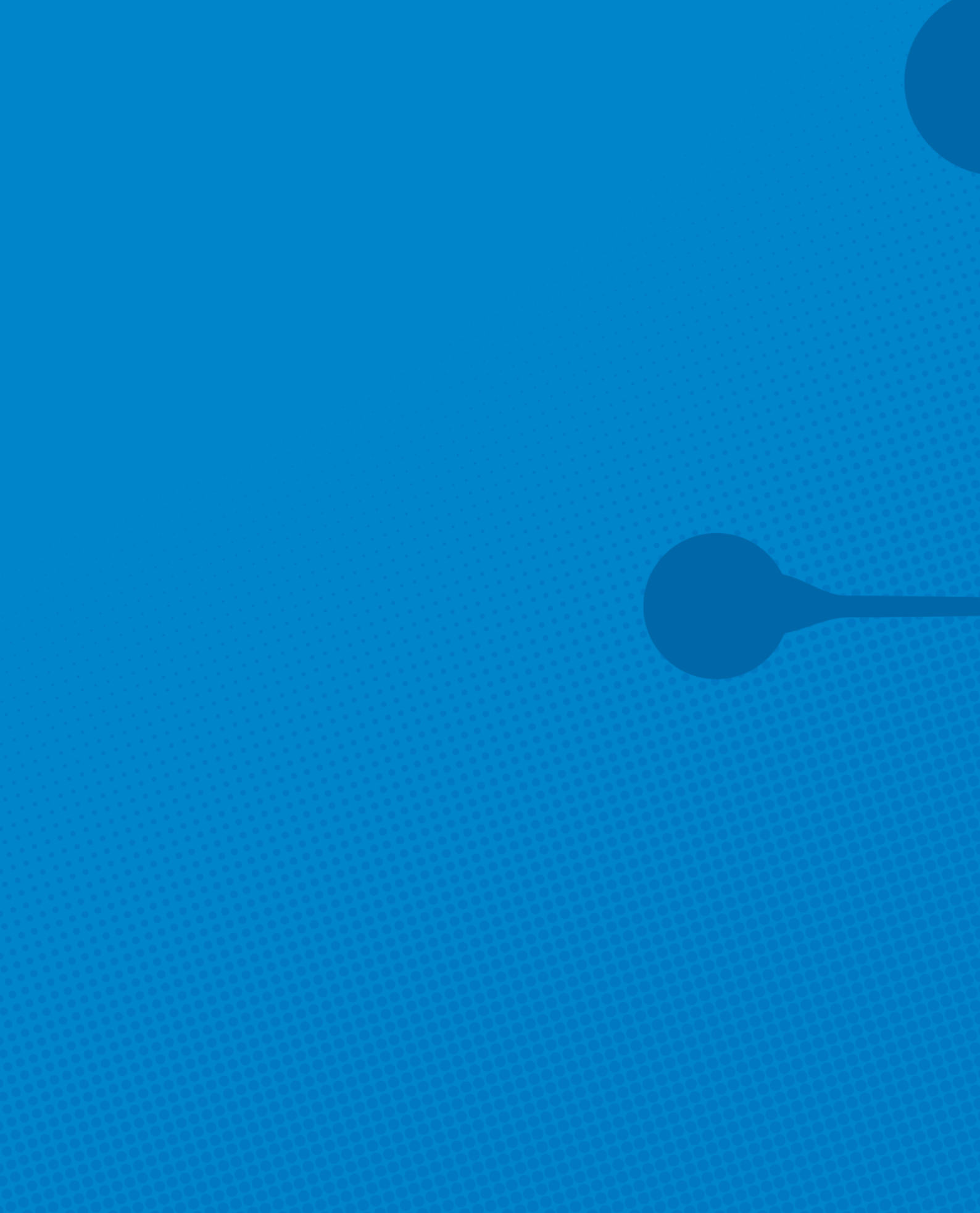

Scientific Activity

Main results

Core-shell magnetic nanoparticles for bio-applications: Magnetic nanoparticles are very suitable for a broad range of applications, like the synthesis of ferrofluids, data storage, catalysis, as solid supports for biomolecule immobilization, and in bio-applications in general. They have become one of the leading research lines at INA. In particular, magnetic iron oxide nanoparticles are amongst the most commonly targeted because they are biocompatible and their size and magnetic behavior can be tailored to obtain ferrimagnetic to superparamagnetic, which makes them suitable for a wide range of biomedical and biotechnological applications, like magnetic separation of biomolecules, magnetic fluid hyperthermia, magnetic resonance imaging and targeted delivery of bioactive molecules. However, further oxidation of the magnetite can result in a degradation of the magnetic properties, so the magnetic core has to be coated with an organic or inorganic material to form a protecting shell. This is also advantageous to avoid the aggregation of the particles due to the large surface-to-volume ratio and therefore to their high surface energies, or due to dipolar magnetic interactions.

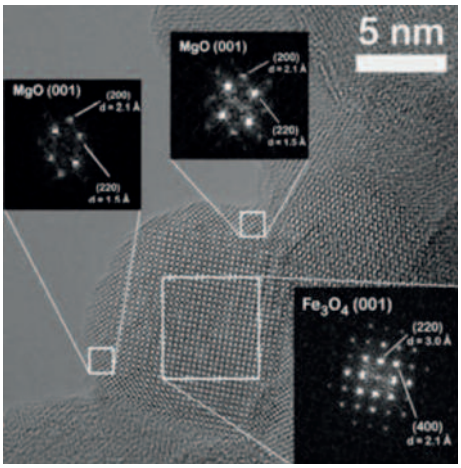

Aberration corrected HRTEM image of a magnetite nanoparticle epitaxially coated by a 1-nm-thick MgO layer. The insets show the FFT calculated from the areas marked with white squares.

The TEM laboratory at the LMA has contributed significantly to the development of new methods and the optimization of synthesis process to produce functional magnetic nanoparticles suitable for bio-applications. The figure illustrates one of the most significant results, in which a new strategy to combine co-precipitation and sol-gel methods have been developed to produce very small superparamagnetic magnetite nanoparticles coated with ultra-thin MgO coating to protect them from oxidation and agglomeration. Only aberration corrected HRTEM in the Titan^3 is capable of unambiguously resolving the ultra-thin layer of MgO that covers the particle, as the images are corrected for spherical aberration and not only the spatial resolution is improved but also delocalization phenomena at the interfaces is minimized

Flexoelectricity in ferroelectric thin films: simultaneous mapping strain and electric polarization: There is an intrinsic coupling between strain and electrical polarization in ferroelectric thin films, the well-known piezoelectricity, which allows functional optimization of polarization by strain engineering with an adequate choice of substrate. Only recently the important role of *strain gradients* coupled with polarization via flexoelectricity has been highlighted. Flexoelectric effects are large at the nanoscale because the size of the strain gradients is inversely proportional to the relaxation length –and hence to the sample size. Small local changes of atomic positions in the range of several pm can have a large impact on strain and electric polarization, so precise experimental structural investigations of the local strain and polarisation distribution are required to check theoretical models for domain wall configurations and to understand the ferroelectric properties.

It has been carried out for the first time the mapping of the elastic strain inside twinned epitaxial $PbTiO_3$ films by aberration corrected HAADF-STEM together with an analysis of the local

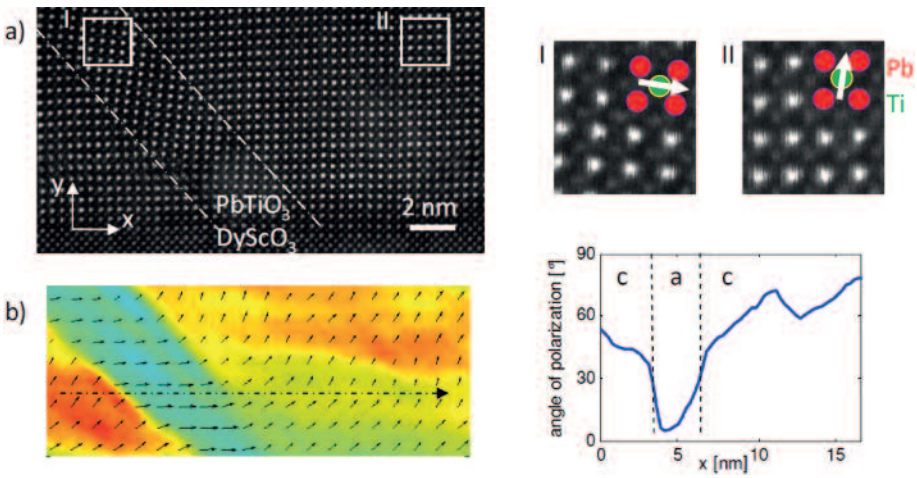

a) HAADF-STEM image with zoom-in showing the a-domain (I) and c-domain (I) atomic column arrangement with the TiO column shifted off-center along the direction of polarization. b) Out-of-plane strain (color map) and electric polarization (vector map). The map confirms the strain difference between acute and obtuse corners and reveals the existence of polar rotations in the c-domains, which are quantified in the line scan

orientation of polarization by measuring the relative displacement of the Ti atoms. As illustrated in the figure, strain gradients have been observed both in the vertical and in the horizontal directions and, more importantly, it is shown that flexoelectric interactions result in a rotated polarization vector associated to those gradients with a magnitude comparable to that of the ferroelectric polarization which is the first direct evidence of the local flexoelectricity in such materials.

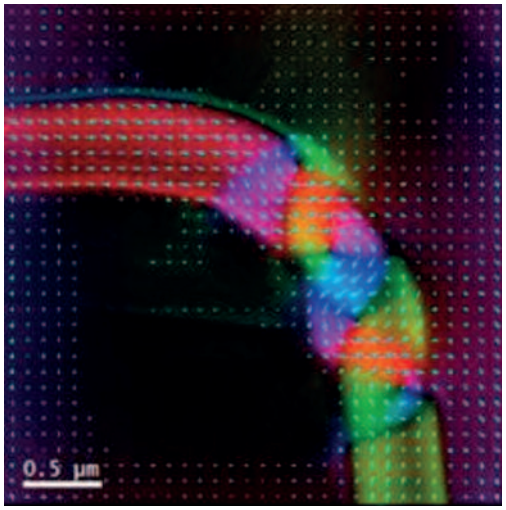

Transport-of-Intensity-Equation reconstruction of the magnetic induction in an L-shape Co nanowire in remanent state by Lorentz microscopy, where the formation of a mulivortex state is observed

Magnetic domain wall behaviour in cobalt nanostructures studied by lorentz microscopy: The design of new magnetic devices based on nano-magnets for applications in magnetic information storage, sensing or magnetic logic requires the precise knowledge of the magnetic state at the nanoscale. These applications also require the accurate control of these magnetic configurations, namely domain walls, vortex structures, etc. by modifying external parameters such as the magnetic field or injected electric current. For that purpose, TEM allows the observation of the magnetic nanostructures with nanometer-range spatial resolution by using Lorentz microscopy (LM).

A comprehensive LM investigation of the magnetic domain wall (DW) configurations has been carried out in nanostructured Co nanowires (NW) fabricated by focused electron beam induced deposition (FEBID) on an electron transparent Si_3N_4 membrane. Studies have been developed in remanent condition and in applied magnetic field in a FEI Titan Cube 60-300 TEM equipped with a Lorentz lens. DW configurations have been studied for different magnetic states (remanence, saturation, nucleation, and propagation) as well as their dependence with the width and thickness. A crossover between thin NW with transverse domain wall states and thick NW with vortex states has been observed at around 13 nm thickness for NWs with a 500 nm width. At this crossover the different between nucleation and propagation fields is maximum, becoming good DW propagators. Focal series in LM were acquired in order to calculate the in-plane magnetic induction orientation in each magnetic state by solving the Transport-of-Intensity Equation (TIE), as shown in the image above.

Study of semiconductor dumbbell polarity by aberration corrected Annular Bright Field STEM imaging. Polarity in binary semiconductors arises from the partial ionicity of their chemical bonds. The charge transfer between the elements of the compound results in the formation of atomic pairs of opposite partial charge (ionicity), which are commonly referred to as "dumbbells". The oppositely signed charge of the atoms constituting the dumbbells implies the existence of this internal electric field in the crystal. Particularly in nanoscale structures such as nanowires (NWs), only a particular polarity drives the unidirectional growth. It influences the growth mechanism, drives the final orientation of the NWs, or can even lead to the formation of new nanostructures such as tripods. In spite of its importance in the growth and final properties of semiconductor NWs, reliable methods for polarity determination of compound semiconductor NWs at the atomic scale are still scarce, although several approaches have been reported, lacking spatial resolution.

In collaboration with Professor J. Arbiol (ICREA-ICMAB) and S. Lopatin (FEI) the newly developed annular bright field (ABF) has been implemented by using a standard annular dark field detector and a particular camera length that enables the detection of the outer part of the bright field disk in STEM configuration, while letting through the central part of the central diffraction disk. These experiments have been carried out in the probe corrected Titan Low Base. As an example, the observation of dumbbels in ZnO is shown in the figure. The same has been performed in GaN. The proposed experimental via opens new routes for the fine characterization of nanostructures, e.g. in electronic and optoelectronic fields, where the polarity is crucial for the understanding of their physical properties (optical and electronic) as well as their growth mechanisms.

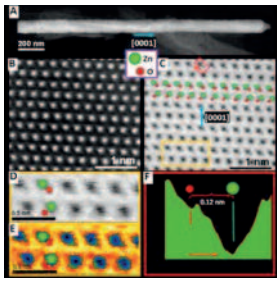

a) HAADF-STEM view of a ZnO NWs. b) Atomic resolution aberration corrected HAADF-STEM of the ZnO wurzite structure a). c) Atomic resolution aberration corrected ABF-STEM detail obtained on the same area as in b). d) ABF-STEM magnified detail of the region marked with an orange rectangle in c). e) Temperature colored detail of the same region in d). f) ABF intensity profile obtained across the Zn-O dumbbell pair inside the red rectangle region in c).

Atomic resolution analysis of zeolites. Zeolites are microporous inorganic solids formed by channels and/or cavities extended through the three-dimensional space. That particular structure in combination with the possibility of incorporating guest elements into their framework have turned zeolites into the most important and versatile heterogeneous catalysts and they are widely employed in petrochemical and detergent industries. Unfortunately, despite their large structural parameters they are tremendously unstable under the electron beam and only few groups have been able to image zeolites by conventional TEM. The purpose of this work is develop C_s corrected STEM experiment to analyze these materials.

Zeolite A (the most beam sensitive zeolite) was studied with and without silver incorporated into the structure. The results obtained (see image below) proved the feasibility of this technique to obtain high-resolution images on STEM mode. It evidences for the first time the clusters formation in the zeolitic cavities where the Ag cations adopted and octahedral structure surrounded by another 8 cations.

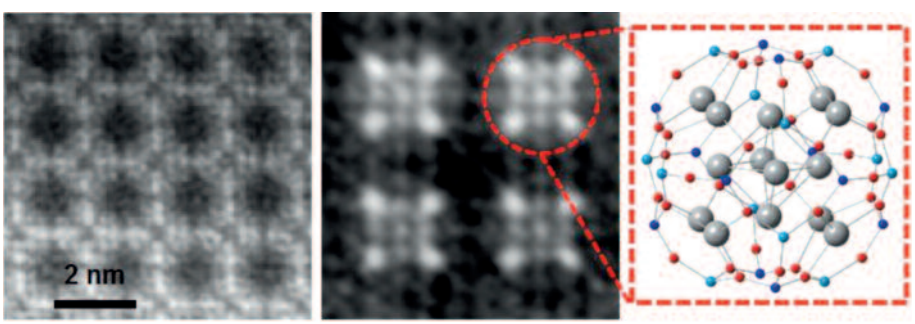

Left: Aberration corrected STEM-HAADF image of the zeolite "A" framework. Centre: Cs corrected STEM-HAADF image of silver occluded zeolite "A". Right: model of the cage with Ag atoms are in grey

Analysis of multibranched Au nanoparticles. Gold nanoparticles have recently regained a great interest due to their potential applications in SERS and cancer treatment. Here, a novel shape based in the combination of two capping agents was produced obtained long branched nanoparticles (see figure), which absorbed energy in the infrared zone. The structure and surface relaxation was studied by means of HRTEM; meanwhile the optical properties were measured by monochromated high resolution EELS analysis.

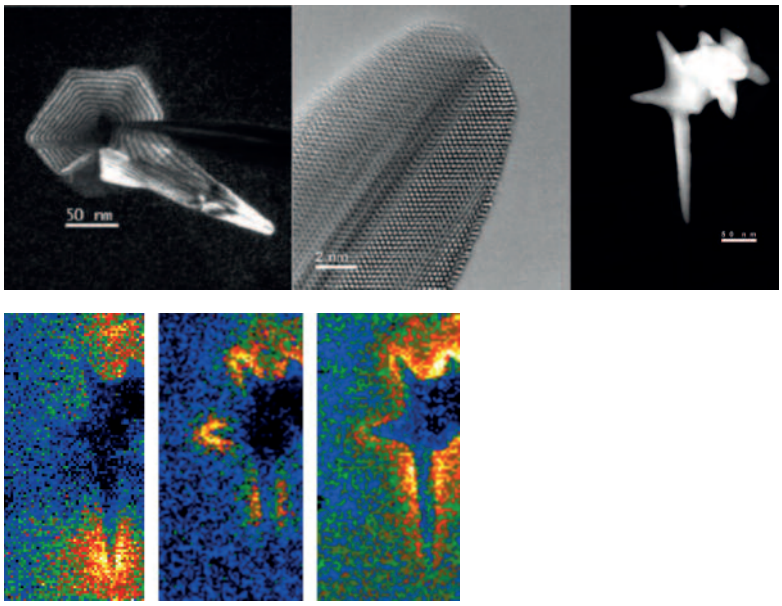

a) Weak-beam DF image of a typical gold crystal. b) Cs corrected HRTEM image of the tip of a branch displaying the monoatomic steps. c) Cs corrected STEM-HAADF image of another nanoparticle where plasmonic analysis was carried out; showing the maps obtained for 0.75, 1.40 and 1.85 eV respectively.

Au-Ag core-shell and Au nanoparticles studied by electron Tomography: Electron tomography is a very powerful technique giving access to crucial structural, morphological and compositional aspects. 3D-STEM-HAADF measurements have been developed in Au-Ag core-shell and Au nanoparticles for analysing their structures and morphologies. These studies have been carried in the FEI Titan – XFEG - Cs probe corrected microscope.

Te figure displays (a) the low magnification high-angle annular dark field STEM image of one of the typical nanoparticles. Their shape is similar to a "stone-age" arrowhead and their size is around 150-340 nm by 50-80 nm. High-resolution HAADF-STEM image of one of the apexes of this nanoparticle is shown in the figure (b). From the analysis of this image it can be interpreted that this structure corresponds to a silver region. This result has been confirmed via EDS measurements developed in this area, as well as in other areas of the particle (see (c) in the figure). From the other EDS spectra it can be inferred that the nanoparticle correspond to a core-shell structure.

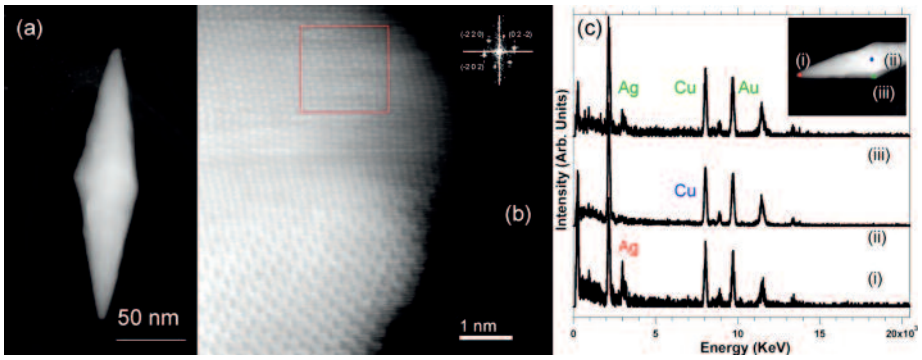

(a) Low magnification HAADF image of one of the Au-Ag core-shell bipyramidal nanoparticles. (b) HR-HAADF image recorded at the apex of this nanoparticle and corresponding to the Ag region. Inset: FFT calculated from the marked area of the HR-HAADF micrograph and that is indexed as Ag. (c) EDS spectra recorded in two different regions marked on the LM-HAADF image.

STEM-HAADF tomography allows obtaining indirect compositional information due to the Z dependence of the inelastic scattered signal. The figure shows in (a) the volume reconstruction of one of these NPs. These studies show that the nanoparticles have a perfect and homogeneous Au-Ag core-shell structure. Their morphology corresponds to a bipyramidal prism, composed by an Au core and covered by an Ag shell of few nm thick, as can be deduced from the sections/slices shown in the figure (b). These results have been partially published in publication 16 and another article is in preparation. Other tomographical studies on Pt NP, Au-Fe core-shell NP, filled mesoporous materials have been carried out.

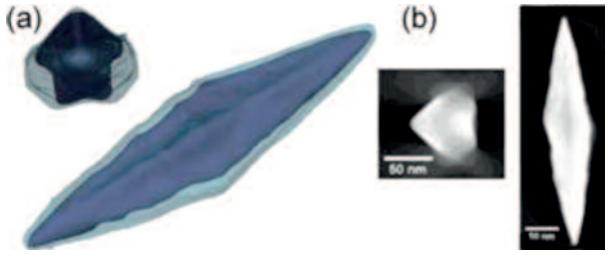

(a) Two different views of the tomographical reconstruction of the Au-Ag core-shell nanoparticle showing the internal gold structure and the outer silver sheath. (b) Examples of two different sections of this reconstructured volume.

Plasmonics: It is well known that in the case of metallic nanoparticles (NPs), their size, morphology, as well as, their local dielectric environment have strong impact on their optical properties. In order to study all these effects, gold NPs with a wide range of sizes, shapes, and dielectric environments have been chosen. These studies have been carried in the FEI Titan – XFEG - Cs probe corrected microscope equipped with a monochromator. The figure displays low-loss spectra recorded on a core-shell Au-Ag bi-pyramidal NP. Similar studies have been carried out in different Au (and other noble metals) nanoparticles, as spherical ones, nanorods, nanostars. Shifts of some of the modes, as well as, other modifications in the response of the surface plasmon modes due to the morphology and the size of the Au-NPs have been observed (more details in publication 14).

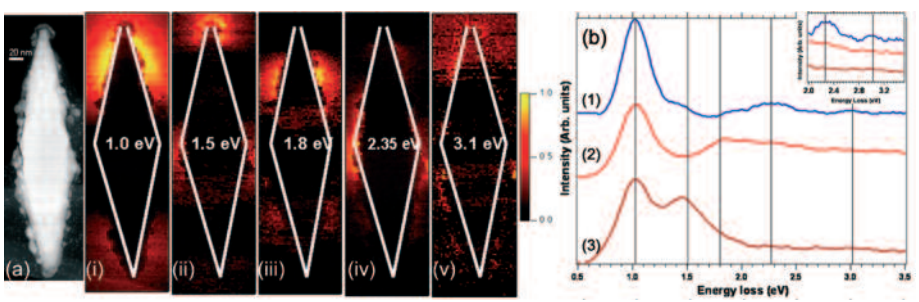

***(a)** HAADF image of a core-shell Au-Ag bi-pyramidal NP where a spectrum-image (SPIM) has been acquired. (i) to (v) Spatial distribution of their excited surface plasmon resonances. **(b)** Spectra extracted from the SPIM of (a), showing the different modes.*

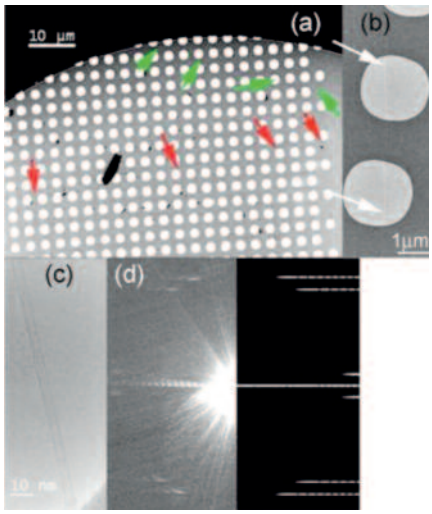

(a) and (b) Low-magnification TEM micrographs corresponding to two different UL-NT. (c) HRTEM Experimental and simulated EDP of this SW-NT, respectively. These EDP are unambiguously assigned to a (35,25) NT.(c) Intensity profiles of the equatorial-line of the experimental and simulated EDP of this NT.

Carbon and heteroatomic materials: structural and analytical studies. HRTEM and electron diffraction techniques have been combined to develop deep structural/atomic studies on individual carbon nanotubes produced by catalytic chemical vapor deposition (CCVD). These NT have high structural quality and no chiral angle modification was observed, nor diameter change along the whole nanotube length. The figure shows one of those NT, which correspond to a (35,25) NT. Most of the studied NT are double-walled. The structural correlation between the two adjacent layers/shells composing a DW (inner and outer NT) was examined. Regarding the chiral angle difference between these 2 shells, it was observed that 78% of the cases is lower than 5°. Moreover, the analysis of the interlayer distance reveals that for most of the DW nanotubes the interlayer distance is close to 0.33 nm which is the interlayer distance in graphite. Thus, from these two complementary data it can be concluded that these DWNT display a strong correlation between the structures of the inner and outer NT.

In addition, a selectivity toward high chiral angles was observed, manifested by the facts that the chiral angle of most of NT ranges between 20 and 30 deg., that 12.5 % of the NT are pure armchair and that no zig-zag NT were observed. From the NT whom chiral indices were fully identified, it is observed that a third of them is metallic. These studies shed light on the structure of very long NT and of DW-NT especially (more details in publication 12).

Heteroatomic NT: analytical (EELS) studies. In order to obtain primarily information on the localisation of the N atoms in the N-CNT, EELS-STEM analyses have been performed. These studies carried out on highly doped N-CNT suggest that the nitrogen is present over the whole structure of the tube (Figure 2(a)). However, some more localized investigations have shown that the nitrogen concentration can vary considerably from one area to another, being higher inside the areas where arches are present (Figure 2 (c)). As a matter of fact, from the analysis of the spectrum-imaging of the figures (a),(b) it can be observed that the amount of N can be almost 20% (area 3, middle of the arch) and only 8% in the region close to it (area 0, inside of one of the compartments). It can be observed in figure (c). The fine structure near (ELNES) of the C-K edge consist of a sharp π^* peak at ~285 eV and a σ^* band starting at ~292 eV. The ELNES analyses of the different EEL spectra extracted of the spectrum-imaging of the figure (b) show that these signatures are typical of graphitic network, sp^2 hybridization of the C atoms, but existing different C configurations in these different positions/areas of this analyzed region: from amorphous-like or less organized carbon (area 3 – middle of the arch) to more graphitic ones as it is the case of the area 0 (in the compartment), see figure (d) and mainly figure (e) which is a zoom in the C-K edge. Thus, this indicates that there is some correlation between the N content and the density of defects or cristallinity/graphitization degree. A detailed analysis of the N-K edge (figure (f)) shows the coexistence of two different atomic configurations of the N atoms: the graphitic (~ 401 eV) and the pyridine-like one (peak at ~398 eV). It is obvious that the insertion of such a high concentration of N within the graphitic planes is at the origin of the high density of defects observed in the high resolution TEM images. Note that the presence of molecular nitrogen species was also occasionally evidenced in some compartments of the tube.

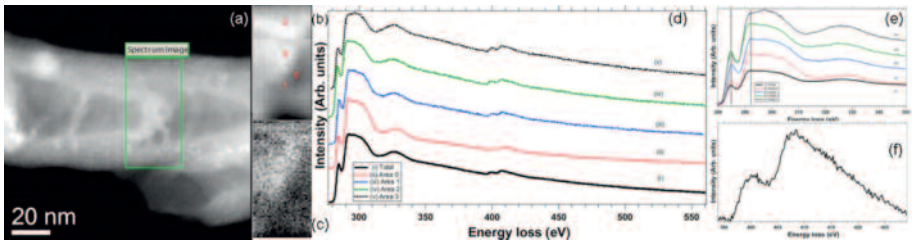

N relative amount (%): Area 0: 8.3; Area 1: 13.8; Area 2: 16.5; Area 3: 19.7; Sum of all spectra: 13.7 %. EELS mapping on a typical area of a highly-doped N-CNT. (a) Global HAADF-STEM view of the analysed N-CNT. An EELS spectrum-image has been recorded in the marked area of the image. (b) HAADF-STEM image of the EELS analysed areas corresponding to the green rectangle from (a). The positions chosen for a more detailed EELS analysis are marked in red. (c) N map extracted from a general spectrum-imaging recorded on the K-edge of nitrogen after the background removal. (d) The individual EELS spectra, after the background removal, corresponding to the positions marked in (b). (e), (f) Zoom on the EELS spectra at C and N K edges, respectively (in the case of N K edge, the curve correspond to the addition of the spectra). The N concentrations corresponding to the different positions that are obtained by the quantification of the spectra are given below the figure.

Atomic manipulation to construct model quantum nanodevices: Individual atoms on a surface can be manipulated one by one using the tip of a low temperature scanning tunnelling microscope (STM). The method requires full stability and control on tip position with sub-atomic control. Once the tip is positioned on an individual atom, it is moved laterally till the desired position, and the chosen atom is dragged to rest at this site. This technique offers the possibility to build functional structures with precision down to the atomic scale. The goal is to explore fundamental properties of quantum mechanics by constructing and investigating atomic-size devices (see below). Unprecedented insight of elementary interactions, excitations and dynamics of individual atoms and molecules become accessible by controlling the site and arrangement at the atomic scale.

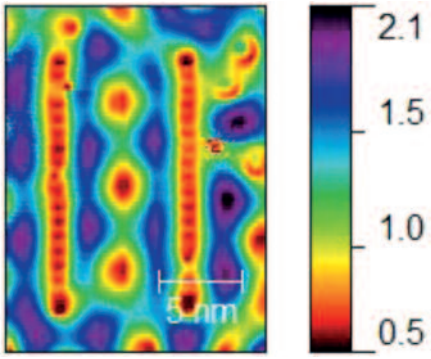

The figure shows an atomic-sized quantum resonator made by two parallel rows formed by 39 Co atoms. The goal for constructing this device is to modulate, in a controlled manner, the substrate LDOS landscape, in order to resolve its role on the strength of Kondo screening of magnetic adatoms. The LDOS oscillates periodically due to standing wave patterns of the surface state of the Ag(111) substrate. Co adatoms precisely positioned inside the resonator exhibited a Kondo temperature (i.e. a parameter determining the strength of magnetic screening) oscillating between 90 K and 145 K, depending on the site. Our data show that the precise control of the substrate LDOS is of crucial importance for a correct quantitative analysis of the Kondo resonance.

Two parallel atomic rows, 19 Co atoms each, representing a electron quantum resonator. The local density of states (LDOS) of the Ag(111) surface is confined within this device, and exhibit a space modulation varying with the width. Hence, it can be tuned at will. The oscillatory false-colour background correspond to the electron states at the Fermi level.

Magnetic ground state of rare-earth atoms: Thulium atoms, thermally deposited on a clean W(110) substrate under UHV conditions, have been investigated at low temperature with STM and STS for coverages below 0.2 monolayer. The adsorbed Tm forms disordered structures consisting of single adatoms and some trimmers with a minimum average separation of 1.7 nm, as determined from the evaluation of the pair distribution function. The Friedel-like oscillatory long range interaction, mediated by the two-dimensional electron gas formed by

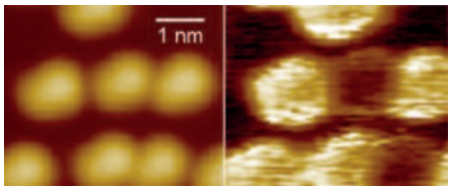

STM and STS images (4.6x3.8 nm2) of 8 Tm atoms deposited on W(110): Left) Topographic image, right) corresponding dI/dV map obtained at Vbias = 2.6 V, were the most intense Tm state shows up; two atoms display opposite magnetic contrast with respect to the others.

the W(110) surface states, and the repulsive dipolar interaction are considered to explain the observed distances distribution between the Tm adatoms. Differential conductance spectra and maps recorded at 4.5 K with a magnetic tip show reversed magnetic contrast on adjacent Tm atoms (see Fig. below), pointing out to a single atom binary magnetic behaviour. This is compatible with a preferred normal to the surface orientation of the prolate 4f magnetogenic shell of Tm. Rare Earth (RE) atoms deposited on metallic surfaces present a relatively large electric moment, 4 D for the W(110) surface; so, below the adatoms, there is an enhanced density of negative charge, promoting a perpendicular orientation of the 4f orbitals. The strong spin-orbit coupling of the rare earth atoms forces their magnetic moment to be also normal to the surface and provides the magnetic anisotropy needed to overcome the thermal instability at the measurement temperature.

Inter atomic interactions probed through their Kondo fingerprint: The comprehension of interactions between single atoms is a fundamental step towards the realization of practical nanodevices with dimensions below the limits of current nanolithography technology. The study of the Kondo screening appearing when a magnetic adatom lies on a metal surface provides deep insight into the involved magnetic interactions. The energy scale of the screening is characterized by the Kondo temperature T_K, which depends strongly on the host LDOS (as shown above) and on the magnetic exchange framework in the vicinity of the atom.

To explore the later, the shape of the Kondo resonance on Co adatoms deposited on the Ag(111) surface is investigated. Co atoms are positioned with sub-nanometer resolution to close-neighbour distances and their Kondo resonance subsequently characterized by means of scanning tunnelling spectroscopy (STS). The interatomic magnetic interactions can be also addressed by arranging atomic chains with different coordination with neighbouring Co atoms and interatomic distances, as shown in the figure below. At a distance of three Ag(111) lattice parameters (8.8 Å), each atom is found to retain its own Kondo resonance, while at two lattice parameters (5.8 Å) the Kondo cloud collapses in one single resonance. The analysis of these data unveils the length scale of magnetic interactions among individual Co adatoms and the onset of the quantum interference of both atomic wave functions. The precise control of the substrate LDOS is of crucial importance for a correct quantitative analysis of the Kondo resonance.

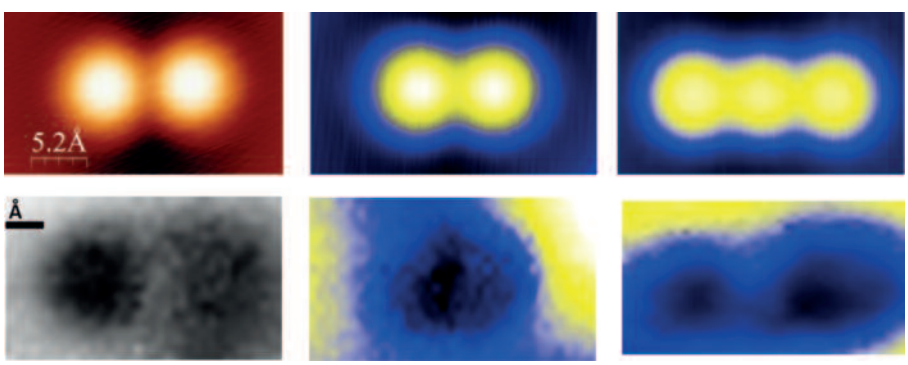

From left to right: topography (top panel) and strength of Kondo resonance at 5 meV (bottom panel) in a dimer with interatomic distance of three Ag(111) lattice parameters, a dimer at two distances and a trimmer at two distances.

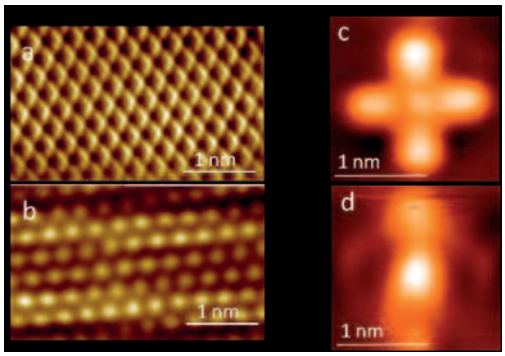

Figure: a) and b) atomic resolution of Ag(111), and Mn/Ag(111), respectively. The Mn layer forms a pseudomorphic lattice entailed from the Ag(111) surface. c) and d) Co-Ph on Ag(111), and on Mn/Ag(111), respectively.

Molecular Magnetism: The investigation of magnetic exchange coupling of metal-organic molecules with magnetic substrate aims to use molecular materials as alternative media for information storage. The study of the adsorption of Co-Phthalocyanine (CoPC) molecules on monolayer islands of Mn on Ag(111). Mn, when adsorbed pseudomorphically on Ag(111) (see figure), exhibits a non-collinear 120° Neel magnetic structure. Our goal is therefore to explore how far the spin pattern of the substrate is leading to spin structures of the adsorbed CoPc networks. CoPc molecules show very strong adsorption properties on Mn islands. Strong chemical binding leads to strong changes in molecular structure, as was observed by comparing STM topographs of CoPC on Mn with those on the Ag(111) substrate.

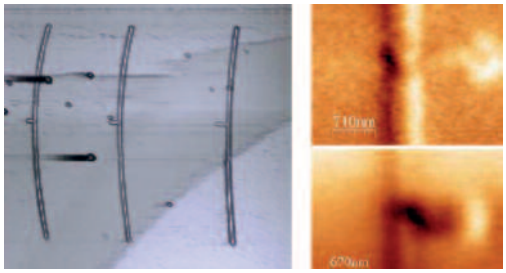

Overview of three Py nanowires with different curvature. On the right side the magnetic signal before and after nucleating a DW at the trap upon application of 2 Tesla perpendicular to the wire is shown (4.2 Kelvin).

Domain wall conduit in magnetic artificial nanostructures (Sample provided by R.H. Cowburn group, U. Cambridge). Domain wall (DW) pinning in ferromagnetic nanowires is in general a complex process. Distortion of the DW shape makes quantitative agreement between modelling and experiment difficult. The pinning and depinning of DW using nanometer scale localized stray fields is here demonstrated. External magnetic fields perpendicular to the Py nanowires (see figures)are applied in order to create a domain wall next to the magnetostatic barrier created by the fingers. Now, a magnetic field parallel to the wire axis can push the DW out of trap. The value of that depinning field depends strongly on the temperature and on the curvature of the conduit wire. This effect is observed by direct imaging of the MFM signal at cryogenic temperatures (4.2 K). Investigating this effect in the temperature range of 4-300 K will provide crucial information on the domain wall energy balance between magnetic anisotropy and exchange interaction.

Tip functionalization for magnetic characterization. A qPlus sensor is a revolutionary method to measure atomic forces using a STM. It consists in a quartz tuning fork brought to oscillate in its characteristic resonance frequency, with a sharp tip at the end of one of its prone acting as the sharp STM sensor. Changes in the resonance frequency of the tuning fork can be directly related with the stiffness of the junction. The force resolution depends critically on the tip radius. To sharpen the tip, tungsten Nanodeposits have been grown directly on the apex using Focused Ion Beam lithography. The result (shown in the figure) is a drastic decrease of the tip radius.
Future development of this line aims at functionalising the tip apex with superconducting or magnetic material. The Tungsten nanodeposits are rich in carbon, what make them superconducting below 5 K. Hence, these structures will be applied to investigate forces in

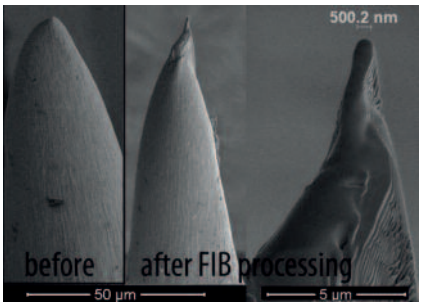

SEM micrographs of the tip of a qPlus sensor before and after growth of a sharp WC apex using FIB

superconducting-vacuum-superconducting junctions using a combination of AFM and STM. In addition, The development of a methodology to quantitatively resolve the magnetic structure of metallic and/or molecular materials at the nanometer scale is being addressed. The measurement of magnetic forces is a logic avenue to expand the field and give it additional quantitative information. Previous attempts using standard non-contact AFM revealed that the magnetic signal is by far weaker than the one obtained using spin-polarized STM. The use of a qPlus sensor will certainly improve the signal to noise because the tip apex can be controlled to oscillate less than 0.1 nm.

Mechanism of action of proteins. Nanopositioning of nanoparticles on sensors: Proteins interact with their ligands through binding forces carrying out enzymatic reactions, gene regulation, electron transfer, etc. Direct measurement by Force Spectroscopy-AFM of the bonds strength in these systems will improve understanding the mechanism of these interactions. Biological processes under relevant physiological conditions using AFM imaging are also being analysed to know the models of binding, estimate parameters on the formation of the complexes and solving mechanisms of enzymes with metabolic interest. At this time we are studying the mechanism of flavoenzymes as Ferredoxin $NADP^+$ Reductase, Human Apoptosis Inducing Factor and FAD Synthetase and clarifying the binding of the Ferric Uptake Regulators to specific gene sequences. This is a new field in which only a few studies have been conducted. Our ability to manipulate proteins and operate with AFM mimicking physiological conditions allows to approach these studies. On the other hand, ferritin containing nanoparticles are synthesized and organized with Dip pen nanolithography–AFM in the most sensitive areas of new microsensors that allows to measure for the first time good coupling signals from magnetic sub-monolayers that differ from the standard bulk measurements.

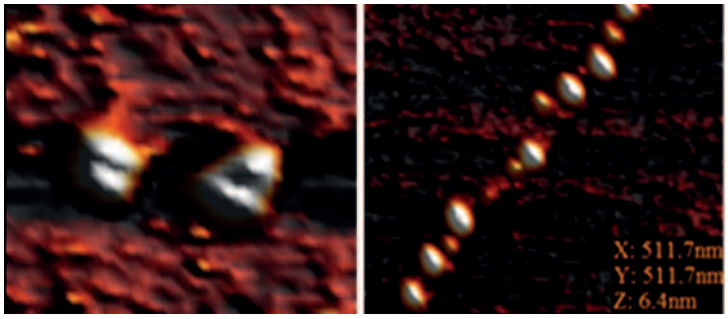

Ferric Uptake Regulators A and B bind the specific regulatory promoter -cloned in a plasmid- using different strategies that define their different role in cyanobacteria involving iron homeostasis, defence against oxidative stress and nitrogen metabolism.

Transport in single molecules and through molecular films: Fundamental parameters influencing the conductance of single molecules and/or small ensembles of molecules have been studied. Langmuir Blodget films of an "asymmetric" OPE derivative (thiol in one side and amine in the other one) were prepared at the air-water interface and transferred onto solid substrate to determine their electrical properties depending on the functional group in contact with the lead. No clear dependence with the linker was observed. In addition, I-V curves were symmetric, despite the inserted asymmetry in the contacting linkers, suggesting that charge flow through the metal-molecule-metal junction proceeds via a (non-resonant) tunnelling mechanism. In addition, charge transport through single oligo-porphyrin wires was determined through electrical measurements in single-molecule junctions. A strong dependence of the molecular conductance with temperature, and with the length of the wire was observed. Although these factors seem to point to an incoherent

thermally assisted hopping mechanism, the transport in these molecular junctions shows to be convincingly described by a theory based on phase-coherent electron tunnelling, using E_F as a simple adjustable parameter. These studies are being complemented with new strategies to make the "top contact" in molecular devices, based on the photo reduction of metal nanoparticles precursors using the LB technique.

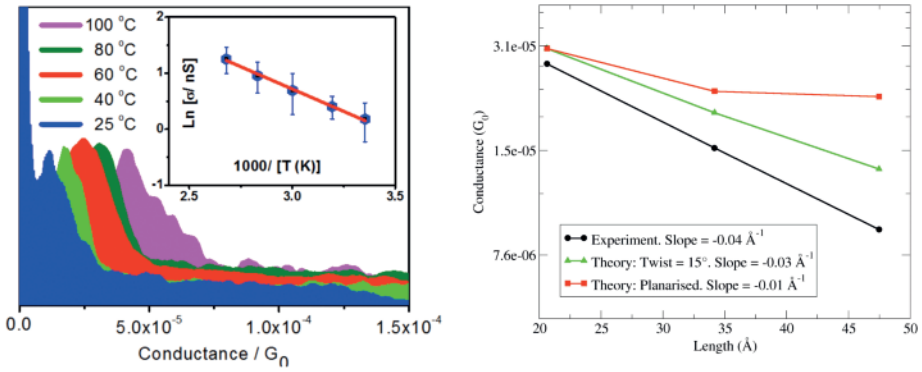

Left side: Conductance histograms for a porphyrin dimer at different temperatures and its dependence on the conductance (inset). Right side: dependence of conductance of oligo-porphyrins on length.

Structural and magnetic characterization of cobalt grown by focused electron-beam-induced deposition. For this, lamellae were prepared from the cobalt nanodeposits and subsequently analyzed by HRTEM and EELS (in collaboration with O. Stephan's group in Orsay). A clear correlation was obtained between the cobalt content and valence state with the observed magnetotransport properties. This type of nanostructures was also investigated by MFM in cooperation with A. Asenjo (ICMM) and her group. This allowed us to conclude that a multidomain structure exists for wide deposits but for narrow ones (below 400 nm) they present single-domain structures, as desired for applications in magnetic logic and sensing. More details in publications 30 and 38.

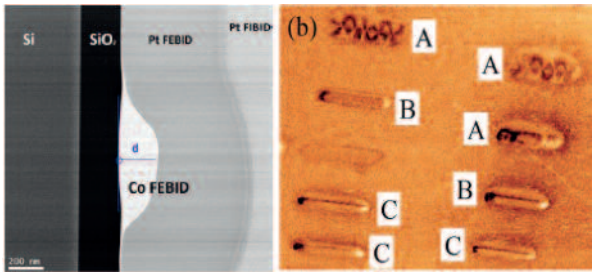

Left: TEM image of a lamella prepared from a cobalt nanodeposit, where precise HRTEM and EELS experiments were performed at the LMA and Orsay. Right: MFM images of several cobalt nanowires of different width.

Growth of ultra-narrow cobalt structures by focused electron-beam-induced deposition. Ultra-small cobalt nanostructures (lateral size below 30 nm) have been successfully grown by optimization of the growth conditions using focused-electron-beam-induced-deposition techniques. This direct-write nanolithography technique is thus shown to produce unprecedented resolution in the growth of magnetic nanostructures. The challenging magnetic characterization of such small structures was carried out by means of electron-holography techniques in cooperation with E. Snoeck and C. Gatel from CEMES (Toulouse). Apart from growing ultra-narrow nanowires, very small Hall sensors have been created and their large response unveiled. More details in publication 35.

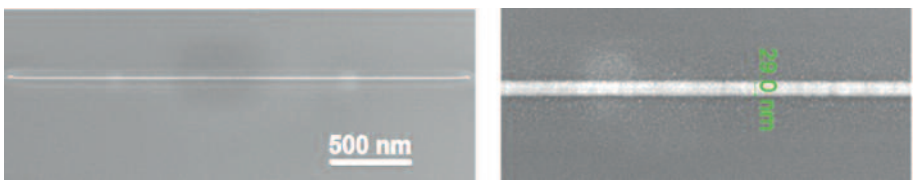

Left: SEM image of a long cobalt nanowire grown by FEBID. Right: High-magnification SEM image of this wire, showing unprecedented lateral resolution for a magnetic nanowire by FEBID.

Left: Topography (STM) image of the studied W nanodeposit, showing very small roughness and a well-defined pinning landscape. Right: The trajectory of a few vortex is indicated when varying the magnetic field from 1 T to 1.2 T.

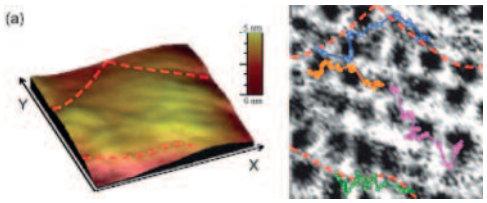

Growth of very smooth W-based nanodeposits by focused ion-beam-induced deposition for subsequent studies of the vortex lattice by scanning tunnelling microscopy. Using flat Si substrates and optimized growth conditions, very smooth W-based nanostructures were grown by FIBID and thoroughly analyzed by STM. The STM experiments have permitted to track the path followed by each individual vortex when slowly increasing the magnetic field, giving access to the dynamics of the vortex lattice. More details in publication 26.

Left: Resistance vs Temperature of one of the nanocontacts under three driving currents. Right: Differential conductance as a function of the applied voltage at different temperatures.

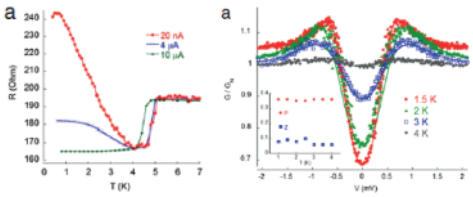

Study of Andreev reflection in ferromagnet-superconductor nanocontacts. Using micro- and nano-lithography techniques, it has been possible to grow ferromagnet-superconductor nanocontacts with controlled final resistance. Andreev reflection has been observed in these nanocontacts, from which the ferromagnet spin polarization and the superconductor gap have been determined. The behavior of these contacts has been additionally studied as a function of the magnetic field. More details in publications 32 and 40.

Left: Variation of the iron content in the microwires grown by FEBID as a function of the H_2O pressure inside the chamber. Right: Anomalous Hall effect measurements at room temperature of the wires with higher Fe content indicating their ferromagnetic behaviour.

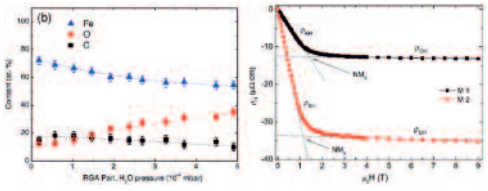

Magnetotransport properties of Fe-based microwires grown by focused electron-beam-induced deposition. In collaboration with the Technical university of Eindhoven, the FEBID technique has been used to grow Fe-based microwires. By precise control of the growth atmosphere, the Fe content has been systematically varied. Lamellae have been prepared out of these wires to study their microstructure by TEM at the LMA. The magnetotransport properties of these wires have been also characterized in Zaragoza, showing their ferromagnetic character. More details in publication 27.

Influence of lithography on graphene properties. Lithography processes have been found to affect severely the physical properties of graphene. First, graphene was grown by mechanical exfoliation techniques. Afterwards, several technological steps were perfomed involving the use of resists and optical and electron-beam exposures as well as FEBID of cobalt. The corresponding influence on the graphene properties have been analyzed by Raman spectroscopy. More details in publications 25 and 36.

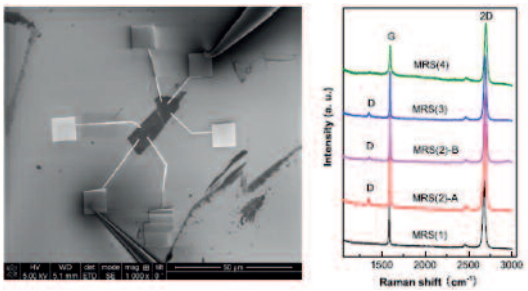

Left: Electrical contacts performed on a graphene flake for the study of the influence of the electron-beam irradiation on graphene. Right: Changes in the Raman spectra when performing several steps of electron beam lithography on a graphene flake.

Focused Electron Beam Induced Etching of Titanium with XeF_2. We have discovered that Ti, which is an important material in nanotechnology, can be etched selectively by focused electron-beam-induced etching using XeF_2 as the etching gas. As an example, a few nanostructures have been created with this method. More details in publication 1.

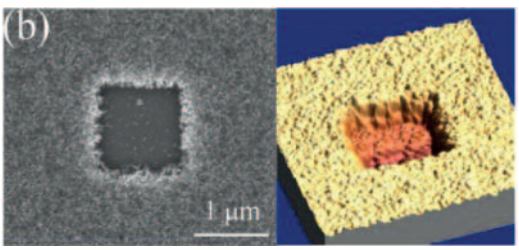

Left: SEM image of a square of etched Ti by FEBIE. Right: The corresponding AFM image of the etched material.

Circuit edit of superconducting microcircuits. Superconducting connections have been proved to be possible with focused-ion-beam-induced deposition of tungsten (W-FIBID) and niobium, which is the standard metal used for superconducting electronics. Our method enables the modification or even the repairing of valuable low-Tc superconducting microcircuits with high resolution; this was previously impossible.

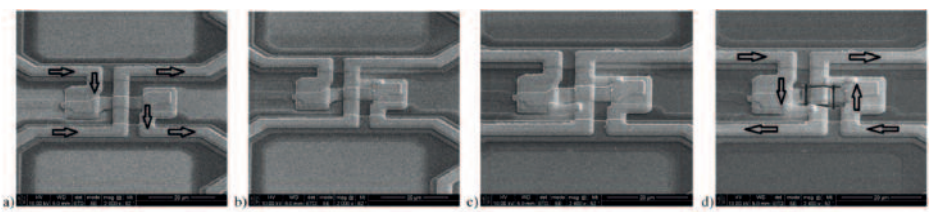

Transformation process for a SQUID susceptometer without intermediate transformer: (a) original connection; (b) first W-FIBID deposit; (c) second W-FIBID deposit; and (d) trenches produced with the FIB to break the original connections. Arrows indicate the direction of the primary current, note the difference in direction between (a) and (d).

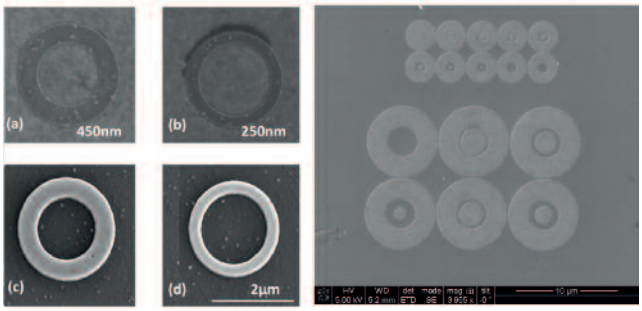

Left, SEM images of rings made by e-beam lithography. (a)-(b) images taken after Cr/Al hard mask evaporation. (c)-(d) images taken after ion milling with argon. Right, SEM images of rings made by ion-beam lithography.

Strain-induced magnetization reorientation and magnetic anisotropy in epitaxial Cu/Ni/Cu rings. Using epitaxial films grown in the MBE facility located at INA, single crystalline rings have been fabricated by means of ion-beam and e-beam lithography and ion-beam etching using an Al-Cr hard mask. The magnetic domain structure of the rings depends on their thickness but, for thin rings, it shows a pattern compatible with a magnetization vector pointing along the radial direction. A transverse magnetoelastic anisotropy, due to an in-plane anisotropic relaxation of the strain existing in the continuous film explains these findings.

Controlled cell death by magnetic hyperthermia: Although important advances regarding early tumour detection have been accomplished, early detection remains among the biggest challenges in oncology. The use of magnetic nanoparticles (MNPs) as heating agents provides a more selective elimination of targeted cells, thus a promising strategy for targeting neoplasic tissues. By magnetically charging system cells ex vivo, our *in vitro* experiments using magnetically-loaded dendritic cells (DCs) as vectors for thermotherapy have shown the potential of this 'Trojan horse' strategy for immune-related therapies. DCs cell death was able to be controlled by a proper choice AMF amplitude and exposure time, depending on the amount of MNPs uploaded. Controlled cell death of MNP-loaded DCs can be obtained by adequate tuning of the physical alternating magnetic field (AMF) parameters and MNPs concentration. Necrotic-like populations were observed after exposure times as short as 10 minutes, suggesting a fast underlying mechanism for cell death. Power absorption by the MNPs might locally disrupt endosomic membranes, thus provoking irreversible cell damage. More details in publication 24

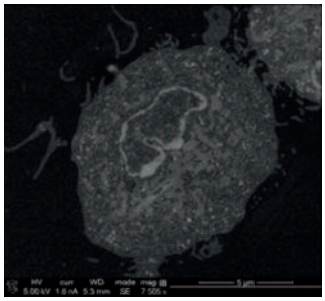

Cross section electron image of a magnetically-loaded dendritic cell, taken at 5 kV and 1.6 nA. The image shows the agglomeration of the magnetic nanoparticles inside endosomal structures of the cell.

Development of ^{90}Y-labelled albumin magnetic microspheres for cancer therapy. Human serum albumin magnetic microspheres were fabricated and ^{90}Y-labelled for their application in bimodal radionuclide-hyperthermia cancer therapy. They were radiolabeled with Y-90 and the stability of Y-90 fixation on the surface of HSAMMS was investigated by both in vitro in saline and human serum and in vivo by biodistribution studies in normal Wistar rats. Appropriately sized radioactive magnetic microspheres were developed as a targeting approach to localize both activity and magnetic energy to a specific organ. The microspheres with encapsulated citric acid-coated 10 nm-magnetite nanoparticles were produced by modified

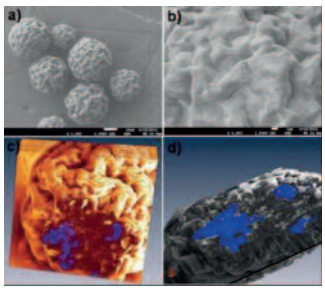

FESEM images (a,b), and 3-D reconstruction of cross-sectional views (c,d) of Human serum albumin magnetic microspheres. Coloured spots show the 3D distribution of the magnetic nanoparticles inside the microspheres

emulsification-heat stabilization technique. It was found that magnetite nanoparticles form inhomogeneous clusters distributed within the albumin microspheres. The magnetic nanoparticles inside the microspheres are in a superparamagnetic state at room temperature.. In vitro experiment revealed a high stability of labeled HSAMMS in saline and in human serum after 72h. Following intravenous administration of 90Y- HSAMMS in rats 88.81% of the activity localizes in the lungs at 30 min, with 82.67 % remaining after 72 h. The promising properties of multifunctional 90Y- HSAMMS complexes based on high radiolabeling yield and suitable magnetic properties constitute a good candidate for application in radionuclide therapy, magnetic field targeting and hyperthermia cancer therapy.

Study of Cell Adhesion Events using Novel Biomaterials using Scanning Electron Microscopy. Sodium hyaluronate has been crosslinked by photoinduced decomposition of a trifunctional diazonium salt to generate new biomaterials called H5. Thin films of formulations of chemically unmodified sodium hyaluronate and the photocrosslinker at different percentages have been processed. 2D patterns of controlled geometry have been generated by direct laser writing to perform cell adhesion studies. Different adhesion behavior of the cell lines, as assessed by scanning electron microscopy, has been observed in the polymeric films depending on the degree of photocrosslinking. These differences on the adhesive/antiadhesive balance could allow to control cell distribution as it happened on H5 patterns, where cells migrate to the glass substrates due to the low affinity for the material. Furthermore, low attachment of cells onto the polymeric pattern promote migration, what yield to a very selective distribution of cells onto the glass areas. More details in publication 70.

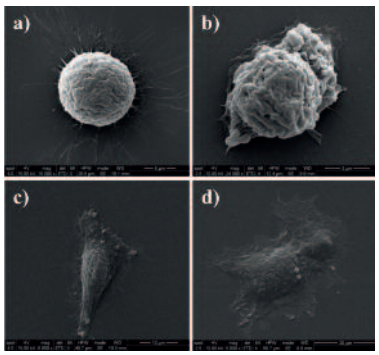

Scanning electron microscopy (SEM) images of HeLa cells (a, c) and COS-7 fibroblasts (b, d) cultured onto flood–exposed substrates of H5 (a, b) and glass substrates (c, d).

Magnetic Loading of Human Neuroblastoma Cells for magnetically assisted neural guidance. In the field of neuroscience, nerve damage and neurological pathologies are two problems of significant medical and economic impact. Nerve regeneration is a central issue in neuroscience, due to the potential benefits of recovering nerve functionality as a consequence of nerve injury or degenerative diseases. Engineered magnetic nanoparticles (MNPs) constitute a promising strategy for noninvasive therapies since they can be used as functional nano-objects to enhance the nerve regeneration and provide guidance to regenerate axons by mechanical forces under the influence of a static magnetic field.
We produced a novel method for obtaining PEI-coated Fe_3O_4 nanoparticles (PEI-MNPs) with controlled sizes between 25 and 80 nm, from oxidative hydrolysis with iron (II) salts (FeSO4). The *in vitro* cell toxicity experiments performed on a SH-SY5Y cell line demonstrated a negligible decrease of cell viability for incubation times up to 168 h and MNPs concentration up to 100 µg/ml MNPs. The intracellular distribution of the PEI-MNPs was

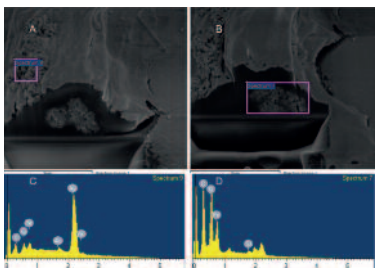

Cross-sectional images (A,B) of SH-SY5Y human neuroblasts with incorporated magnetic nanoparticles. The lower panels (C, D) show the spectral analysis of specific cell areas (pink boxes in the upper panels), demonstrating the presence of the iron constituent of the MNPs.

studied at the single-cell level by SEM-EDX and dual-beam (FIB/SEM) analysis. The results showed large clusters of the PEI-MNPs a strongly attached to the cell membrane, with partial internalization crossing the membrane. The results obtained indicate that these polymer-coated particles have great potential to be used for neuroscience applications**.**

Growth and structural characterization of epitaxial magnetite thin films. (001)-oriented thin films of Fe_3O_4 were grown by pulsed laser deposition (PLD) on MgO(001) single-crystal substrates. X-ray diffraction proves cube-on-cube epitaxial growth of high crystal quality films.

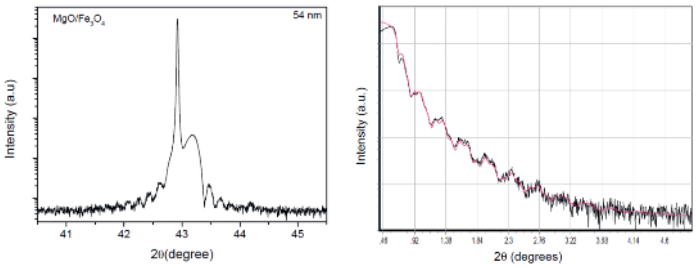

Left: Symmetric θ/2θ scan in a 54-nm-thick epitaxial film of Fe_3O_4. Von-Laue oscillations are clearly visible at both sides of the 004 Fe_3O_4 reflection, showing coherent growth along the whole film thickness. Right: XRR measured in an LCMO/STO/LCMO magnetic tunnel junction. The simulation (red line) fits the measured curve (black line), allowing to get the thickness and roughness of all the films and interfaces in the epitaxial heterostructure. Both measurements were done in the Bruker D8 high-resolution diffractometer.

Thickness and roughness measurement in epitaxial heterostructures. Magnetic tunnel junctions made of $La_{1-x}Ca_xMnO_3$ electrodes and $SrTiO_3$ barrier were grown by PLD. X-ray reflectivity was used to precisely determine all the thickness and roughness values in the multilayer.

Antibody-functionalized hybrid superparamagnetic nanoparticles. XPS analysis showed that the main elements before functionalization of the iron oxide-silica particles were Si and O, in addition to the usual adventitious carbon. Concentrations of Fe and N were less than 0.6 atom %. The peak positions detected for Fe $2p_{3/2}$ and $2p_{1/2}$ at 710.8 and 724.3 eV, respectively are consistent with the presence of iron in magnetite. The particles were again analyzed by XPS after the chemical functionalization showing the presence of amine and carboxyl groups The presence of the monoclonal antibody in the amine functionalized nanoparticles after the washing protocol was demonstrated by means of XPS analysis. The main elements present in the surface were C, O, N, Na, Si, S, and Cl. Sulphur was detected in the spectrum . This sulphur can only come from the antibody because the monoclonal antibody anti-hCG contains inter- and intrachain disulfides. The sodium detected would also come from the antibody since it was not present previously in the amine-functionalized particles.

Absence of Ni on the surface of Nitinol used in biomedical applications. XPS angle-resolved experiments were carried out. The trend of Ni 2p core-level peak with the emission angle is shown in the figure. It can be seen that at high surface sensitivity, at θ= 60º, the peak corresponding to Ni is undetectable and the amount of Ni in the outermost surface layers is below the threshold values detectable by XPS (≤ 1 at. %). The Ni/Ti atomic ratio decreases from 0.29 for θ= 0º to 0 for θ= 60º.

Comparative study of the synthesis of silica nanoparticles in micromixer–microreactor and batch reactor systems: Usually in the XPS spectra the C 1s peak is related to the presence of atmospheric contamination, but in these samples it would also came from the non-reacted precursor. XPS results showed an important decrease in the concentration of carbon after 30 min reaction in the micromixer, and it is even lower after 90 min of reaction. On the other

hand, the sample obtained in the batch reactor showed the presence of a high amount of superficial carbon that would came from remaining un-reacted TEOS. On the other hand, the O/Si ratio for the nanoparticles obtained in the batch reactor shows a value close to that of TEOS molecule (O/Si = 4) while the nanoparticles obtained in the interdigital micromixer at 90 min. residence time have a O/Si ratio close to that of the SiO2 molecule (O/Si = 2).

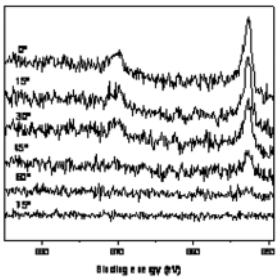

XPS angle resolved results for freshly polished NiTi. The angle is referred to the surface normal.

Characterization of the interfacial activity of PEG at the silica/PCL interface. the interactions between the PEG and the silica and between the PEGand the PCL have been studied by XPS. The XPS analyses performed for SiO_2, PEGylated nanoparticles and PCL nanocomposites showed that the binding energy (BE) of the Si 2p peak measured in the bare particles is 103.5 eV, typical for silicon atoms coordinated with oxide anions in SiO_2. In the PEGylated sample, the Si 2p BE shifted to lower values (101.8 eV) indicating a different electronic environment for the Si related to the interaction between the silica particles and the organic compound. The Si 2p BE in the nanocomposite materials is also similar to that in the PEGylated nanoparticles, suggesting the location of the PEG at the interface between PCL and silica. On the other hand, in the composite with non-functionalized particles the Si 2p BE is again 103.8 eV, showing the lack of interaction between the polymer and the inorganic particles.

Determination of the chemical state of elements and their relative proportions on different zeolite-supported Pt catalysts. For all catalysts the Pt 4f signal showed three components, the main one at 71.0 eV can be clearly assigned to Pt^0. The second component on all the catalysts appears at higher binding energies (71.8–72.0 eV) and is more difficult to assign, because it could indicate the presence of Pt^{2+} on the surface but could also be due to metallic Pt particles of 1–2 nm. Since all catalysts were calcined and reduced ex situ before XPS analysis and therefore exposed to atmospheric conditions during handling, the presence of Pt^{2+} could not be ruled out; these platinum species would be associated to oxide particles, since Pt in Exchange positions is expected to show higher binding energies. On the other hand, small metallic particles could be produced by the reduction of platinum in exchange sites. The last component would be associated to Pt^{2+} at exchange sites of the zeolite. Regarding XPS determined compositions, for the MFI support (before ion-exchange) the Na/Si ratio was 0.034 while for the Pt–MFI catalysts no Na could be detected by XPS, indicating a high degree of ion-exchange for this solid. This is also in agreement with the Pt/Si ratio which is almost the same as the Al/Si ratio measured by XPS. A high degree of exchange was also found for the MOR catalyst, where looking at the initial Al/Si ratio and to the M/Si and Pt/Si ratios after ionexchange it can be estimated that exchange took place at over 70% of the sites. For the other solids the exchange achieved was lower as shown by the high M/Si ratios remaining after exchange.

Development of microstructured zeolite films as highly accessible catalytic coatings for microreactors. XPS analysis on zeolite-coated and uncoated microneedles confirmed the excellent coverage of the microneedle structure by the zeolite films. The uncoated microneedles showed a Si 2p peak at 102.4 eV that is the result of contributions from the Si substrate (99.6 eV) and the SiO_2 microneedles (103.6 eV) . In contrast, the zeolite-coated material exhibited an Si 2p BE at 103.1 eV. This value is in agreement with values reported for siliceous zeolites, indicating that all of the microneedles and the Si substrate are well coated by the silicalite film.

Loss of permeance and selectivity of the ETS-10 membranes exposed to propylene/propane mixtures. For the ETS-10 powder the O 1s region was decomposed into two contributions; the high-intensity peak at a binding energy of 532.3–532.4 eV is attributed to O in Si–O–Si and Si–O–Ti linkages. The low binding energy (BE) peak with lower intensity (530.4–530.8 eV) is due to Ti–O–Ti bonds. Avery high carbon concentration was found in the surface of the used membranes that had lost their separation properties, around twice the concentration found in the powder. The C 1s spectrum of the powder consists of a peak with a shoulder on the high-binding energy side but on the surface of the used membranes a third contribution at higher BE appeared. The C 1s spectrum in this case was deconvoluted into three peaks: the one at lower BE (284.7–284.9 eV) can be attributed to C–C and/or C C, the second at 286.2–286.8 eV would be related to C–O bonds, and the last one at the highest binding energy could indicate the presence of ROC O groups. As was expected, after 1200 s etching, the amount of carbon on the sample diminished in the membranes, whereas the peak at high-binding energy disappeared. This would indicate a different nature of the carbon deposit on the surface and inside the pores of the membrane.

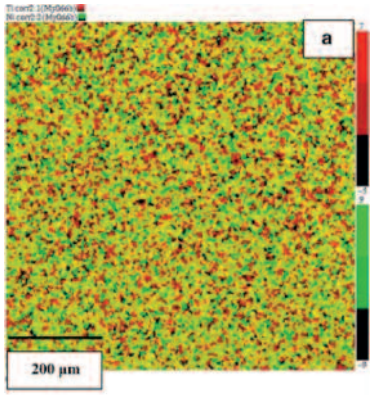

XPS mapping showing the atomic distribution of titanium and nickel. The darker the red, the more titanium is present. The darker the green, the more nickel is present.

Characterisation of silica-based coatings on Nitinol substrates. According to the XPS results, the thickness of the TiO_2 oxide layer is at least 20.8 nm thick because after etching Ti^{4+} was still detected, although Ti^{3+} and Ti^{2+} appeared as well. The titanium and nickel distribution is macroscopically homogeneous. The Ti 2p3/2 peak has only one component at 459.2 eV assigned to TiO_2, Ni 2p; on the other hand, it presents the main component at 856.6 eV, that would correspond to Ni–O (Ni^{3+}) bonding, and a small contribution (0.1% area) at 853.6 eV that could be associated to NiO or to Ni in intermetallic NiTi state]. The absence of a peak at 454.5 eV in the Ti 2p spectrum, that would correspond to the NiTi compound, indicates that there is NiO present on the surface. After etching there is an increase in the Ni atomic concentration. The Ti 2p3/2 can be fitted into 3 peaks, at 456.2 eV (Ti2+), 457.4 eV (Ti^{3+}) and 459.0 eV (Ti^{4+}) [25], while Ni 2p3/2 has one component at 855.8 eV assigned to Ni_2O_3 oxide.

Anisotropic magnetotransport in $SrTiO_3$ surface electron gases generated by Ar^+ irradiation. Metallic surface layers are fabricated by doping (100) $SrTiO_3$ (STO) single crystals with oxygen vacancies generated by bombardment with Ar ions from an rf plasma source. The presence of oxygen vacancies is confirmed by x-ray photoemission spectroscopy. Pristine STO and Nb-doped crystals were consistently analyzed in terms of a single Ti^{4+} species. In the Ar-irradiated sample relative spectral weights were consistent with an 87.5/12.5 Ti^{4+}/Ti^{3+} ratio, indicating a strong electron doping of the surface layer which suggests a large amount of oxygen vacancies (0.0625 per formula) in this layer.

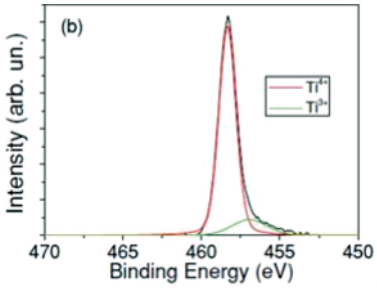

Ar^+-irradiated STO sample. High resolution XPS Ti 2m spectra. F.Y. Bruno et al., Phys. Rev. B83, 245120 (2011)

Scientific Publications

1. **Focused electron beam induced etching of titanium with XeF_2**

   > *Schoenaker, FJ ; Cordoba, R ; Fernandez-Pacheco, R ; Magen, C ; Stephan, O ; Zuriaga-Monroy, C ; Ibarra, MR De Teresa, JM*

   Nanotechnolgy 22, 265304 (2011)

   Impact factor (IF): 3.652

2. **Effect of tantalum nitride supporting layer on growth and morphology of carbon nanotubes by thermal chemical vapor deposition**

   > *Bouchet-Fabre, B ; Fadjie-Djomkam, A ; Fernandez-Pacheco, R ; Delmas, M ; Pinault, M ; Jegou, P Reynaud, C ; Mayne-L'Hermite, M ; Stephan, O ; Minea, T*

   Diamond and Related Materials 20, 999-1007 (2011)

   IF: 1.825

3. **Composite phenolic resin-based carbon molecular sieve membranes for gas separation**

   > *Teixeira, M ; Campo, MC ; Tanaka, DAP ; Tanco, MAL ; Magen, C ; Mendes, A*

   Carbon 49, 4348-4358 (2011)

   IF: 4.896

4. **Three-Dimensional Multiple-Order Twinning of Self-Catalyzed GaAs Nanowires on Si Substrates**

   > *Uccelli, E ; Arbiol, J ; Magén, C ; Krogstrup, P ; Russo-Averchi, E ; Heiss, M ; Mugny, G ; Morier-Genoud, F ; Nygard, J ; Morante, JR ; Morral, AFI*

   Nano Letters 11, 3827-3832 (2011)

   IF: 12.219

5. **Role of growth mode in the formation of magnetic properties of InMnAs grown by MOVPE**

   > *Novak, J ; Vavra, I ; Hasenohrl, S ; Reiffers, M ; Strichovanec, P ; Magen, C*

   Journal of Crystal Growth 318, 576-579 (2011)

   IF: 1.746

6. TEM studies of zeolites and ordered mesoporous materials

> *Diaz, I; Mayoral, A*

Micron 42, 512-527 (2011)

IF: 1.649

7. Hydrodechlorination of chloromethanes with a highly stable Pt on activated carbon catalyst

> *Alvarez-Montero, MA ; Gomez-Sainero, LM ; Mayoral, A ; Diaz, I ; Baker, RT ; Rodriguez, JJ*

Journal of Catalysis 279, 389-396 (2011)

IF: 5.415

8. In-situ immobilization of enzymes in mesoporous silicas

> *Santalla, E ; Serra, E ; Mayoral, A ; Losada, J ; Blanco, RM ; Diaz, I*

Solid State Sciences 13, 691-697 (2011)

IF: 1.828

9. High yield production of long branched Au nanoparticles characterized by atomic resolution transmission electron microscopy

> *A. Mayoral, C. Magen, M. Jose-Yacaman*

Crystal Growth and Design 11, 4538-4543 (2011)

IF: 4.390

10. Flexoelectric tuning of polar rotations in ferroelectric thin films

> *G. Catalan, A. Lubk, A. H. G. Vlooswijk, E. Snoeck, C. Magen, A. Janssens, G. Rispens, G.* Rijnders, D.H.A. Blank and B. Noheda

Nature Materials 10, 963-967 (2011) doi 10.1038/nmat3141

IF: 29.920

11. Nanoalloying in real time. A high resolution STEM and computer simulation study

> *M. M. Mariscal, A. Mayoral, J. A. Olmos-Asar, C. Magén, S. Mejía-Rosales, E. Pérez-Tijerina, M. José Yacamán*

Nanoscale 3, 5013-5019 (2011) doi 10.1039/c1nr11052g

IF: 4.109

12. First evidence of a mechanical coupling between shells in an individual double-walled carbon nanotube

> *D. Levshov, T. Than, R. Arenal, V. N. Popov, R. Parret, M. Paillet, V. Jourdain, A. A. Zahab, T. Michel, J.-L. Sauvajol*

Nano Letters 11, 4800 (2011)

IF: 12.219

13. Electrical and mechanical properties of single-walled BNNTs

> *R. Arenal, M.S. Wang, Z. Xu, A. Loiseau, D.Golberg*

Nanotechnology 22, 265704 (2011)

IF: 3.652

14. Low-Loss Measurements on metallic and insulating nanostructures using a monochromatic electron beam

> *Arenal R*

Microscopy and Microanalysis 17, 768 (2011)

IF: 3.259

15. EELS Measurements on Heteroatomic Single-Walled Nanotubes

> *R. Arenal, O. Stephan, A. Loiseau*

Microscopy and Microanalysis 17, 1512 (2011)

IF: 3.259

16. Gold nanoparticles: 3D-STEM-HAADF analyses and plasmonic studies by EELS

> *R. Arenal, L. Roiban, O. Ersen, J. Burgin, M. Treguer-Delapierre*

Microscopy and Microanalysis 17, 948 (2011)

IF: 3.259

17. Charge transfer in conjugated oligomers encapsulated into carbon nanotubes

> *Y. Almadori, L. Alvarez, R. Arenal, R. Babaa, T. Michel, R. Le Parc, J-L Bantignies, B. Jouselme, S. Palacin, P. Hermet, J-L Sauvajol*

Physica status Solidi B 248, 2560-2563 (2011)

IF: 0.727

18. Charge transfer evidence between carbon nanotubes and encapsulated conjugated oligomers

> *L. Alvarez, Y. Almadori, R. Arenal, R. Babaa, T. Michel, R. Leparc, J-L. Bantignies, P. Hermet, J-L. Sauvajol*

Journal of Physical Chemistry C 115, 11898-11905 (2011)

IF: 4.524

19. Nitrogen-doped single-walled carbon nanotube thin films exhibiting anomalous sheet resistances

> *T. Susi, A. Kaskela, Z. Zhu, P. Ayala, R. Arenal, Y. Tian, P. Laiho, J. Mali, A.G. Nasibulin, H. Jiang, T. Jiang, G. Lanzani, O. Stephan, K. Laasonen, T. Pichler, A. Loiseau, E.I. Kauppinen*

Chemistry of Materials 23, 2201 (2011)

IF: 6.400

20. Processes Controlling the Diameter Distribution of Single-Walled Carbon Nanotubes during Catalytic Chemical Vapor Deposition

> *M. Picher, E. Anglaret, R. Arenal, V. Jourdain*

ACS Nano 5, 2118 (2011)

IF: 9.865

21. Applications of Aberration Corrected Scanning Transmission Electron Microscopy and Electron Energy Loss Spectroscopy to Complex Oxide Materials

> *M. Varela, J. Gazquez, T. J. Pennycook, C. Magén, M. P. Oxley, and S. J. Pennycook*

Scanning Transmission Electron Microscopy: Imaging and Analysis 429-466 (2011)

22. Structural and magnetic properties of amorphous Co-W alloyed nanoparticles

> *A.I. Figueroa, J. Bartolome, L.M. Garcia, F. Bartolome, C. Magen, A. Ibarra, L. Ruiz, J. M. Gonzalez-Calbet, F. Petroff, C. Deranlot, S. Pascarelli, and P. Bencok*

Physical Review B Phys. Rev. B 84, 184423 (2011)

IF: 3.774

23. Anisotropic magnetotransport in $SrTiO_3$ surface electron gases generated by Ar(+) irradiation

> *Bruno, FY; Tornos, J ; del Olmo, MG ; Santolino, GS ; Nemes, NM ; Garcia-Hernandez, M ; Mendez, B ; Piqueras, J ; Antorrena, G ; Morellon, L ; De Teresa, JM; Clement, M ; Iborra, E; Leon, C; Santamaria, J*

Physical Review B 83, 245120 (2011)

IP 3.774

24. Cell death induced by the application of alternating magnetic fields to nanoparticle-loaded dendritic cells

> *Marcos-Campos, I ; Asin, L ; Torres, TE ; Marquina, C ; Tres, A ; Ibarra, MR ; Goya, GF*

Nanotechnology 22, 205101 (2011)

IP 3.652

25. Quantification and minimization of disorder caused by focused electron beam induced deposition of cobalt on grapheme

> *Michalik, JM; Roddaro, S ; Casado, L ; Ibarra, MR ; De Teresa, JM*

Microelectronic Engineering 88, 2063-2065 (2011)

IF: 1.575

26. Direct Observation of Stress Accumulation and Relaxation in Small Bundles of Superconducting Vortices in Tungsten Thin Films

> *Guillamon, I ; Suderow, H ; Vieira, S; Sese, J ; Cordoba, R ; De Teresa, JM; Ibarra, MR*

Physical Review Letters 106, 077001 (2011)

IF: 7.622

27. Fe:O:C grown by focused-electron-beam-induced deposition: magnetic and electric properties

> *Lavrijsen, R ; Cordoba, R ; Schoenaker, FJ ; Ellis, TH Barcones, B ; Kohlhepp, JT; Swagten, HJM; Koopmans, B; De Teresa, JM; Magen, C ; Ibarra, MR; Trompenaars, P ; Mulders, JJL*

Nanotechnology 22, 025302 (2011)

IP 3.652

28. Enhanced exchange and reduced magnetization of Gd in an Fe/Gd/Fe trilayer

> *Romera, M ; Munoz, M ; Maicas, M ; Michalik, JM ; de Teresa, JM; Magen, C ; Prieto, JL*

Physical Review B 84, 094456 (2011)

IF: 3.774

29. Quantitative analysis of the weak anti-localization effect in ultrathin bismuth films

> *Sangiao, S ; Marcano, N ; Fan, J; Morellon, L; Ibarra, MR ; De Teresa, JM*

EPL 95, 37002 (2011)

IF: 2.753

30. Hysteresis loops of individual Co nanostripes measured by magnetic force microscopy

> *Jaafar, M; Serrano-Ramon, L Iglesias-Freire, O ; Fernandez-Pacheco, A ; Ibarra, MR ; De Teresa, JM; Asenjo, A*

Nanoscale Research Letters 6, 407 (2011)

IF: 2.560

31. Tunneling magnetoresistance in epitaxial discontinuous Fe/MgO multilayers

> *Garcia-Garcia, A ; Pardo, JA ; Strichovanec, P ; Magen, C; Vovk, A; De Teresa, JM; Kakazei, GN; Pogorelov, YG; Morellon, L; Algarabel, PA; Ibarra, MR*

Applied Physics Letters 98, 122502 (2011)

IF: 3.841

32. Ferromagnet-superconductor nanocontacts grown by focused electron/ion beam techniques for current-in-plane Andreev Reflection measurements

> *Sangiao, S ; Morellon, L; Ibarra, MR; De Teresa, JM*

Solid State Communications 151, 37-41 (2011)

IF: 1.981

33. Designing Novel Hybrid Materials by One-Pot Co-condensation: From Hydrophobic Mesoporous Silica Nanoparticles to Superamphiphobic Cotton Textiles

> *Pereira, C; Alves, C ; Monteiro, A ; Magen, C; Pereira, AM; Ibarra, A ; Ibarra, MR; Tavares, PB ; Araujo, JP; Blanco, G Pintado, JM ; Carvalho, AP; Pires, J; Pereira, MFR ; Freire, C*

ACS Applied Materials & Interfaces 3, 2289-2299 (2011)

IF: 2.925

34. Distinguishing Magnetic and Electrostatic Interactions by a Kelvin Force Microscopy-Magnetic Force Microscopy Combination

> *Jaafar M; Iglesias-Freire O; Serrano-Ramón L; Ibarra MR; De Teresa JM; Asenjo A*

Beilstein Journal of Nanotechnology 2, 552-560 (2011)

35. Ultrasmall Functional Ferromagnetic Nanostructures Grown by Focused Electron-Beam-Induced Deposition

> *Serrano-Ramon L; Cordoba R; Rodriguez LA; Magen C; Snoeck E; Gatel C; Serrano I; Ibarra MR; De Teresa JM*

ACS Nano 5, 7781-7787 (2011)

IF: 9.865

36. Investigation of the Influence on Graphene by Using Electron-Beam and Photo-Lithography

> *Fan J; Michalik JM; Casado L; Roddaro S; Ibarra MR; De Teresa JM*

Solid State Communications 151, 1574-1578 (2011)

IF: 1.981

37. Morphology, magnetic and resonance properties of Fe/MgO multilayers

> *García-García, A. Vovk, P. Štrichovanec, J. A. Pardo, C. Magén, V. Golub, O. Salyuk, P. A. Algarabel, M. R. Ibarra*

Journal of Physics Conference Series 303, 012052 (2011)

38. Nanoscale chemical and structural study of Co- based FEBID structures by STEM-EELS and HRTEM

> *R. Córdoba, R. Fernández-Pacheco, A. Fernández-Pacheco, A. Gloter, C. Magén, O. Stéphan, M. R. Ibarra, J. M. De Teresa*

Nanoscale Research Letters 6, 592 (2011)

IF: 2.560

39. Effect of the capping on the local Mn oxidation state in buried (001) and (110) $SrTiO_3/La_{2/3}Ca_{1/3}MnO_3$ interfaces

> *S. Estradé, J. M. Rebled,M. G. Walls, F. de la Peña, C. Colliex, R. Córdoba, I. C. Infante, G. Herranz, F. Sánchez, J. Fontcuberta,and F. Peiró*

Journal of Applied Physics 110, 10391-10395 (2011)

IF: 2.079

40. Andreev reflection under high magnetic fields in ferromagnet-superconductor nanocontacts

> *S. Sangiao, J. M. de Teresa, M.R. Ibarra, I. Guillamón, H. Suderow, S. Vieira, L. Morellón*

Physical Review B 84, 233402 (2011)

IF: 3.774

41. On the role of the colloidal stability of mesoporous silica nanoparticles as gene delivery vectors

> *Cebrian, V; Yague, C; Arruebo, M; Martin-Saavedra, FM; Santamaria, J; Vilaboa, N*

Journal of Nanoparticle Research 13, 4097-4108 (2011)

IP 3.253

42. Comparative study of the synthesis of silica nanoparticles in micromixer-microreactor and batch reactor systems

> *Gutierrez, L ; Gomez, L ; Irusta, S ; Arruebo, M ; Santamaria, J*

Chemical Engineering Journal 171, 674-683 (2011)

IP 3.074

43. Hollow porous implants filled with mesoporous silica particles as a two-stage antibiotic-eluting device

> *Perez, LM ; Lalueza, P ; Monzon, M ; Puertolas, JA ; Arruebo, M ; Santamaria, J*

International Journal of Pharmaceutics 409, 1-8 (2011)

IP 3.607

44. Antibacterial action of Ag-containing MFI zeolite at low Ag loadings

> *Lalueza, P ; Monzon, M ; Arruebo, M; Santamaria, J*

Chemical Communications 47, 680-682 (2011)

IP 5.787

45. Microgels for Efficient Protein Purification

> *Mizrahi, B ; Irusta, S ; McKenna, M ; Stefanescu, C ; Yedidsion, L ; Myint, M ; Langer, R ; Kohane, DS*

Advanced Materials 23, H258-H262 (2011)

IP 10.880

46. Efficient tuning of the Pt nano-particle mono-dispersion on Vulcan XC-72R by selective pre-treatment and electrochemical evaluation of hydrogen oxidation and oxygen reduction reactions

> *Kumar, SMS ; Hidyatai, N ; Herrero, JS ; Irusta, S ; Scott, K*

International Journal of Hydrogen Energy 36, 5453-5465 (2011)

IF: 4.057

47. Magnetically Triggered Nanocomposite Membranes: A Versatile Platform for Triggered Drug Release

> *Hoare, T ; Timko, BP ; Santamaria, J ; Goya, GF ; Irusta, S; Lau, S ; Stefanescu, CF ; Lin, DB ; Langer, R; Kohane, DS*

Nano Letters 11, 1395-1400 (2011)

IF: 12.219

48. Zeolite-coated interdigital capacitors for humidity sensing

> *Urbiztondo, M ; Pellejero, I ; Rodriguez, A ; Pina, MP ; Santamaria, J*
Sensors and Actuators B-Chemical 157, 450-459 (2011)
IF: 3.370

49. Size-dependent transfection efficiency of PEI-coated gold nanoparticles

> *Cebrian, V ; Martin-Saavedra, F ; Yague, C ; Arruebo, M Santamaria, J ; Vilaboa, N*
Acta Biomaterialia 7, 3645-3655 (2011)
IF: 4.824

50. Development of Stable, Water-Dispersible, and Biofunctionalizable Superparamagnetic Iron Oxide Nanoparticles

> *Miguel-Sancho, N ; Bomati-Miguel, O ; Salvador, JP ; Marco, MP ; Santamaria, J*
Chemistry of Materials 23, 2795-2802 (2011)
IF: 6.400

51. Al-promoted increase of surface area and adsorption capacity in ordered mesoporous silica materials with a cubic structure

> *Caremona D; Balas F; Mayoral A; Urriolabeitia E; Luque R; Santamaría J*
Chemmical Communications 47, 13337-12339 (2011)
IF: 5.787

52. Bactericidal effects of different silver-containing materials

> *Lalueza P; Monzon M; Arruebo M; Santamaria J;*
Materials Research Bulletin 46, 2070-2076 (2011)
IF: 2.146

53. Explosives detection using nanoporous coatings

> *Pina, MP ; Pellejero, I ; Urbiztondo, M ; Sese, J ; Santamaria, J*
Proc. SPIE 8031, 803124 (2011); doi:10.1117/12.883780

54. Membranes and films based on zeolites: emerging applications

> *Pina M.P., Mallada, R., Arruebo, M., Urbitzondo, M., Navascués, N., de la Iglesia, O., Santamaria, J.*
Microp. Mesop. Mater., 144, 19-27 (2011).

55. Structural study on the Al distribution in zeolites Nu-6(1) and Nu-6(2)

> *Galve, A ; Gorgojo, P ; Navascues, N ; Casado, C; Tellez, C ; Coronas, J*

Microporous and Mesoporous Materials 145, 211-216 (2011)

IF: 3.220

56. Synthesis, Swelling, and Exfoliation of Microporous Lamellar Titanosilicate AM-4

> *Casado, C ; Ambroj, D ; Mayoral, A ; Vispe, E ; Tellez, C ; Coronas, J*

European Journal of Inorganic Chemistry 14, 2247-2253 (2011)

IF: 2.910

57. Chiral Imprinting with Amino Acids of Ordered Mesoporous Silica Exhibiting Enantioselectivity after Calcination

> *Lacasta, S ; Sebastian, V ; Casado, C ; Mayoral, A ; Romero, P; Larrea, A ; Vispe, E ; Lopez-Ram-de-Viu, P ; Uriel, S ; Coronas, J*

Chemistry of Materials 23, 1280-1287 (2011)

IF: 6.400

58. Direct exfoliation of layered zeolite Nu-6(1)

> *Gorgojo, P ; Galve, A ; Uriel, S ; Tellez, C; Coronas, J*

Microporous and Mesoporous Materials 142, 122-129 (2011)

IF: 3.220

59. Copolyimide mixed matrix membranes with oriented microporous titanosilicate JDF-L1 sheet particles

> *Galve, A ; Sieffert, D ; Vispe, E ; Tellez, C; Coronas, J; Staudt, C*

Journal of Membrane Science 370, 131-140 (2011)

IF: 3.673

60. Mixed matrix membranes comprising glassy polymers and dispersed mesoporous silica spheres for gas separation

> *Zornoza, B ; Tellez, C ; Coronas, J*

Journal of Membrane Science 368, 100-109 (2011)

IF: 3.673

61. Hollow silicalite-1 sphere-polymer mixed matrix membranes for gas separation

> *Zornoza, B ; Esekhile, O ; Koros, WJ; Tellez, C ; Coronas, J*

Separation and Purification Technology 77, 137-145 (2011)

IF: 2.775

62. Insight into the crystal synthesis, activation and application of ZIF-20

> *Seoane B; Zamaro JM; Tellez C; Coronas J*

RSC Advances 1, 917-922 (2011)

63. Combination of MOFs and Zeolites for Mixed-Matrix Membranes

> *Zornoza B; Seoane B; Zamaro JM; Tellez C; Coronas J*

ChemPhysChem 12, 2781-2785 (2011)

IF: 3.340

64. Manifold domain structure of double films with perpendicular magnetic anisotropy

> Coffey, D ; Diez-Ferrer, JL ; *Corredor, EC;* Arnaudas, JI; Ciria, M

Journal of Physics D – Applied Physics 11, 115001 (2011)

IP 2.109

65. Long-range electron tunnelling tunnelling in oligo-porphyrin molecular wires.

> G. Sedghi, V. M. García-Suárez, L. J. Esdaile, H. L. Anderson, C. J. Lambert, S. Martin, D. Bethell, S. J. Higgins, M. Elliott, N. Bennett, J. E. Macdonald, R. J. Nichols

Nature Nanotechnology 6, 517-523 (2011)

IF: 30.306

66. Ultrasensitive Broad Band SQUID Microsusceptometer for Magnetic Measurements at Very Low Temperatures

> Martinez-Perez, MJ ; Sese, J ; Luis, F; Cordoba, R ; Drung, D Schurig, T; Bellido, E ; de Miguel, R ; Gomez-Moreno, C ; Lostao, A ; Ruiz-Molina, D

IEEE Transactions on Applied Superconductivity 21, 345-348 (2011)

IF: 1.035

67. Alternating current magnetic susceptibility of a molecular magnet submonolayer directly patterned onto a micro superconducting quantum interference device

> Martinez-Perez, MJ ; Bellido, E ; de Miguel, R ; Sese, J ; Lostao, A ; Gomez-Moreno, C ; Drung, D; Schurig, T ; Ruiz-Molina, D ; Luis, F

Applied Physics Letters 99, 032504 (2011)

IF: 3.841

68. Ferritin: nanotechnology at the service of the new biomedicine

> De Miguel, R ; Martinez-Perez, MJ ; Martinez-Julvez, M ; Fiddyment, S ; Garcia-Ortin, AL ; Gomez-Moreno, C; Luis, F; Lostao, A

FEBS Journal 278, 155-156 (2011)

IF: 3.129

69. Molecular Prototypes for Spin-Based CNOT and SWAP Quantum Gates

> Luis, F ; Repolles, A ; Martinez-Perez, MJ ; Aguila, D ; Roubeau, O ; Zueco, D Alonso, PJ ; Evangelisti, M; Camon, A ; Sese, J ; Barrios, LA ; Aromi, G

Physical Review Letters 107, 117203 (2011)

IF: 7.622

70. "In Situ" Photopolymerization of Biomaterials Via Thiol-yne Click Chemistry

> *Lomba M; Oriol L; Alcala R; Sanchez C; Moros M; Grazu V; Serrano JL; de La Fuente JM*

Macromolecular Bioscience 11, 1505–1514 (2011)

IF: 3.458

71. Magnetoelastic Effects in Nanostructures

> *Arnaudas, JI; Badia-Majos, A; Berbil-Bautista, L; Bode, M; Castano, FJ; Ciria, M; de la Fuente, C; Diez-Ferrer, JL ; Krause, S; Ng, BG ; O'Handley, RC; Ross, CA; Wiesendanger, R*

Solid State Phenomena 168-169, 177-184 (2011)

Highlights

Evidence of flexolectricity in $PbTiO_3$

The strain and polarization distribution inside twinned epitaxial films of perovskite ferroelectric $PbTiO_3$ has been successfully mapped by STEM-HAADF on the LMA Titan G2 STEM microscope. Quantitative image analysis was used to map both strain and polarization across the layer (see fig.). They reveal the appearance of strain gradients both in the vertical and, unexpectedly, the horizontal direction. These strain gradients have a geometric origin, and generate a horizontal flexoelectricity that forces the spontaneous polarization to rotate away from the normal direction. Polar rotations are otherwise a feature of compositionally engineered morphotropic phase boundary ferroelectrics with giant piezoelectricity.

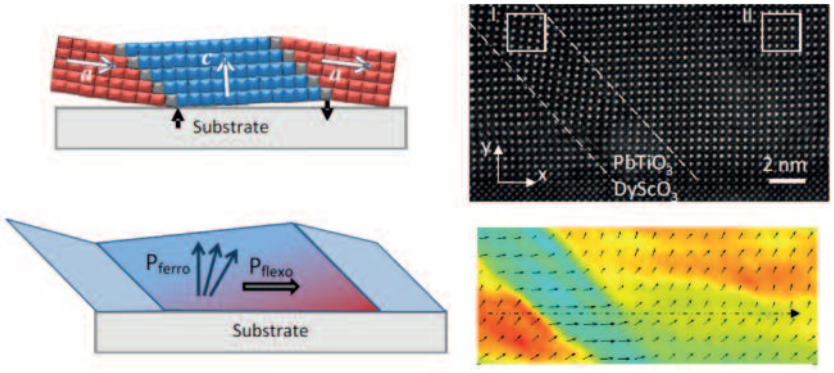

(a) Schematic representation of the domain structure in a film with a-c domains. The black arrows represent the stresses that must be applied to the twinned film in order to flatten it onto the substrate. (b) the flexoelectric polarization (grey) induces a rotation of the ferroelectric polarization of the c domain (blue), c) HAADF STEM image showing the two ferroelectric a-c domains. d) Out-of-plane strain (colour map) and electric polarization (vector map).The colour map confirms the strain difference between acute and obtuse corners as well as the polar rotations in the c-domains, while the line scan confirms that the rotation angle tends towards 10 degrees off the normal direction.

Reference(s):

G. Catalan, A. Lubk, A. H. G. Vlooswijk, E. Snoeck, C. Magen, A. Janssens, G. Rispens, G. Rijnders, D.H.A. Blank and B. Noheda. Nature Materials 10, 963–967 (2011) doi:10.1038/nmat3141

Highlights

Atomic analysis of zeolites

The three-dimensional structure of Ag ion-exchanged zeolite A was studied by powder XRD and aberration corrected scanning transmission electron microscopy. Despite the difficulties in the microscopic investigation of zeolites with high Al content, the arrangement of isolated Ag ions and Ag clusters of six atoms was visualized.

After recording several micrographs along the main crystallographic orientations, it could be elucidated that the Ag_6 adopted an octahedral morphology surrounded by 8 Ag cations (see figure).

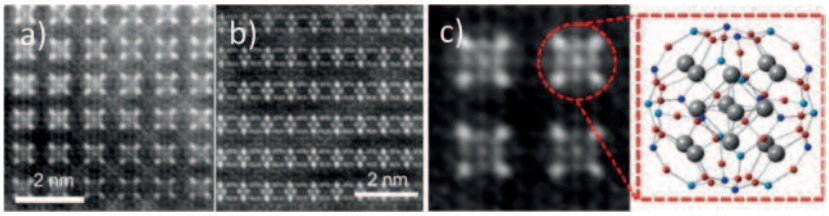

a) HAADF-STEM recorded along the [001] and b) the [011] orientations.
c) Closer observation of the zeolite cavities where the Ag ions and Ag clusters (white) can be unambiguously elucidated. The proposed atomistic model (Ag in grey) corresponding to one the zeolite cages, marked by a red dashed circle, is also shown.

Reference(s):

A. Mayoral,* T. Carey, P. A. Anderson, A. Lubk, and Isabel Diaz
Angew. Chem. Int. Ed. 2011, 50, 11230 –11233

Highlights

Atomic structure of individual suspended carbon nanotubes

These studies have combined HRTEM and electron diffraction techniques to develop deep structural/atomic studies on individual carbon nanotubes produced by catalytic chemical vapor deposition (CCVD). These NT have high structural quality and no chiral angle modification was observed, nor diameter change along the whole nanotube length. Figure shows one of those NT, which correspond to a (21,21) @ (28,26) @ (36,29) NT. Most of the studied NT are double-walled. The structural correlation between the two adjacent layers/shells composing a DW (inner and outer NT) was examined. Regarding the chiral angle difference between these 2 shells, it was observed that 78 % of the cases is lower than 5°. These studies shed light on the structure of very long NT and of DW-NT especially which is necessary in order to apply them in real devices.

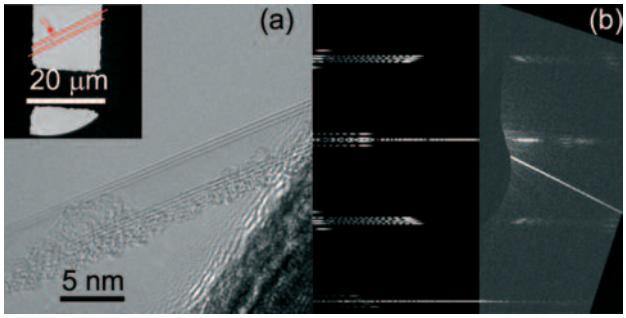

(a) HRTEM image of a triple-walled (TW) carbon nanotube (inset: low-magnification micrograph of this NT). (b) Experimental and simulated EDP of this TW-NT, respectively. These EDP were unambiguously assigned to a (21, 21) @ (28, 26) @ (36, 29) NT.

References:

(1) R. Arenal, P. Loehtman, M. Picher, V. Jourdain, submitted to J. Phys. Chem. C (2011).
(2) D. Leshov, T. Than, R. Arenal et al., Nano Letters 11, 4800 (2011).

Highlights

Alternating current magnetic susceptibility of a molecular magnet submonolayer directly patterned onto a micro superconducting quantum interference device

The article reports the controlled integration, via dip pen nanolithography (DPN), of submonolayer arrays of ferritin-based 2 nm CoO nanoparticles (12 μ_B) into the most sensitive areas of a microSQUID sensor. Furthermore, the molecular deposition is carried out under ambient conditions and implies no chemical functionalization of the sensor neither of the sample. The nearly optimum flux coupling between these nanomagnets and the microSQUID improves the achievable sensitivity by a factor 10^2, enabling us to measure the linear susceptibility of the molecular array down to very low temperatures (13 mK). This method opens the possibility of applying ac susceptibility experiments to characterize two-dimensional arrays of single molecule magnets within a wide range of temperatures and frequencies.

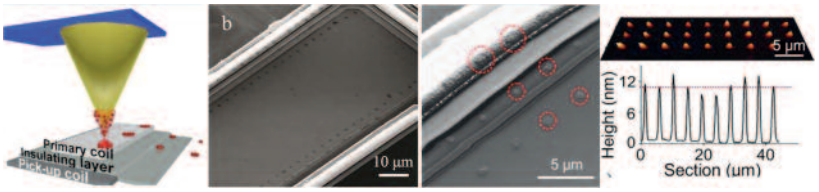

Scheme, SEM and AFM images of 3 rows of monolayer CoO@ferritin dots organized on the most active areas of the sensor using DPN.

Reference(s):

Martínez-Pérez MJ; Bellido E; de Miguel R; Sesé J; Lostao A; Gómez-Moreno C; Drung D; Schurig T; Ruiz-Molina D; Luis F, Appl. Phys. Lett. 99 032504 (2011) (selected for the August 1, 2011 issue of Virtual Journal of Nanoscale Science & Technology)

Highlights

Long-range electron tunnelling in oligo-porphyrin molecular wires

Based on electrical measurements of single-molecule junctions, show that the conductance of oligo-porphyrin wires has a strong dependence on temperature, and a weak dependence on the length of the wire. Although it is widely accepted that such behaviour is a signature of a thermally assisted incoherent (hopping) mechanism, density functional theory calculations and an accompanying analytical model strongly suggest that the observed temperature and length dependence is consistent with phase-coherent tunnelling through the whole molecular junction.

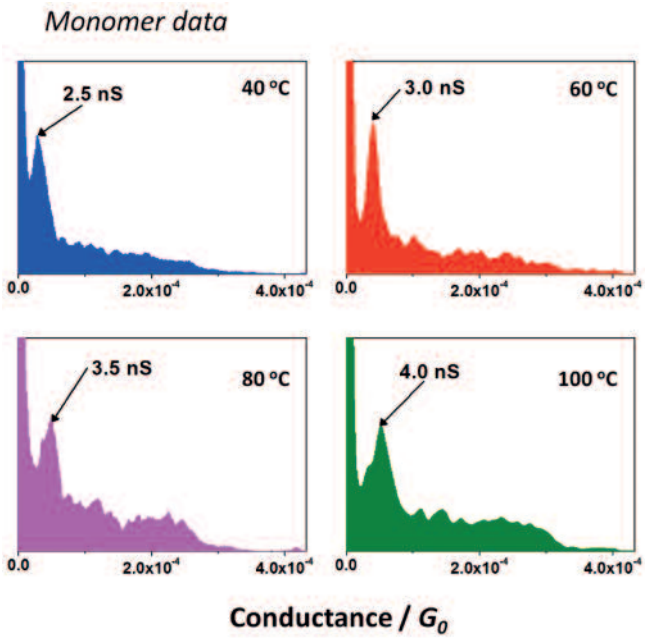

Conductance histograms for a porphyrin recorded for the temperatures shown in the figure. Vbias = 0.6 V and with a set point current of 8 nA.

Reference:

G. Sedghi, V. M. García-Suárez, L. J. Esdaile, H. L. Anderson, C. J. Lambert, S. Martin, D. Bethell, S. J. Higgins, M. Elliott, N. Bennett, J. E. Macdonald, R. J. Nichols, Nature Nanotechnology, 6 517-523 (2011)

Highlights

Controlled manipulation of the word "ARAGÓN" employing 68 Co atoms and one atom of silver

Individual Co atoms on a surface were manipulated one by one using the tip of a low temperature scanning tunneling microscope (STM) to construct the word "ARAGÓN". The method requires full stability and control of tip position with sub-atomic control. Once the tip is positioned on an individual atom, it is approached and moved laterally till the desired position, dragging the atom to rest at this final site. The manipulation persecuted to lay the atom at the same type of adsorption site (on a (111) surface of fcc crystal there are two possible hollows adsorption sites). Chemical identification of Co atoms and Ag adatoms was done by tunneling spectroscopy; in particular, by the presence or absence of a characteristic Kondo resonance in Co and Ag adatoms, respectively.

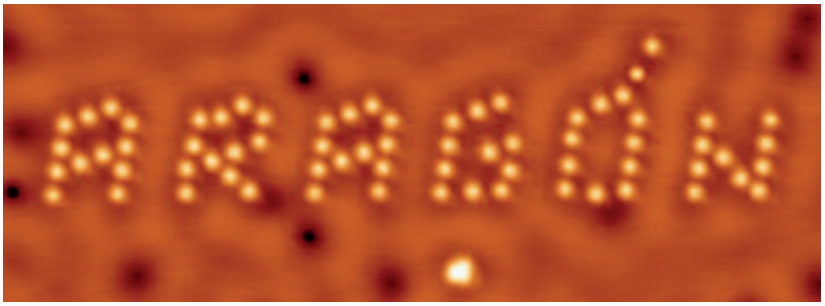

"ARAGÓN" nanostructure composed of 68 Co atoms manipulating by dragging them to selected locations on a Ag(111) surface. This shows the ultimate control on atomic manipulations.

Highlights

Ultrasmall Functional Ferromagnetic Nanostructures Grown by focused Electron-Beam-Induced Deposition

Ultra-small cobalt nanostructures (lateral size below 30 nm) have been successfully grown by optimization of the growth conditions using focused-electron-beam-induced-deposition techniques. This direct-write nanolithography technique is thus shown to produce unprecedented resolution in the growth of magnetic nanostructures. The challenging magnetic characterization of such small structures was carried out by means of electron-holography techniques. Apart from growing ultra-narrow nanowires, very small Hall sensors have been created and their large response unveiled.

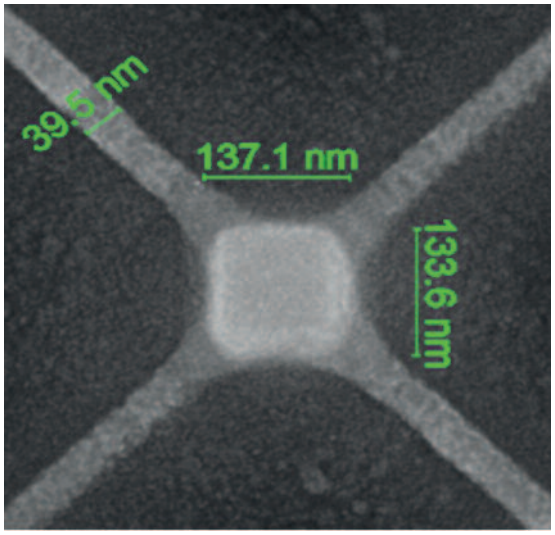

Ultra-narrow Hall sensor based on cobalt grown by focused electron-beam-induced deposition

Reference(s): Serrano-Ramon L; Cordoba R; Rodriguez LA; Magen C; Snoeck E; Gatel C; Serrano I; Ibarra MR; De Teresa JM, ACS Nano 5 (10) 7781-7787 (2011)

Highlights

Direct observation of stress accumulation and relaxation in small superconducting vortex bundles

The behavior of bundles of superconducting vortices when increasing the magnetic field have been studied using scanning tunneling microscopy and spectroscopy (STM/S) at 100 mK. Pinning centers are given by features on the surface corrugation. Strong net vortex motion in a bundle towards a well defined direction has been found. It has also been observed continuous changes of the vortex arrangements, and identified small displacements, which stress and deform the vortex bundle, separated by larger re-arrangements or avalanches, which release accumulated stress.

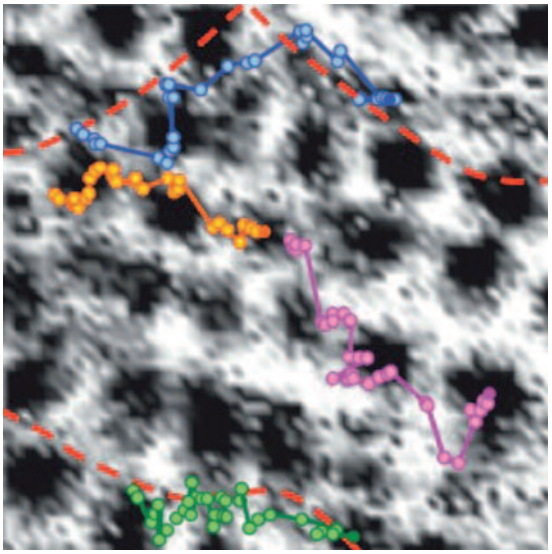

Movement of selected vortices in superconducting W nanostructures grown by focused ion-beam-induced deposition. The images have been taken at 100 mK under application of magnetic field (from 1 T to 1.2 T) using scanning tunneling spectroscopy

Reference(s):

I. Guillamón, H. Suderow, S. Vieira, J. Sesé, R. Córdoba, J M De Teresa, M R Ibarra, Phys. Rev. Lett. 106 (2011) 077001

Highlights

Andreev reflection under high magnetic fields in ferromagnet-superconductor nanocontacts

The magnetic-field dependence of the conductance in planar ferromagnet-superconductor nanocontacts created with focused-electron/ion-beam techniques has been studied. From the fits of the differential conductance curves in high magnetic fields, the magnetic field dependences of the superconducting gap and the broadening parameter are obtained. Orbital depairing is found to be linear with magnetic field. The magnetic field dependence of the quasiparticle density of states is evaluated and compared with the value obtained by scanning tunneling spectroscopy experiments.

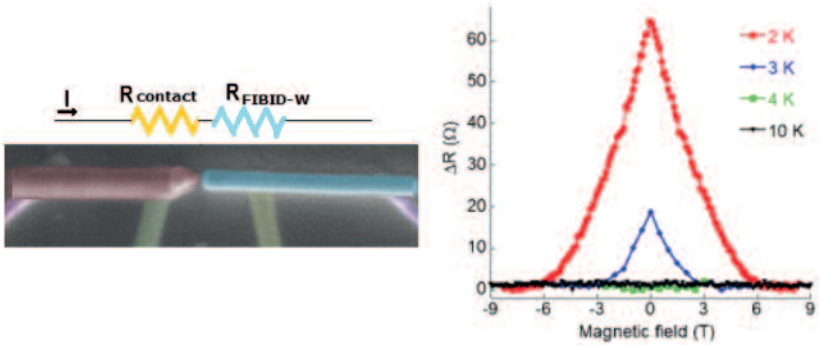

In the shown Co ferromagnetic-W superconducting nanocontact, change in resistance (relative to the value just below the resistive transition) with the applied perpendicular magnetic field at different temperatures for an applied current of 50 nA.

Reference(s):

S. Sangiao, J. M. de Teresa, M.R. Ibarra, I. Guillamón, H. Suderow, S. Vieira, L. Morellón, Phys. Rev. B 84 (2011) 233402

Highlights

Focused electron beam induced etching of titanium with XeF_2

Titanium is a relevant technological material due to its extraordinary mechanical and biocompatible properties, its nanopatterning being an increasingly important requirement in many applications. The successful nanopatterning of titanium by means of focused electron beam induced etching using XeF_2 as a precursor gas is reported. Etch rates up to 1.25×10^{-3} $\mu m^3 s^{-1}$ and minimum pattern sizes of 80 nm were obtained. Different etching parameters such as beam current, beam energy, dwell time and pixel spacing were systematically investigated, the etching process being optimized by decreasing both the beam current and the beam energy. The etching mechanism was investigated by transmission electron microscopy.

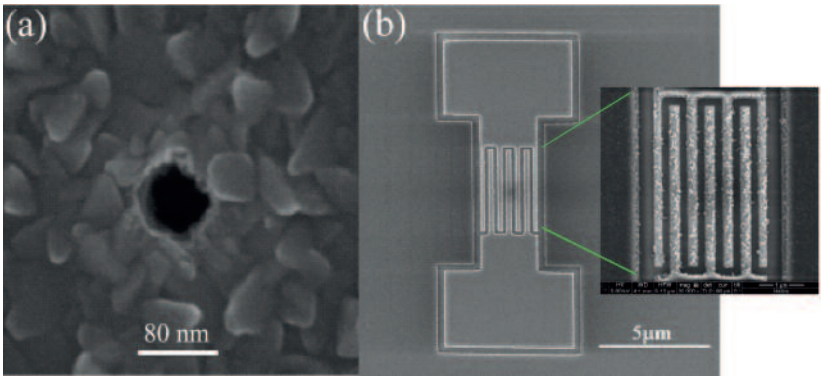

(a) SEM image of a spot etching with a 5.1 pA beam current and 120 s etching time. (b) Interdigitated nanoelectrodes with 200 nm resolution patterned by XeF_2-based FEBIE.

Reference(s):

F J Schoenaker, R Córdoba, R Fernández-Pacheco, C Magén, O Stéphan, C. Zuriaga-Monroy, M R Ibarra, J M De Teresa, Nanotechnology 22 (2011) 265304

Highlights

Strain-induced magnetization reorientation and magnetic anisotropy in epitaxial Cu/Ni/Cu rings

Ni rings of different widths (w) with diameters (D) of 1 and 3 μm have been obtained by means of a subtractive process on epitaxial Cu/Ni/Cu films grown by e-beam evaporation in ultra high vacuum. The lithography techniques include focused ion beam and electron-beam writing as well as ion-beam etching using a Al-Cr hard mask. MFM images taken on the rings with D = 3 μm and w=250 nm (see image) show a domain structure compatible with a magnetization vector pointing along the radial direction. This fact is explained by the existence of a transverse magnetoelastic anisotropy, due to an in-plane anisotropic relaxation of the strain existing in the continuous film that suggests that the fabrication process does not degrade the crystalline structure of the Ni films.

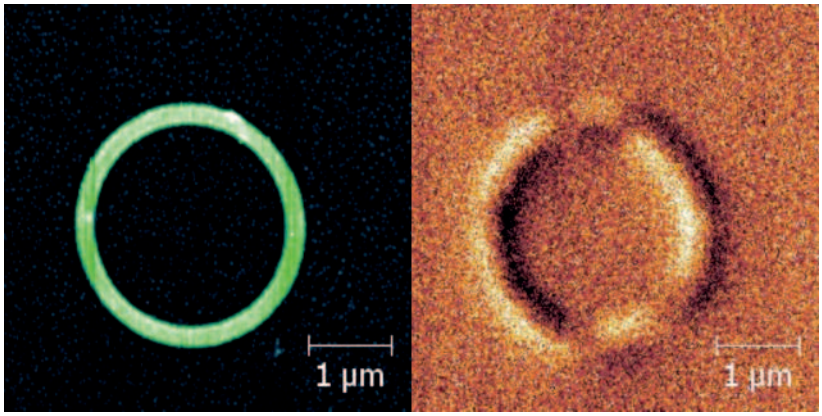

Images of a ring (left) and its magnetic domain structure (right) taken with a magnetic force microscope .

Reference(s):

E.C. Corredor, D. Coffey, J. I. Arnaudas, and Miguel Ciria, "Strain-induced magnetization reorientation and magnetic anisotropy in epitaxial Cu/Ni/Cu rings" in preparation

Highlights

Ultrasensitive Broad Band SQUID Microsusceptometer for Magnetic Measurements at Very Low Temperatures

This work reports the development and calibration of an ultrasensitive SQUID susceptometer capable of operating over an extremely wide frequency range (0.001Hz–1 MHz) at extremely low temperatures (13 mK). Starting with 2-stage SQUID sensors fabricated at PTB-Berlin, an integrated susceptometer with experimental spin sensitivity of 10^4 Bohr magneton/$Hz^{1/2}$ is obtained by rerouting some SQUID input circuit connections. Modification of the chips is carried out using Focused Ion Beam Induced Deposition (FIBID) of amorphous W, using $W(CO)_6$ as precursor gas. We have demonstrated that superconducting connections between W FIBID lines and Nb films can be fabricated and that they operate at 4.2 K, providing a powerful technique for fixing errors in device designs, repairing damaged circuits, or modifying existing ones. The microsusceptometer is used for the study of monolayers of nanosized magnets, and has potential applications in diverse fields such as quantum computing, high-density information storage or on-chip magnetic refrigeration.

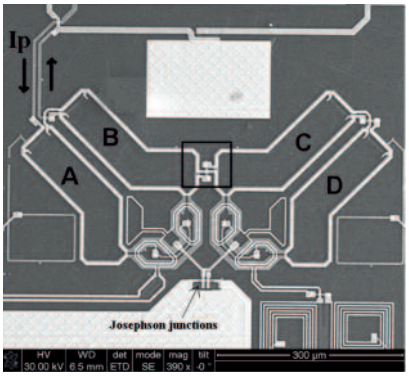

Figure caption: SEM picture of the front-end SQUID. The main contribution of the SQUID loop inductance comes from the four coils A. B, C and D that are connected in parallel. Those are the sensitive areas used to locate the sample to be measured. Ip is the primary current that creates the exciting field. The center square is the modified region using a Helios DualBeam.

Reference(s):

Martínez-Pérez MJ; Sesé J; Luis F; Cordoba R; Drung D; Schurig T; Bellido E; de Miguel R; Gómez-Moreno C; Lostao A; Ruiz-Molina D *IEEE Trans. Appl. Supercond.* 21 (3) 345-348 (2011)

Martínez-Pérez MJ; Bellido E; de Miguel R; Sesé J; Lostao A; Gómez-Moreno C; Drung D; Schurig T; Ruiz-Molina D; Luis F *Appl. Phys. Lett.* 99 art. nr. 032504 (2011)

Luis F; Repollés A; Martínez-Pérez MJ; Aguila D; Roubeau O; Zueco D; Alonso PJ; Evangelisti M; Camón A; Sesé J; Barrios LA; Aromí G *Phys. Rev. Lett.* 107 art nr 117203 (2011)

Highlights

Study of Cell Adhesion Events using Novel Biomaterials using Scanning Electron Microscopy

Sodium hyaluronate has been crosslinked by photoinduced decomposition of a trifunctionaldiazonium salt to generate new biomaterials called H5. Thin films of formulations of chemically unmodified sodium hyaluronate and the photocrosslinker at different percentages have been processed. 2D patterns of controlled geometry have been generated by direct laser writing to perform cell adhesion studies. Different adhesion behavior of the cell lines, as assessed by scanning electron microscopy, has been observed in the polymeric films depending on the degree of photocrosslinking. These differences on the adhesive/antiadhesive balance could allow to control cell distribution as it happened on H5 patterns, where cells migrate to the glass substrates due to the low affinity for the material. Furthermore, low attachment of cells onto the polymeric pattern promote migration, what yield to a very selective distribution of cells onto the glass areas.

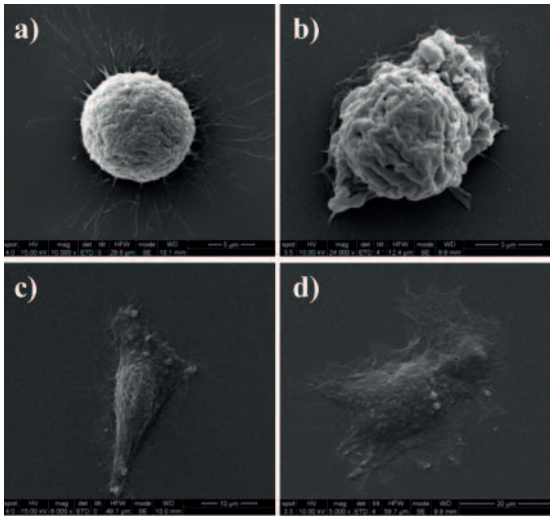

Scanning electron microscopy (SEM) images of HeLa cells (a, c) and COS-7 fibroblasts (b, d) cultured onto flood–exposed substrates of H5 (a, b) and glass substrates (c, d).

Reference:

Lomba M.; Oriol L.; Alcalá R.; Sánchez C.; Moros M.; Grazú V.; Serrano J.L.; De la Fuente, J.M. "In situ" photopolymerization of biomaterials via thiol-yne click chemistry. Macromolecular Bioscience 11 (2011) 1505-1514.

Highlights

Cross sectional analysis of magnetically-loaded human neuroblastoma cells for neural regeneration

We have obtained cross-sectional analysis of human neuroblastoma SH-SY5Y cell line loaded magnetic nanoparticles (MNPs) used as functional nano-objects to enhance the nerve regeneration and provide guidance to regenerate axons by mechanical forces under the influence of a static magnetic field. The intracellular distribution of the MNPs at the single-cell level was successfully obtained from combined SEM-EDX and dual-beam (FIB/SEM) analysis. The results showed large clusters of the MNPs strongly attached to the cell membrane, with partial internalization crossing the membrane. This novel strategy for analyzing intracellular fate of MNPs demonstrated its flexibility and simplicity for determining the physical state of magnetically loaded cells.

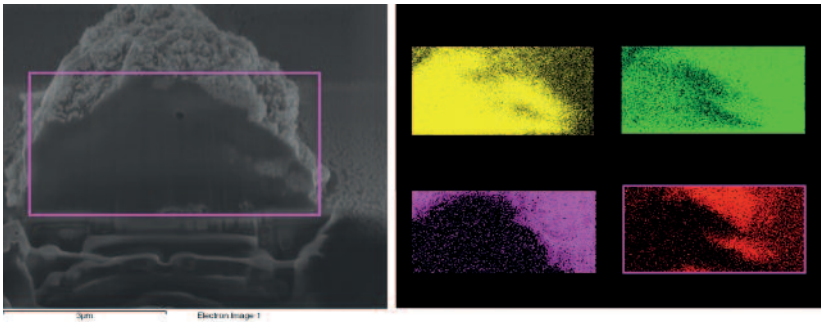

Figure caption: cross section image of magnetically-loaded SH-SY5Y neuroblasts, and EDX mapping showing distribution of carbon C, oxygen (O) and iron (red)..

Reference:
M.P. Calatayud, C. Riggio, V. Raffa, B. Sanz, T.E. Torres, M. R. Ibarra, C. Hoskins, A. Cuschieri, L.Y. Wang and G.F. Goya; "Magnetic Loading of Human Neuroblastoma Cells for magnetically assisted neural guidance", ACS Nano, submitted.

Highlights

Microgel for efficient Protein Purification

Immobilized metal affinity chromatography (IMAC) is the most frequently used method for the separation and purification of histidine –tagged (his – tagged) proteins. In collaboration with MIT researchers, the internal structure of particles where the metal –chelating moiety, nitrilotriacetic acid (NTA), is distributed throughout the entire matrix was analized. The nickel ions density in the microgel were examined by dual beam miscroscopy (a combination of a focused ion beam with an electron beam that allows SEM imaging and local elemental analysis by energy –dispersive X-ray (EDX) of localized cross-sections (FEI Nova 200 Nanolab). The microgel particles exhibited micrometer scale corrugated features with channels on the outer surface on pores in the body. This technique confirmed that our method produced high concentrations of nickel from surface to core.

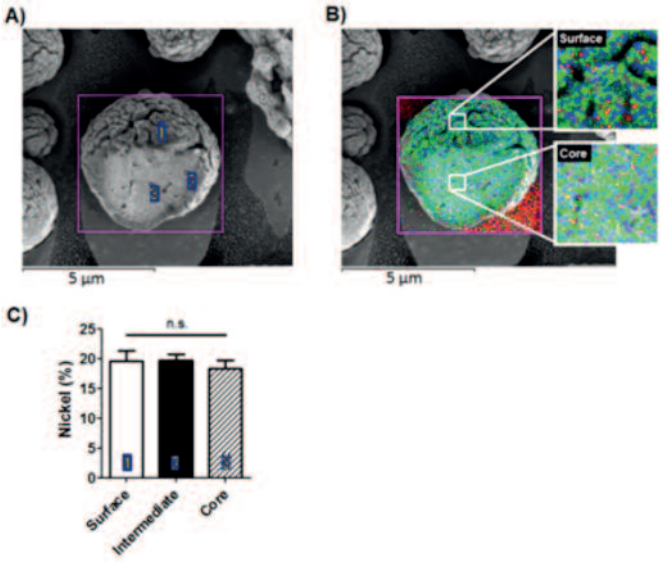

A) SEM micrographof ion-milled microgel particle displaying the surface and the core. Numbers indicate locations analyzed for nickel content at (1) the surface, (2) an intermediate location, and (3) the core. B) SEM/EDZ map for nickel in the same particles shown in A). Nickel is indicated by turquoise dots. Insets: enlargement of the surface and the core. Pores are in black. C) Nickel mean density (% w/w) throughout the microgel particle at the locations indicate in A).

Reference:

Boaz Mizrahi, Silvia Irusta, Marshal McKenna, Liron Yedidsion, Robert Langer, and Daniel S. Kohane. Advanced Materials 23 (2011) H258-H262

List of Activities

Summer Course July 9-8, 2011	**Técnicas de nanofabricación para aplicaciones en Nanotecnología** University of Zaragoza Summer Courses. Jaca (Huesca)
Users course March 8, 2011	**Basics of Transmission Electron Microscopy (TEM) I** Alfonso Ibarra (INA-LMA/UZ)
Users Course March 15, 2011	**Basics of Transmission Electron Microscopy (TEM) II** Alfonso Ibarra (INA-LMA/UZ)
Users Course July 11 & 15, 2011	**Local Probe Microscopy. Theory and Practice** José Luis Díez (INA-LMA/UZ)
Users Course Dec 12 & 16, 2011	**Local Probe Microscopy. Theory and Practice** José Luis Díez (INA-LMA/UZ)
Course Dec 14-16, 2011	**1st School on Advanced Transmission Microscopy** Jointly organized by INA-LMA/UZ – CEMS Toulouse & CICNanogune
Lecture January 11, 2011	**Principles and Prospects of Electron Tomography** Zineb Shagy (University of Cambridge, UK)
Lecture March 31, 2011	**Focused electron beam induced deposition** Hans Mulders (FEI International)

Lecture
April 28, 2011

TEM studies on nanocrystals: HR(S)TEM, tomography...
Lionel Cervera Gontard (Oxford University, UK)

Lecture
May 12, 2011

Cryo-Electron Microscopy
Matthijn Vos (FEI International)

Lecture
July 13, 2011

Magnetic characterization of single nanostructures
Hans Peter Oepen (University of Hamburg)

Lecture
Sept 15, 2011

EELS & FIB investigation of nanostructures in Materials and Life sciences
Cécile Hébert (Interdisciplinary Center for Electron Microscopy, Ecole Polytechnique Federale de Lausanne, Switzerland)

Lecture
October 17, 2011

New techniques for TEM nano-analysis: precession diffraction and 3D diffraction tomography for structure determination and (EBSD-TEM like) high resolution phase/orientation maps
Stavros Nicolopoulos (Consultant at the International Union of Crystallography, Electron crystallography Comission; Director NanoMEGAS SPRL, Belgium)

Lecture
Dec 9, 2011

In-situ science in a corrected TEM: iTEAM project
Néstor Zaluzec (Argonne National Laboratory, USA)

Course
Dec 14-16, 2011

Advanced Transmission Electron Microscopy.
Jointly organized by LMA, CICNanoGune and CEMES Toulouse

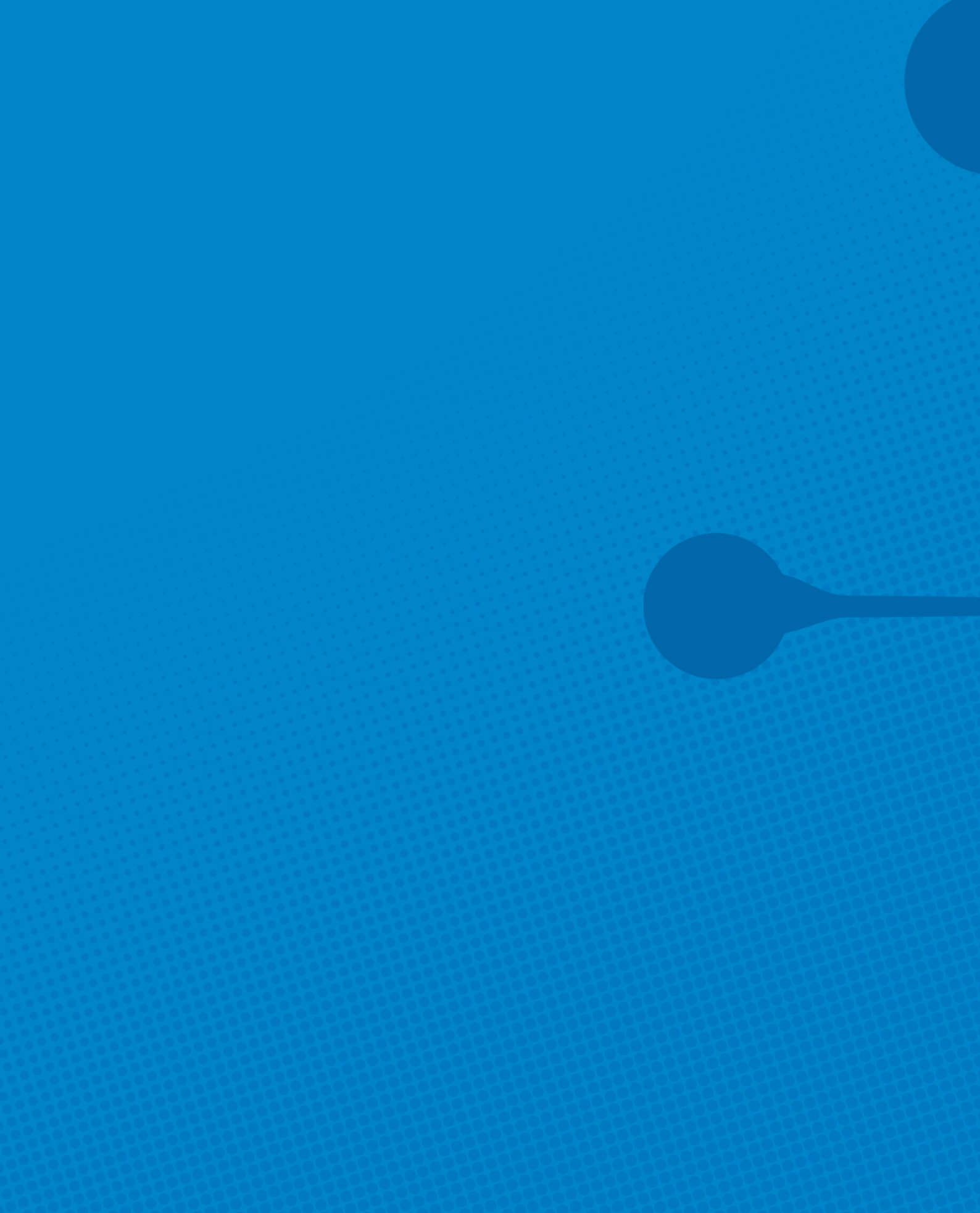

LMA and the industry

LMA and the industry

In 2011, the Advanced Microscopy Laboratory has offered the experience of their researchers and technical staff to provide service to several private companies in order to help them to solve production problems and advance in their R&D projects. They have been able to benefit from the transfer of our technical knowledge and experience in highly advanced characterization and fabrication techniques. These companies belong to branches of industry as diverse as electronics and microelectronics, biotechnology, white goods industry, telecommunications, chemistry, logistic or automotive industry. A list of several private companies from Spain and from abroad which have benefited from these services is provided below. A short description of their industrial activity and the type of study carried out at the LMA is also mentioned.

Laboratorios Argenol, S.L. > *manufacture and sale of Silver-based products.* Morphology and distribution analysis of Ag and Cu Nanoparticles (STEM, EDS, instrument F30)

Soluciones Extractivas Alimentarias, S.L. (SOLUTEX) > *Supercritical CO_2 Extraction Technology applied to Food & Beverage, Cosmetics and Pharmacy.* Morphology analysis of Nanoparticles using Transmission Electron Microscopy (TEM, Tecnai T20)

Abalonyx AS > *cleantech SME with focus on nanostructured, biomimetic materials based on nano-composites, nano-laminates and coatings.* Whole characterization of graphene based samples by Ultra-High resolution Transmission Electron Microscopy (Cs-corrected HRTEM), Atomic Force Microscopy (AFM), and x-ray photoelectron microscopy (XPS)

Enagas, S.A. > *Technical Manager of the Gas System and Common Carrier for the high pressure gas network in Spain.* Characterization by Scanning electron Microscopy (SEM) and Energy-dispersive X-ray Spectroscopy (EDX) of unknown powder detected in some pipes.

Industrias químicas del Ebro, S.A. (IQE) > *Specialized in the field of basic inorganic chemistry, it produces soluble silicates and derivatives.* Characterization by Scanning electron Microscopy (SEM) and Energy-dispersive X-ray Spectroscopy (EDX) of silicate based samples

AlphaSIP > *Design, development and production of molecular diagnostic chips.* Microfabrication in Clean Room using photolithography laboratory. Optical lithography training of Alphasip selected staff. Surface characterization of nanomaterials by High resolution Spectroscopy and imaging modes of XPS. Scanning electron Microscopy (SEM / EDX) analysis of functionalized nanomaterials for chips.

Baolab Microsystems, S.L. > *design and commercialization of products based on Nano Embedded Mechanical Systems technology (NanoEMS™).* CMOS devices fabricated by optical lithography techniques were tested by cross-sectional FIB (focused ion beam).

BSH Electrodomésticos España, S.A. > *BSH Group is the largest manufacturer of home appliances in Europe.* Evaluation of the plasma cleaning process in steel surfaces in order to characterize the growth and adhesion of silica films and perform the usability of silicon based glues Techniques: SEM-EDX, AFM and XPS. SEM-EDX, AFM and XPS characterization of Si-coated steel based samples in order to evaluate cleaning process and optimize parameters. XPS characterization of laser marking effects in several samples as a characterization tool of process parameters. (Research project in collaboration with UZ).

Valeo Térmico, S.A. > *Valeo Grup is fully focused on the design, production and sale of components, integrated systems and modules for the automotive industry.* Study of soldering processes by X-ray Photoelectron Spectroscopy (XPS) and analysis of production samples.

Faci Metalest, S.L. > *production of carboxylic acid derivatives.* Morphology analysis of organic samples.

Teltronic > World leader in the design and manufacturing of mission-critical radio communications equipment and systems. Scanning electron microscopy and EDX analysis of defective parts (screws).

Eficiencia Energética Aplicada > SME company with projects in the synthesis of graphene. Scanning electron microscopy and EDX analysis.

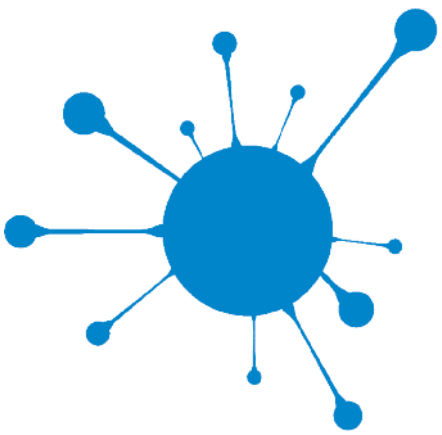

EDITA:
Laboratorio
de Microscopías Avanzadas
C/ Mariano Esquillor, s/n.
50018 Zaragoz (Spain)
Tel. +34 976 762 980
Fax +34 976 762 777
Email: lma@unizar.es
http://ina.unizar.es/lma

DISEÑO GRÁFICO:
José Luis Lizano

DEPÓSITO LEGAL:
Z-771-2012


LMA
LABORATORIO
DE MICROSCOPIAS
AVANZADAS

GOBIERNO DE ESPAÑA
MINISTERIO DE ECONOMÍA Y COMPETITIVIDAD

Universidad Zaragoza
1542

GOBIERNO DE ARAGON